Aus dem Fachbereich Medizin
der Johann Wolfgang Goethe-Universität
Frankfurt am Main

betreut am
Gustav Embden-Zentrum der Biochemie
Institut für Biochemie II (Kardiovaskuläre Biochemie)
Direktor/in: Prof. Dr. Ivan Dikic

The F-BAR protein NOSTRIN in endothelial signal transduction

Dissertation
zur Erlangung des Doktorgrades der Medizin
des Fachbereichs Medizin
der Johann Wolfgang Goethe-Universität
Frankfurt am Main

vorgelegt von
Miriam Müller

aus Frankfurt am Main

Frankfurt am Main, 2016

Dekan/in:	Prof. Dr. Josef M. Pfeilschifter
Referent/in:	Prof. Dr. Ivan Dikic
Koreferent/in:	Prof. Dr. Nina Wettschureck
Tag der mündlichen Prüfung:	07.03.2017

1 Table of Contents

2 Summary

NOSTRIN belongs to the family of F-BAR proteins, which are multi-domain adaptor proteins that have emerged as important regulators of membrane remodeling and actin dynamics in a variety of vital cellular processes. They have been analyzed structurally and biochemically and overexpression studies have revealed their potential in inducing membrane curvature and tubulation. Several studies have begun to decipher the function of individual proteins, but the understanding of F-BAR protein functions in vivo is still quite limited.

The F-BAR protein NOSTRIN is mainly expressed in endothelial cells and has originally been described as interaction partner of the endothelial nitric oxide synthase (eNOS), modulating eNOS subcellular localization. The phenotypic characterization of NOSTRIN knockout mice revealed decreased nitric oxide (NO) and cGMP levels, an increase in systolic blood pressure and an impairment of the acetylcholine-induced, NO-dependent relaxation of aortic rings from mice with global as well as endothelial cell-specific knockout of the NOSTRIN gene (ECKO) . These findings implied that NOSTRIN plays a role in regulating NO production *in vivo*, but the underlying molecular mechanisms were unclear. Therefore, this study was aimed at addressing the mechanism causing the inhibited vasodilation specifically upon stimulation with acetylcholine in NOSTRIN KO and ECKO mice, and at exploring additional roles of NOSTRIN in the signal transduction of endothelial cells.

The major acetylcholine receptor that mediates vessel relaxation upon stimulation with acetylcholine is the muscarinic acetylcholine receptor subtype M3 (M3R). In the present study NOSTRIN was identified as novel interaction partner of the M3R and important factor for the correct spatial distribution and functionality of the M3R. Moreover, it provides the first example of an F-BAR protein regulating a GPCR. Confocal immunofluorescence microscopy analysis of isolated aortae from NOSTRIN KO and WT mice indicated that NOSTRIN was necessary for the proper subcellular localization of the M3R and targeted it to the plasma membrane. A series of pulldown experiments revealed a direct interaction of NOSTRIN with the M3R. The binding required the SH3 domain of NOSTRIN and the third intracellular loop of the M3R, which has a recognized

role in receptor regulation. The interaction of NOSTRIN with the M3R was confirmed by co-localization of NOSTRIN and the M3R upon overexpression in mammalian cells. Expression levels of the M3R as well as eNOS were not affected by the loss of NOSTRIN in accordance with the finding, that NOSTRIN impacts on the acetylcholine/eNOS signaling axis through regulation of the subcellular trafficking of its binding partners.
Furthermore, there were first indications for a role of NOSTRIN in facilitating the carbachol-induced calcium response in M3R-expressing cells, suggesting that NOSTRIN might influence M3R activation. in the absence of NOSTRIN, the function of the M3R in mammalian cells overexpressing the M3R was markedly impaired, resulting in abolition of the calcium response to the M3R agonist carbachol. In accordance, the activated eNOS fraction associated with the Golgi complex was markedly reduced in aorta explants from NOSTRIN knockout and ECKO mice. Moreover, NOSTRIN knockout inhibited the carbachol-induced, activating phosphorylation of eNOS in murine aortae as well as primary mouse lung endothelial cells confirming its role as important regulator of eNOS activity in vivo.

Exploring the additional roles of NOSTRIN in the signal transduction of endothelial cells, it was found that in the absence of NOSTRIN aortic endothelial cells showed misarranged cortical actin, loss of actin stress fibers, and loss of PECAM-1 membrane staining. Both the actin cytoskeleton and PECAM-1 are crucial for the endothelial cell's response to shear stress. To address the question if NOSTRIN is needed for the (re-)alignment of actin stress fibers in the direction of flow, a flow chamber was constructed. This flow chamber allowed fixing pieces of aorta explants within the flow chamber either in the physiological direction of flow or perpendicular to it. En face immunofluorescence staining of the aorta explants indicated that the endothelial cell's ability to realign their shape and stress fibers upon the change of the direction of flow was lost in NOSTRIN KO aortae. These data suggest that NOSTRIN might play a role in shear sensing or mediating the response to shear stress in endothelial cells and lay the basis for more future studies addressing the role of NOSTRIN in endothelial mechanoactivated pathways.

3 Zusammenfassung

F-BAR Proteine sind eine Familie von Adapterproteinen, die über verschiedene funktionelle Domänen verfügen und an der Schnittstelle zwischen Membran und Aktinzytoskelett eine Vielzahl essentieller zellulärer Prozesse regulieren. Die strukturellen und biochemischen Eigenschaften einer Reihe von F-BAR Proteinen wurden bereits detailliert untersucht und Überexpressionsstudien belegen die Fähigkeit von F-BAR Proteinen, Membrankrümmungen und kleine Membrankanäle zu erzeugen. Das Wissen über die spezifische Funktion einzelner F-BAR Proteine *in vivo* ist hingegen noch immer begrenzt.

Das F-BAR Protein NOSTRIN wird vor allem von Endothelzellen exprimiert und wurde ursprünglich als Interaktionspartner und Regulator der subzellulären Lokalisation der endothelialen Stickstoffmonoxid-Synthase (eNOS) beschrieben. NOSTRIN-KO-Mäuse weisen erniedrigte Stickstoffmonoxid (NO) und cGMP-Spiegel, einen erhöhten systolischen Blutdruck und eine deutliche Beeinträchtigung der acetylcholinabhängigen Relaxation isolierter Aortenringe auf, was darauf hindeutet, dass NOSTRIN eine wichtige Rolle in der Regulation der NO-Produktion *in vivo* spielt. Die Zielsetzung der vorliegenden Arbeit war, den molekularen Mechanismus aufzuklären, der der Beeinträchtigung der acetylcholin-abhängigen Vasorelaxation zugrunde liegt, und darüberhinaus weitere mögliche Funktionen von NOSTRIN in der Signaltransduktion von Endothelzellen zu untersuchen.

Die acetylcholinabhängige Vasorelaxation wird über den muskarinergen Acetylcholinrezeptor vom Subtyp M3 (M3R) vermittelt. In der vorliegenden Arbeit wurde NOSTRIN als neuer Interaktionspartner des M3R identifiziert. Dies stellt die erste Beschreibung eines F-BAR Proteins als Regulator eines G-Protein-gekoppelten Rezeptors dar.

Mit Hilfe von konkofaler Immunfluoreszemzmikroskopie an Aortenexplantaten konnte nachgewiesen werden, dass NOSTRIN für die korrekte räumliche Lokalisation des M3R an der Plasmamembran von Endothelzellen verantwortlich ist. Mit einer Reihe von *Pulldown*-Experimenten wurde die Wechselwirkung von NOSTRIN mit dem M3R als eine direkte Protein-Protein-Interaktion charakterisiert. Die Interaktion wird über die SH3-Domäne von NOSTRIN und die dritte intrazelluläre Schleife des M3R vermittelt, welche eine wichtige Rolle

in der Regulation der Rezeptorfunktion einnimmt. Die Interaktion von NOSTRIN mit dem M3R wurde zusätzlich durch die Kolokalisation der beiden überexprimierten Proteine in Säugerzellen bestätigt. Darüber hinaus konnte gezeigt werden, dass NOSTRIN keinen Einfluss auf die Expression des M3R hat, was unterstreicht, dass NOSTRIN die Acetylcholin/eNOS-Signalkaskade durch die Regulation der subzellulären Lokalisation seiner Interaktionspartner beeinflusst.

Die Ergebnisse der vorliegenden Arbeit gaben zudem erste Hinweise darauf, dass NOSTRIN den Carbachol-induzierten Kalziumeinstrom in M3R-exprimierenden Zellen ermöglicht. Das deutet darauf hin, dass NOSTRIN die Funktionalität des M3R beeinflusst. In Übereinstimmung damit war die Carbachol-induzierte aktivierende Phosphorylierung der eNOS in Aorten und primären Endothelzellen in der Abwesenheit von NOSTRIN inhibiert und die mit dem Golgi-Apparat-assozieerte eNOS-Fraktion im NOSTRIN-KO und -ECKO deutlich reduziert. NOSTRIN stellt somit einen neuen, wichtigen Interaktionspartner des M3R dar und der Verlust von NOSTRIN beeinträchtigt die dem M3R nachgeschalteten Signalwege, einschliesslich der Aktivierung der eNOS.

Bei der Untersuchung weiterer Funktionen von NOSTRIN wurde in Endothelzellen von NOSTRIN-KO-Mäusen eine Beeinträchtigung der Anordnung von kortikalem Aktin, Aktin-Stressfasern und der PECAM-1-Membranfärbung beobachtet. Sowohl das Aktinzytoskelett als auch PECAM-1 sind maßgeblich an der Reaktion der Endothelzellen auf Schubspannung beteiligt. Um der Frage nachzugehen, ob NOSTRIN an der Ausbildung und Ausrichtung von Stressfasern in Richtung des Blutflusses beteiligt ist, wurde eine Flusskammer gebaut. Mit Hilfe dieser konnten Aortenexplantate definiertem Fluss entweder in der physiologischen Flussrichtung oder rechtwinklig dazu ausgesetzt werden. Immunofluoreszenzfärbungen der Aortenexplantate ergaben Hinweise darauf, dass die Fähigkeit der Endothelzellen, ihren Zellkörper und ihre Stressfasern mit der Flussrichtung auszurichten, in Aorten von NOSTRIN-KO-Mäusen beeinträchtigt war. Diese Daten bilden die Grundlage für zukünftige Studien zur Rolle von NOSTRIN bei der Mechanotransduktion in Endothelzellen.

4 Abbreviations

aa	Amino acid
ACh	Acetylcholine
APS	Ammonium persulfate
Arp2/3	Actin related protein 2/3
AUC	Area under the curve
BAR domain	Bin-amphiphysin-Rvs domain
BH_4	Tetrahydrobiopterin
BSA	Bovine serum albumin
Ca^{2+}	Calcium ion
Cav-1	Caveolin-1
Cdc42	Cell division control protein 42 homolog
cDNA	Complementary DNA
cGMP	Cyclic guanosine monophosphate
CHO cells	Chinese hamster ovary cells
CIP4	Cdc42-interacting protein 4
CTL	Control
DAAM1	Disheveled associated activator of morphogenesis 1
DABCO	1,4-diazabicyclo[2.2.2]octane
DAG	Diacyl glycerol
DAPI	4',6-diamidino-2-phenylindole
DMEM	Dulbecco’s modified Eagle's medium
DNA	Deoxyribonucleic acid
DTT	Dithiothreitol
EC	Endothelial cell
EC_{50}	Half maximal effective concentration
ECKO	Endothelial cell specific knockout
EDTA	Ethylenediaminetetraacetic acid
EEA1	Early Endosome Antigen 1
EGF	Epidermal growth factor
EGFP	Enhanced green fluorescent protein
EGFR	Epidermal growth factor receptor
eNOS	Endothelial nitric oxide synthase

eps15	Epidermal growth factor receptor substrate 15
ERK	Extracellular-signal-regulated kinase
F-BAR domain	FCH and BAR domain
FAP52	Focal adhesion protein 52
FBP17	Formin-binding protein 17
FBS	Fetal bovine serum
FCH domain	Fes and CIP4 homology domain
FCHo	FCH domain only
FGF	Fibroblast growth factor
FGFR	Fibroblast growth factor receptor
FITC	Fluorescein isothiocyanate
GAP	GTPase activating protein
GAPDH	Glyceraldehyde 3-phosphate dehydrogenase
GEF	Guanine exchange factor
GFP	Green fluorescent protein
GLUT1	Glucose transporter type 1
GLUT4	Glucose transporter type 4
GMP	Guanosine monophosphate
GPCR	G-protein coupled receptor
GRK2	G-protein coupled receptor kinase 2
GSH	Glutathione
GST	Glutathione S-transferase
GTP	guanosine triphosphate
HBSS	Hanks' Balanced Salt Solution
HFpEF	Heart failure with preserved ejection fraction
HR1 motif	Homology region 1 motif
HRP	Horseradish peroxidase
i3loop	3rd intracellular loop
IgG	Immunoglobulin G
iNOS	inducible nitric oxide synthase
IP3	inositol-1,4,5-trisphosphate
IPTG	Isopropyl β-D-1-thiogalactopyranoside
kb	Kilo-base pair
KO	Knockout

LB medium	Lysogeny broth medium
M3R	Muscarinic acetylcholine receptor subtype M3
mAChR	Muscarinic acetylcholine receptor
MBP	Maltose binding protein
mDia	Mammalian diaphanous related formin
MLEC	Mouse lung endothelial cells
N-WASP	Neural Wiskott-Aldrich-Syndrome protein
NMDA receptor	N-methyl-D-aspartate receptor
nNOS	neuronal nitric oxide synthase
NO	Nitric oxide
NOSIP	NOS-interacting protein
NOSTRIN	eNOS traffic inducer
PACSIN	Protein kinase C and casein kinase substrate in neurons
PBS	Phosphate-buffered saline
PCH	Pombe/cdc15 homology
PCR	polymerase chain reaction
PDGFRβ	Platelet-derived growth factor receptor type β
PECAM-1	Platelet endothelial cell adhesion molecule-1
PFA	Paraformaldehyde
PMSF	Phenylmethane sulfonyl fluorid
PSTPIP	Proline-serine-threonine phosphatase-interacting protein
Rac1	Ras-related C3 botulinum toxin substrate 1
Ras	Rat sarcoma
RhoA	Ras homolog gene family, member A
SDS	Sodium dodecyl sulfate
SDS-PAGE	Sodium dodecyl sulfate polyacrylamide gel electrophoresis
sGC	Soluble guanylyl cyclase
SH2	Src homology 2
SH3	Src homology 3
SNP	Sodium nitroprussid
Sos	Son-of-Sevenless
srGAP	Slit-Robo RhoGTPase-activating protein
STAT3	signal transducer and activator of transcription 3
TEMED	Tetramethylethylenediamine

U	Unit
v/v	Volume per volume
VE-Cadherin	Vascular endothelial cadherin
VEGF	Vascular endothelial growth factor
w/v	Weight per volume
WASP	Wiskott-Aldrich-Syndrome protein
WT	Wildtype
µHD	µ homology domain

5 Introduction

5.1 F-BAR proteins and the BAR protein family

F-B4AR proteins belong to the superfamily of BAR proteins and have emerged as important regulators of membrane remodeling and actin dynamics in a variety of fundamental cellular processes including endocytosis, cell migration, division and development[1,2]. Formerly referred to as PCH (Pombe/cdc15 homology) proteins[3], F-BAR proteins have been identified in most eukaryotes except plants[4].

The term BAR is derived from the first letters of the initially identified members of the family, the mammalian tumor suppressor Bin1, the mammalian neuronal protein amphiphysin and the yeast protein Rvs167p. The defining feature of all BAR proteins is the crescent-shaped BAR domain that allows binding to membranes that fit their structure and/or deform membranes according to their shape, thus generating specific membrane geometries[2]. At the structural level, BAR domains are dimers of an antiparallel helix bundle that displays various degrees of intrinsic curvature[5,6].

The BAR family is composed of several subfamilies, namely N-BAR, I-BAR and F-BAR. N-BAR proteins contain N-terminal amphipathic helices preceding the BAR domain. Although sensing and generation of membrane curvature are thought to be critically dependent on the curved shape of the BAR domain, these amphipathic helices fold upon membrane interaction and penetrate like wedges into the lipid bilayer enhancing the N-BAR domain's membrane bending activity and stabilizing the curvature[7,8].
In contrast to the concave-shaped lipid-binding interface of BAR and F-BAR domains, the positively charged lipid-binding surface of I-BAR or inverse BAR domains displays a convex geometry which resembles the shape of a cigar or a zeppelin (Fig. 1). This finding provides a possible structural explanation for the observation that I-BAR domains induce membrane protrusions rather than invaginations[9,10,11].

5.2 Structure and domain architecture of F-BAR proteins

F-BAR domains are composed of an N-terminal FCH (Fes and CIP4 homology) module followed by a coiled-coil BAR domain[12] with a positively charged surface that allows the association with the negatively charged inner surface of cellular membranes[2]. Due to their structural similarity with BAR domains, the combined domain has been renamed as F-BAR domain. In comparison to canonical BAR domains, both individual monomers and the dimer are more elongated in the F-BAR structure and monomers are set in a wider angle in the dimer giving the dimers a more gentle curvature (Fig. 1). This is consistent with the wider diameter of F-BAR versus BAR domain-induced tubules[6,13]. In addition, BAR and F-BAR domains show different preferences for differently sized liposomes *in vitro*[14].

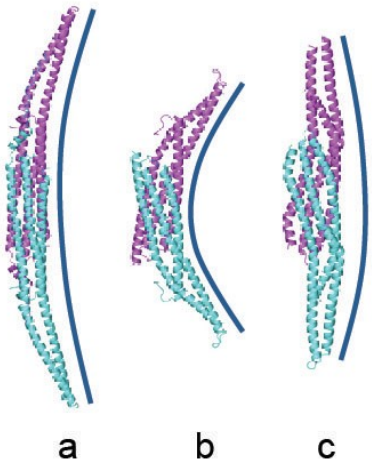

Figure 1 Structure of F-BAR, BAR, and I-BAR domains. BAR domains are crescent-shaped dimers of an antiparallel helix bundles that display various degrees of intrinsic curvature: The curvature of F-BAR domains (a) is more gentle compared to canonical BAR domains (b). In contrast to the concave-shaped lipid-binding interface of BAR and F-BAR domains, the positively charged lipid-binding surface of I-BAR domains (c) displays a convex geometry. This figure was modified from[6].

F-BAR proteins can be further divided into six subfamilies: The Fes subfamily of non-receptor tyrosine kinases, the protein kinase C and casein kinase substrate in neurons protein (PACSIN) subfamily, the Cdc42-interacting protein 4 (CIP4) subfamily, the Slit–Robo RhoGTPase-activating proteins (srGAPs), the FCH-domain-only (FCHo) and the proline-serine-threonine phosphatase-interacting protein (PSTPIP) subfamilies[15,16] (Fig. 2). As primary sequence homology

between the family members is low[3], the similarity is defined mainly by the (predicted) domain structure.

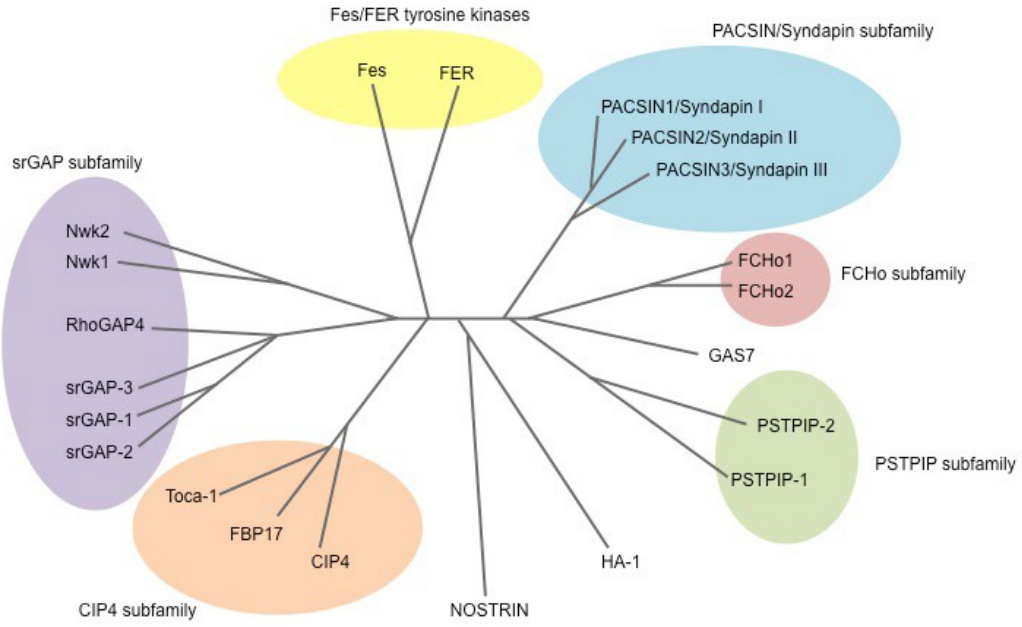

Figure 2 Phylogenetic tree of F-BAR protein subfamilies F-BAR proteins can be divided into six subfamilies: the srGAPs (purple), the Fes subfamily (yellow), the PACSIN subfamily (blue), the FCHo subfamily (red), the PSTPIP subfamily (green) and the CIP4 subfamily (orange). GAS7, HA-1 and NOSTRIN are currently not assigned to any of the six subfamilies. This figure was modified from[4]

Just like the majority of BAR protein family members, F-BAR proteins are scaffolding proteins that combine the membrane remodeling F-BAR domain with various combinations of additional protein-protein interaction motifs or catalytic domains[17] (Fig. 3). Most of the F-BAR proteins contain SH3 (Src homology 3) domains, important protein-protein interaction modules that specifically recognize proline-rich ligands and regulate the assembly of multi-protein complexes and thus the local concentration and subcellular distribution of binding partners[18]. Members of the Fes subfamily contain tyrosine kinase domains as well as SH2 (Src homology 2) domains, which allow binding to phosphorylated tyrosine residues[19]. Some F-BAR proteins are linked to small GTPases: CIP4, FBP17 and Toca-1 possess a domain for binding to Rho GTPases, and the srGAPs and HA-1 have a RhoGAP domain, which enhances the slow intrinsic GTPase activity of Rho GTPases leading to their

inactivation[20]. Members of the FCHo subfamily contain μ homology domains (μHD) that allow the recruitment of adaptor proteins, which promote the formation of clathrin-coated pits[21].

The assembly of these different modules and domains allows F-BAR proteins not only to aid membrane remodeling by imposing, stabilizing or preferentially binding particular membrane curvatures, but, at the same time, to recruit effector proteins and couple distinct curvature states to specific biological processes[17,14].

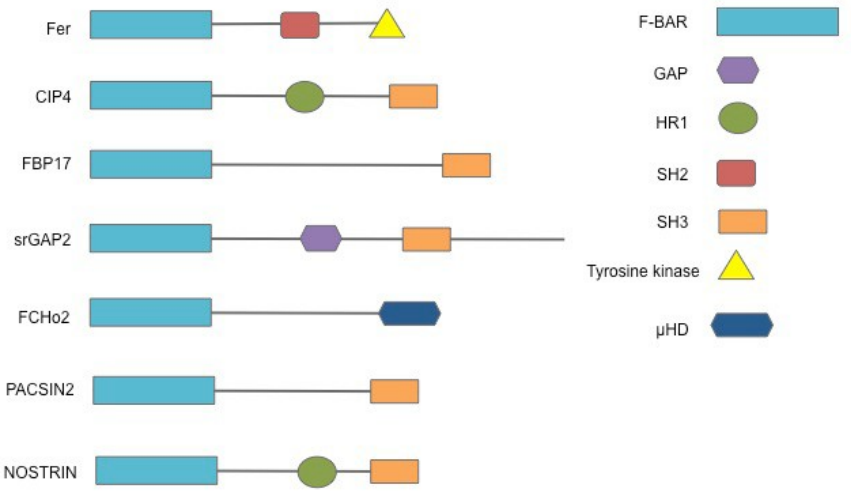

Figure 3 Domain structure of F-BAR proteins. Schematic representation of typical members of the F-BAR protein family. F-BAR proteins are multidomain adaptor proteins. Their common feature is the F-BAR domain. In addition, F-BAR proteins contain other domains, including protein-protein interaction motifs (e.g. SH3 and SH2) or catalytic domains (e.g. tyrosin kinases and GAP). This figure was modified from[22] .

5.3 F-BAR proteins and the actin cytoskeleton

The regulation of the actin cytoskeleton is a commonly reported function of F-BAR proteins and is conserved from yeast to higher eukaryotes[16]. More precisely, F-BAR proteins regulate the interplay between the actin cytoskeleton and the machinery that controls membrane dynamics. This is required in a

variety of vital processes, like endocytosis, phagocytosis, filopodium and lamellipodium formation, cytokinesis, and adhesion[23].

The best-characterized mechanism through which F-BAR proteins act on the actin filament system is the interaction with the Wiskott-Aldrich-Syndrome protein (WASP) family via the F-BAR proteins' SH3 domain, which has been reported for Toca-1[24], CIP4[25], PACSINs[26], and NOSTRIN[27]. Proteins of the WASP family are scaffolding proteins that mediate the activation of the Arp2/3 (actin related protein 2/3) complex, which catalyzes the nucleation of new actin filaments in the form of branches off the sides of preexisting actin filaments[28].

A second mechanism by which F-BAR proteins interact with the actin cytoskeleton is through their interaction with diaphanous-related formins, which catalyze the assembly of long unbranched actin filaments that are found in filopodia and stress fibers. It has been reported that Cip4, FBP17 and Toca-1 interact via their SH3 domains with the mammalian diaphanous-related formins mDia1 and mDia2 and with DAAM1 (disheveled associated activator of morphogenesis) in the formation of filopodia[29].

Moreover, some F-BAR proteins interact directly with actin or actin regulating proteins modulating the architecture of F-actin. PSTPIP2 bundles actin[30] and FAP52 interacts with the actin crosslinking protein filamin and colocalizes with actin and filamin in focal adhesions[31]. Overexpression of FAP52 leads to disorganization of the actin cytoskeleton and redistribution of filamin from the linear pattern of actin fibers to dot-like structures[31].

PACSIN2 associates with actin filaments using the same concave surface of the F-BAR domain that is needed to bind to membranes[32]. However, this seems to be a specific feature of some BAR domain proteins and not a general property of the protein family, as two other F-BAR proteins (FCHo2 and CIP4) as well as the N-BAR protein endophilin did not interact with F-actin[32].

5.4 F-BAR proteins in endocytosis

F-BAR proteins are particularly important in endocytosis where the generation of membrane curvature is tightly coupled to actin dynamics. Whereas the F-BAR domain shapes the membrane, the highly dynamic actin cytoskeleton provides the force that drives membrane invagination, helps to constrict the neck of a nascent vesicle, and propels the vesicle away from the plasma membrane[33,34].

There are at least five different endocytic pathways in mammalian cells: Clathrin-dependent, caveolae-dependent, clathrin- and caveolae-independent endocytosis, macropinocytosis and phagocytosis[35], with clathrin-mediated endocytosis being most thoroughly studied. Clathrin assembles with different coat proteins at the nascent endocytic pit and cooperates with the large GTPase dynamin in the process of invagination and vesicle scission. Vesicles bud and pinch off from the plasma membrane, move deeper into the cell and fuse later with the early endosome or recycle back to the cell surface[36].

The crescent-shaped BAR and F-BAR domains display positively charged residues on their surface allowing direct interactions with negatively charged membrane lipids such as phophoinositides or phosphatidylserine[6,37,5]. By end-to-end association and lateral interactions, F-BAR protein dimers can form a helical coat around membrane invaginations that promotes and stabilizes tubulation[6]. The differences in diameter of both the BAR domain and the endocytic intermediates suggest a sequential involvement of BAR and F-BAR proteins during the process of endocytosis. While BAR proteins are involved in constricting the neck of the endocytic vesicle thus leading to vesicle scission, F-BAR proteins might play a role in the early steps of endocytosis by associating to rather broad invaginations of the nascent endocytic pit and deepen the initial invagination[38] (Fig. 4).

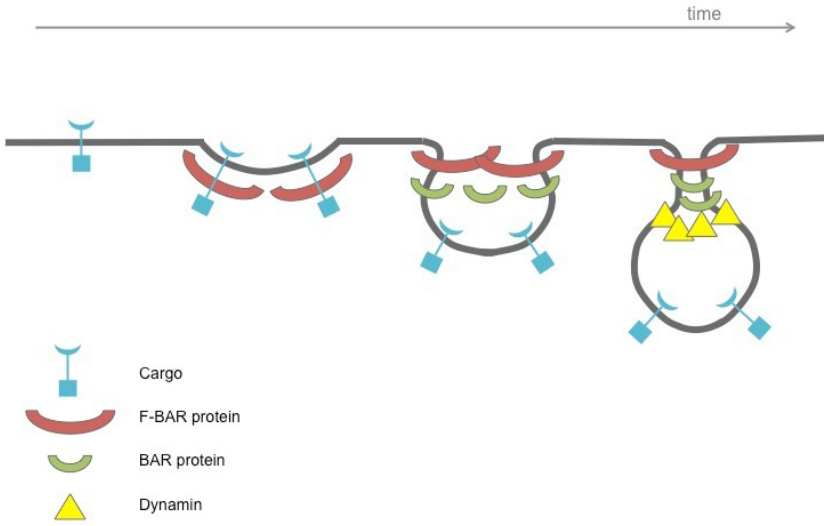

Figure 4 F-BAR and BAR proteins in endocytosis. The differences in diameter of F-BAR and BAR domains suggest a sequential involvement during the process of endocytosis: Whereas F-BAR proteins with the more gentle curved F-BAR domain could play a role in the early steps of endocytosis, BAR proteins are involved in constricting the neck oft he nascent vesicle leading to vesicle scission. This figure was modified after[38].

In addition to their lipid-binding and membrane-sculpting activity, FCHo proteins directly bind epidermal growth factor receptor substrate 15 (eps15) and intersectin thus initiating the maturation of clathrin-coated vesicles[21].

Endocytosis is also fundamental for the trafficking of membrane receptors. The regulation of their level of surface expression, internalization and degradation is crucial for the outcome of downstream signaling. Several F-BAR family members have been found to be involved in the trafficking of different receptors: PACSIN1 regulates endocytosis of developmentally expressed NMDA (N-methyl-D-aspartate) receptors in rat hippocampal cells. By binding to the receptor and assembling a complex of proteins including dynamin and clathrin, PACSIN1 promotes the removal of immature NMDA receptor forms from the synaptic sites, which is a key step in glutamergic synapse maturation and essential for synaptic plasticity[39].
Furthermore, PACSIN2 has been described to regulate EGFR internalization. Internalized EGFR translocates to PACSIN2-positive endosomes and the loss of PACSIN2 leads to an increased expression of EGFR at the plasma membrane as well as an enhanced EGF-induced phosphorylation of the EGFR.

Accordingly, both downstream signaling and cell proliferation were enhanced [40]. Moreover, CIP4 and Toca-1 regulate late events in EGFR trafficking. CIP4 localizes to Rab5-positive vesicles and promotes the EGF induced transit of EGFR from EEA1-positive endosomes to lysosomes[41]. Therefore a more complex picture of F-BAR function emerges in the coordination of intracellular vesicular trafficking and membrane dynamics beyond their role at the plasma membrane.

5.5 Roles of F-BAR proteins in human diseases

Acting at the interface of membrane remodeling and cytoskeleton dynamics, F-BAR proteins are critical in a wide range of normal and pathological cellular functions. Disturbed functionality of several members of the F-BAR protein family has been associated with a variety of human diseases and disorder conditions, including neurologic and autoinflammatory disease, chronic kidney disease and cancer. However, the understanding of the underlying mechanisms is still quite limited and there is currently no common mechanism for F-BAR protein action in disorder conditions.

To name a few examples, members of the srGAP subfamily have been described in the context of several neurological disorders including mental retardation[42,43,44], Parkinson's disease[45], and schizophrenia[46,47]. srGAP3 is part of the Slit-Robo pathway that regulates neuronal migration and axonal branching suggesting a role of srGAP3 in the maturation of neuronal structures which is essential for mental development and normal cognitive function[48]. Being among the many interaction partners of huntingtin protein, PACSIN1 and CIP4 are implied in the pathogenesis of Huntington's Disease. PACSIN1 serves as endocytic adaptor for juvenile NMDA receptors and the interference of mutated huntingtin with PACSIN1 led to inappropriate synapse destabilization[49]. Overexpression of CIP4 induced death of striatal neurons, and it has been suggested that it may contribute to early changes in the pathogenesis of Huntington's Disease by interfering with Rho GTPases and signal transduction essential to neuronal survival[50].

Evidence has been accumulating to suggest roles for several F-BAR proteins in cancer, often in the context of enhanced cancer cell motility and invasion through invadopodia formation. Invadopodia are actin-rich membrane protrusions formed by invasive tumor cells that promote degradation of the extracellular matrix and invasiveness of tumor cells. In this regard, FBP17 was found to play a critical role in bladder tumor cell invasion by mediating invadopodia formation[51] and CIP4 promotes breast cancer invasiveness by invadopodia formation through activation of N-WASP[52]. Conversely, CIP4 knockdown in a breast tumor cell line inhibited internalization of matrix metalloproteases, limiting their surface expression and leading to increased extracellular matrix degradation and tumor cell invasion[53].

There are first studies that implicate a role of F-BAR proteins in glucose uptake and renal dysfunction. CIP4 controlled endocytosis of the glucose transporter GLUT4 in myoblasts by interacting with N-WASP and dynamin-2 in an insulin-dependent manner[54]. Overexpression of PACSIN3 in adipocytes lead to an increased glucose uptake through inhibition of GLUT1 endocytosis and thus elevation of GLUT1 surface expression[55].

Furthermore, CIP4 is highly expressed in tubular epithelia of nephrectomized rats and overexpression of CIP4 in human kidney cells induced renal-epithelial-mesenchymal transition, a process that involves dissolving of tight junctions, loosening of cell-cell-adhesions and apical-basal polarity, reorganization of the actin cytoskeleton and an increase of cell mobility, finally leading to progressive kidney failure and fibrosis[56].

In addition, several F-BAR proteins have been described in the context of auto-inflammatory diseases, including pyogenic sterile arthritis, pyoderma gangraenosum and acne (PAPA) syndrome[57,58,59], Wiskott-Aldrich-Syndrom[60], and chronic recurrent multifocal osteomyelitis[61].

5.6 The F-BAR protein NOSTRIN

NOSTRIN is expressed in endothelial cells and highly vascularized tissues, the strongest expression is found in heart, placenta, kidney and lung[62]. It has first been identified as regulator of the endothelial nitric oxide synthase (eNOS) subcellular localization[62], hence the name eNOS traffic inducer.

NOSTRIN is composed of 506 amino acids. As a prototypic member of the F-BAR protein family, it displays a typical domain structure, consisting of an N-terminal F-BAR domain, an HR1 motif, the intermediate domain and a C-terminal SH3 domain (Fig. 5). The NOSTRIN SH3 domain mediates the interaction with eNOS, dynamin and the guanine exchange factor (GEF) Sos. Although NOSTRIN contains only one SH3 domain, oligomerization via the F-BAR domain enables it to interact with different interaction partners at the same time[27].

Figure 5 Domain structure of NOSTRIN. The F-BAR protein NOSTRIN is composed of 506 amino acids. Amino acids 1 to 224 form the F-BAR domain, amino acids 304 to 386 the HR1 motif, and amino acids 441 to 506 the C-terminal SH3 domain. This Figure was modified from[63]

In cultured cells, NOSTRIN is known to facilitate the translocation of eNOS from the plasma membrane into intracellular vesicular structures that are associated with actin filaments through the interaction with the large GTPase dynamin and N-WASP[27]. Furthermore, NOSTRIN forms a ternary complex with eNOS and caveolin-1, mediating the subcellular localization of eNOS and possibly playing a role in caveolar trafficking[64] (Fig. 6).

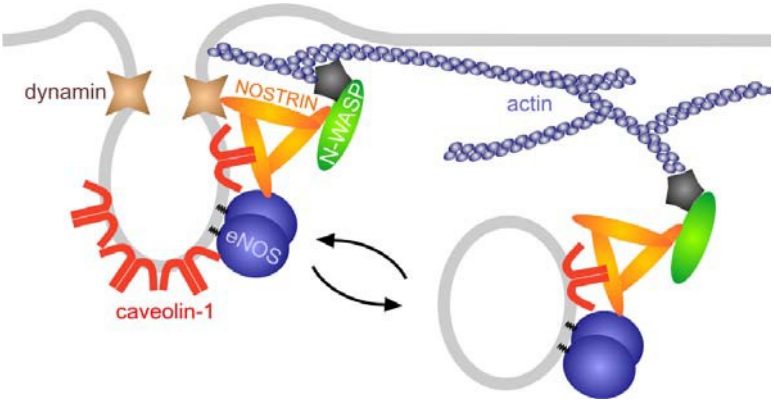

Figure 6 Model for NOSTRIN-dependent regulation of eNOS subcellular localization by interacting with dynamin and N-WASP. NOSTRIN (NST) is enriched at caveolar membranes and forms a ternary complex with eNOS and the caveolar protein caveolin-1 (Cav). Moreover, NOSTRIN serves as oligomeric adaptor protein for the large GTPase dynamin (Dyn) and the Arp2/3 activating protein N-WASP, suggesting a role of NOSTRIN in eNOS internalization and trafficking. This figure was modified from[65].

A shortened variant of NOSTRIN, termed NOSTRINβ, which is lacking essential parts of the F-BAR domain and is mainly localizing to the nucleus, was found in cirrhotic liver[66]. NOSTRINβ has been suggested to be a nucleo-cytoplasmic shuttling protein, which negatively regulates the transcription of the NOSTRIN gene[67].

There are first studies that begin to decipher the function of NOSTRIN *in vivo* and suggest a role of NOSTRIN in the pathogenesis of several human diseases.

First, it has been shown that NOSTRIN plays a crucial role in developmental angiogenesis in both zebrafish and mice and the loss of NOSTRIN impairs endothelial tip cell function and endothelial cell proliferation. It has been suggested that NOSTRIN serves as multivalent adaptor for fibroblast growth factor receptor 1 (FGFR1), the small GTPase Rac1 and it's guanine exchange factor (GEF) Sos1, and that the assembly of this signaling complex regulates the FGF-2-dependent activation of Rac1. Both FGF signaling and Rac1 are known to be important in pro-angiogenic signaling[63].

Furthermore, the NOSTRIN gene was identified in gene regions that are associated with hypertension in humans[68] as well as in rats[69]. In the kidney, NOSTRIN is expressed in podocytes and colocalizes with the cell-cell-contact proteins β-catenin and zonula-occludens-1 and interacts with the slit-membrane

associated adaptor protein CD2AP. Knockdown of NOSTRIN in zebrafish larvae alters the glomerular filtration barrier, leading to proteinuria and morphological changes of the kidney. These findings suggest a role of NOSTRIN in hypertensive kidney disease[70].

Additionally, patients with alcoholic hepatitis and liver cirrhosis had significantly higher hepatic levels of NOSTRIN suggesting a role of NOSTRIN in the development of increased intrahepatic resistance in these patients, a condition that is associated with reduced eNOS activity[66].

NOSTRIN may also play a role in the pathogenesis of maternal hypertensive disorders, as high expression levels of NOSTRIN were found in placental tissues of patients with pre-eclampsia[71] and pregnancy-induced hypertension[72].

5.7 Endothelial cell function and dysfunction

Situated at the interface between the blood and the vessel wall, the endothelium is a major regulator of vascular tone and homeostasis and exerts anticoagulant, antiplatelet and fibrinolytic properties[73]. Many of these effects rely on nitric oxide (NO), which is synthetized from the amino acid L-arginine in an enzymatic reaction catalyzed by eNOS[74,75,76,77].

The maintenance of vascular tone is mediated by the release of numerous dilator and constrictor substances, as well as hemodynamic stimuli like fluid shear stress, that regulate eNOS activity and NO availability. NO diffuses to underlying vascular smooth muscle cells and causes relaxation by activating soluble guanylyl cyclase (sGC), thereby increasing intracellular cyclic guanosine monophosphate (cGMP) levels (Fig. 7)[73].

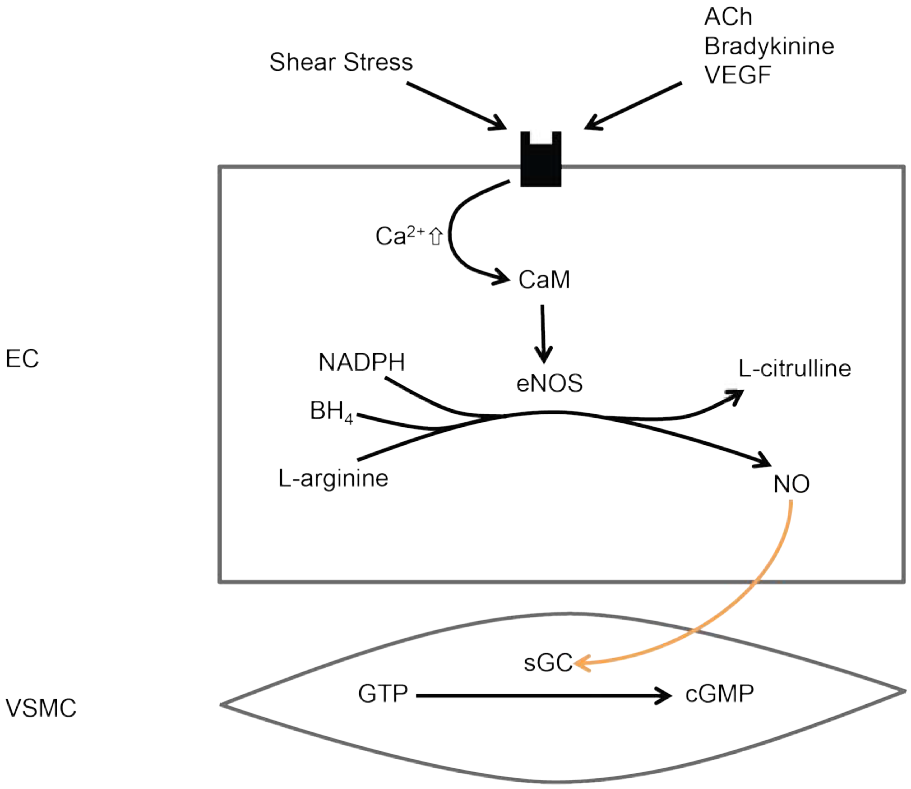

Figure 7 Regulation of the vascular tone (simplified schematic presentation). Increased intracellular calcium levels in response to vasodilator agonists or shear stress lead to an activation of eNOS through interrupting the eNOS-Cav-1-complex and calcium/calmodulin binding. eNOS catalyzes the synthesis of NO from L-arginine in an NADPH and BH4 dependent reaction. NO diffuses to underlying vascular smooth muscle cells (VSMCs), activates soluble guanylyl cyclase (sGC), leading to an increase of intracellular cGMP and finally to relaxation. This figure was modified from[78].

Damage to the endothelium upsets the balance between vasoconstriction and vasodilation. Reduced activity of eNOS and decreased NO bioavailability are important characteristics of endothelial dysfunction, an early event in the development of cardiovascular diseases, such as hypertension, atherosclerosis, and heart failure[78,73,79].

5.7.1 Regulation of eNOS activity

Since NO is a highly reactive free radical which can diffuse freely through cell membranes, its synthesis must be kept under tight control.

eNOS consists of two protein modules, the reductase and the oxygenase domain, which are connected via a flexible protein strand. The reductase domain generates the electrons required for NO synthesis by binding reduced NADPH and catalyzing its dehydrogenation. The electrons are then transferred to the oxygenase domain, that binds heme, L-arginine and tetrahydrobiopterin (BH_4) and contains the catalytic center for NO synthesis[73].

eNOS is constitutively expressed, but its expression and enzymatic activity is affected by numerous agonists, for example, acetylcholine, vascular endothelial growth factor (VEGF), bradykinin, sphingosine-1-phosphate, or hemodynamic stimuli like fluid shear stress from the viscous drag of the blood flow[75].

Regulation of eNOS activity is relatively complex and includes cellular events such as increased intracellular calcium levels, substrate and co-factor availability, protein-protein interactions with a spectrum of adaptor and regulatory proteins, posttranslational modifications, and shuttling between distinct subcellular compartments[75].

At the posttranslational level, eNOS is regulated by the availability of its substrate L-arginine. Under physiological conditions, the intracellular level of L-arginine is generally high enough. However, cardiovascular disease and the associated oxidative stress have been linked with reduced L-arginine transport and competition with other L-arginine-utilizing enzymes like arginase [80]. Furthermore, protein degradation is associated with the generation of endogenous NOS inhibitors like asymmetric dimethylarginine (ADMA), which is a competitive inhibitor of eNOS associated with endothelial dysfunction. The lack of the cofactor BH_4 leads to the uncoupling of eNOS, resulting in the generation of reactive oxygen species, reduced NO bioavailability, and endothelial dysfunction[75].

Shuttling between distinct subcellular compartments and spatially and temporally coordinated association and dissociation with a spectrum of interacting proteins, is essential for controlled eNOS activity and efficient NO production. Localization of eNOS to plasma membrane caveolae is associated with reduced eNOS activity. Caveolin-1, a major coat protein of caveolae, interacts directly with eNOS resulting in eNOS inhibition. The disruption of this complex through increase in intracellular calcium in response to various stimuli

is required for eNOS activation. The rate of electron transfer is increased by calcium-dependent binding of calmodulin, a major interaction partner and activator of eNOS[75,79].
Interaction with NOSTRIN, NOSIP (NOS-interacting protein) and dynamin contribute to the dynamically regulated intracellular distribution of eNOS[65].

Furthermore, eNOS activity is highly regulated by reversible phosphorylation. There are numerous potential phosphorylation sites on serine, threonine and tyrosine residues and the phosphorylation status is regulated by a number of kinases and phosphatases, which vary with the stimulus applied. The two most thoroughly studied phosphorylation sites are the ones at Thr495 and at Ser1177 in humans, Ser1179 in mice respectively. The activation of eNOS is associated with concomitant changes in the phosphorylation state of Ser1177 and Thr495. In the basal state, eNOS is phosphorylated at Thr495, which is associated with reduced eNOS activity as it prevents its interaction with calmodulin. On the contrary, Ser1177 is not phosphorylated in unstimulated cultured endothelial cells. Upon stimulation, eNOS is dephosphorylated at Thr495 allowing calmodulin to bind and activate the enzyme, and gets rapidly phosphorylated at Ser1177[75].

5.7.2 Muscarinic acetylcholine receptors and their role in ECs

Acetylcholine (ACh) is a major neurotransmitter in the central and peripheral nervous system and the first neurotransmitter ever identified[81]. ACh receptors are traditionally divided into nicotinic and muscarinic ACh receptors (mAChR). Whereas nicotinic ACh receptors are ion channels, mAChR are prototypical G-protein coupled receptors (GPCRs) containing seven hydrophobic transmembrane domains[82].
Five mAChR subtypes have been identified, designated M1, M2, M3, M4 and M5. In general, M2 and M4 couple to $G_{i/0}$ proteins resulting in an inhibition of adenylate cyclase, whereas M1, M3 and M5 couple to G-proteins of the $G\alpha_{q/11}$ family, leading to an activation of phospholipase C. Phospholipase C cleaves phosphoinsositol-4,5-bisphosphate to yield diacylglycerol (DAG) and inositol-

1,4,5-trisphosphate (IP3). While DAG remains bound to the membrane, IP3 diffuses through the cytosol to bind to its receptors, particular calcium channels in the endoplasmic reticulum. Binding causes an increase of intracellular calcium levels and influences a variety of signaling events in the cell[83].
Five distinct genes encode the receptor subtypes. Whereas they share 26,3% overall amino acid identity, the third intracellular loop (i3loop, between the 5th and the 6th transmembrane domain) shows the largest variety between the subtypes with only 2,7% amino acid identity in contrast to an average of 66% amino acid identity in the transmembrane domains. Compared to other GPCRs, the i3loop of mAChRs is relatively long, consisting of 160-240 amino acid residues. Mutagenesis studies have shown that the N- as well as the C-terminal parts of the i3loop are important for the coupling to G-proteins. Additionally, the i3loop provides sites for agonist- and second messenger-dependent phosphorylation and thus the regulation of G-protein and receptor activity[84].

mAChRs are expressed in virtually all organs, tissues and cell types and frequently multiple subtypes coexist in the same tissues and cells[82]. The presence of mAChRs on endothelial cells has first been described in 1980 by Furchgott and Zawadzki, who could demonstrate that endothelial mAChRs mediate vasodilation in isolated rabbit aortae upon stimulation with ACh[85]. The M3 receptor (M3R) has been found to be the major mAChR subtype that mediates vessel relaxation upon stimulation with ACh. This has been demonstrated by comparative analysis of knockout mice for the different muscarinic acetylcholine receptor subtypes M1 – M5 for the aorta[86,87], as well as for smaller arteries, such as pulmonary[88], ophthalmic[89], cutaneous, skeletal muscle and renal interlobar arteries[90], retinal[91] and coronary arteries[92]. In addition the subtype M2 is predominantly expressed by smooth muscle cells together with a smaller proportion of M3R[93].

5.8 Vascular phenotype of mice with global or endothelial cell-specific deletion of the NOSTRIN gene

Both mice with global (NOSTRIN KO) or endothelial cell-specific deletion of the NOSTRIN gene (NOSTRIN ECKO) are viable, but phenotypic characterization revealed a vascular phenotype:

The systolic blood pressure of NOSTRIN KO and ECKO mice was significantly increased when compared to control animals. Accordingly, NO release and cGMP levels were significantly reduced in the absence of NOSTRIN. Expression of eNOS, however, was not affected by the loss of NOSTRIN ([94], Tanja Hindemith and Igor Kovacevic, unpublished data).

Furthermore, myograph vascular reactivity analysis revealed an impairment of the ACh-induced, NO-dependent relaxation of aortic rings from NOSTRIN KO and ECKO mice. This finding was accompanied by a significant increase in the half maximal effective concentration (EC_{50}). An unimpaired vasoconstrictor response of the vessel to phenylephrine and the unaltered vasorelaxation in response to the NO donor sodium nitroprussid (SNP) indicated preserved reactivity of the vascular smooth muscle cells and functionality of the signaling cascade downstream of eNOS ([94], Tanja Hindemith and Igor Kovacevic, unpublished data).
Importantly, stimulation of aortic rings with the α2-agonist UK14304, which also induces a Ca^{2+}-mediated eNOS activation and the calcium ionophore A23187 did not show any significant difference in the vasorelaxation response between NOSTRIN KO and ECKO mice and their respective controls ([94], Tanja Hindemith and Igor Kovacevic, unpublished data). Therefore, of the agents tested, the inhibitory effect of the loss of NOSTRIN on endothelium-dependent relaxation seemed to be specific to stimulation with ACh ([94], Tanja Hindemith and Igor Kovacevic, unpublished data)(Fig. 8).

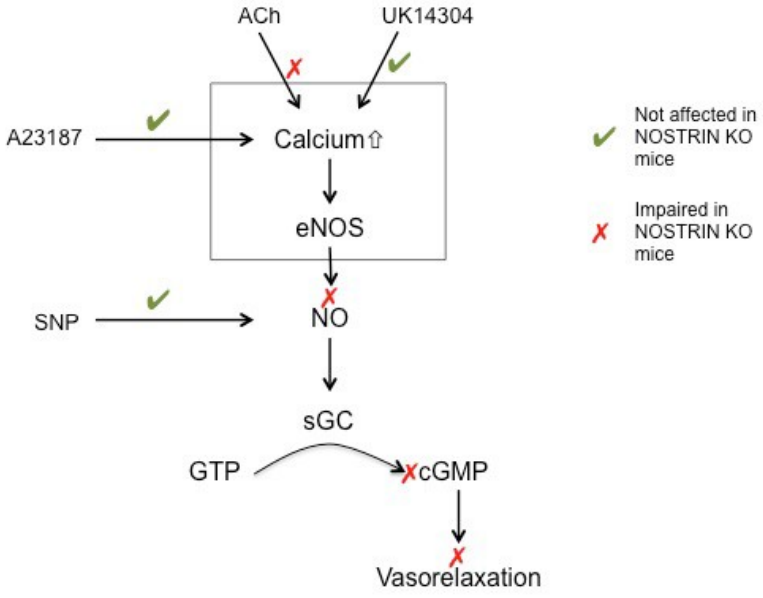

Figure 8 Schematic presentation of the vascular phenotype of NOSTRIN KO and ECKO mice. Mygraph experiments revealed an impairment of the ACh-induced NO-dependent relaxation of aortic rings from NOSTRIN KO and ECKO mice. The vasorelaxation response in response to the α2-agonist UK14304, the Ca^{2+}-ionophore A23187, and the NO donor sodium nitroprussid (SNP) were unaltered.

5.9 Aims of the present study

F-B AR family members have been identified in an ever-increasing number of pathways. They have been analyzed structurally and biochemically and overexpression studies have revealed their potential to induce membrane curvature and tubulation. Several studies have begun to decipher the function of individual proteins, but the understanding of F-BAR protein function *in vivo* is still quite limited.

The F-BAR protein NOSTRIN has been described as interaction partner of eNOS and modulates its subcellular localization in cultured cells. The phenotypic characterization of NOSTRIN knockout mice revealed decreased NO and cGMP levels, an increase in systolic blood pressure and an impairment of the ACh-induced, NO-dependent relaxation of aortic rings from NOSTRIN KO and ECKO mice compared to controls. These findings clearly indicate that NOSTRIN plays an important role in regulating NO production *in vivo*, but the underlying molecular mechanisms were unclear to date.

Therefore, the present study aims at

- Addressing the mechanism causing the inhibited vasodilation specifically upon stimulation with ACh in NOSTRIN KO and ECKO mice.
- Exploring additional roles of NOSTRIN in the signal transduction of endothelial cells.

6 Material and methods

6.1 Material

6.1.1 Vectors, cDNA and constructs

Vectors

pEGFP-N1, Takara Bio/Clontech, Saint-Germain-en-Laye, France

pIRESpuro2, Takara Bio/Clontech, Saint-Germain-en-Laye, France

pMal-C2X, New England Biolabs, Beverly, USA

pmCherry-N1, Takara Bio/Clontech, Saint-Germain-en-Laye, France

Primers

All primers were purchased from Sigma-Aldrich Chemie GmbH, Steinheim, Germany.

Primer	**Sequence 5' →→ 3'**
Flp10	AGGTTTATAGGAGAGCCAGGGACCTAGC
Flp11	CTCATACTGGTAAGCAGAAAAGCATCGTTT
FW2	CAGGACCAGGAAAGATCTGAGGCTG
Hom 28	CCTAGAGCTGACTCCTGCTGTGAGAGG
i3loop fw	TATAGAATTCAGGATCTATAAGGAAACTGAAAAG
i3loop rev	TATATCTAGACTAGGTCTGGGCCGCTTTCTTCTC
NST-mCherry fw	TATAAAGCTTATGAGGGACCCACTGACAG
NST-mCherry rev	TATAGGATCCGCTTTGTAGCTGTGTTGCC
NST-ΔSH3-mCherry fw	TATAGCTAGCATGAGGGACCCACTGACAG
NST-ΔSH3-mCherry rev	TATAAAGCTTGCTGAGCTGGGCTGCACCAGG
REV2	GCTGTGTAATCAAGTCTGATCTTG

cDNAs and constructs

The constructs for the following proteins used in this study were generated and described previously or supplied from commercial sources/depositories: human NOSTRIN, aa 1-506, in the vector pME18SFL3[62]; GST-NOSTRIN, aa 1-506 in pGEX2T[27]; GST-NOSTRIN-Δ-SH3, aa 1-440 in pGEX2T[27]; GST-SH3, aa 433-506 in pGEX2T[27]; His-Sos1-PRD [63,95]; full-length human M3 muscarinic Acetylcholine receptor cDNA (MGC Human CHRM3 Sequenced-Verified cDNA (Clone-ID: 40117429), glycerol stock) was obtained from Fermentas GmbH, St. Leon-Rot, Germany.

The following constructs were generated in this study according to the protocols described:

MBP-i3loop, aa 253-492 in pMal-C2x, inserted using the XbaI and EcoRI restriction sites; M3R-GFP, full length, in pEGFP-N1 using the EcoRI and SalI restriction sites; M3R-GFP, full length, in frame with EGFP in pIRESpuro2 using EcoRI and BamHI restriction sites; NOSTRIN-mCherry, full length, in mCherry-N1 using the HindIII and BamHI restriction sites; NOSTRIN-Δ-SH3-mCherry, aa 1-440, in mCherry using the NheI, and HindIII restriction sites.

6.1.2 Bacteria strains and cell lines

Escherichia coli strain BL21 Star (DE3)	Invitrogen, Karlsruhe, Germany
Escherichia coli strain Mach1	ThermoScientific, Schwerte, Germany
Escherichia coli strain TOP10	Invitrogen, Karlsruhe, Germany
Escherichia coli strain XL-10 Gold	Invitrogen, Karlsruhe, Germany

CHO/G5A cells[96] were a kind gift from S.Tunaru and S. Offermanns, Max-Planck-Institute for Heart and Lung Research, Bad Nauheim

U2OS cells were obtained from the Leibniz Institute DSMZ - German Collection of Microorganisms and Cell Cultures GmbH

6.1.3 Antibodies

Primary antibodies

Antigen	Host species	Dilution for IB	IF	Generated by
Protein-specific antibodies				
eNOS	Mouse	1:2000	1:200	BD Transduction Lab.
eNOS pSer 1177	Mouse	1:100	1:50	BD Transduction Lab.
ERK1/2	Mouse	1:2000	-	Cell Signaling
GAPDH	Mouse	1:10 000	-	Abcam
Giantin	Rabbit	-	1:200	Abcam
M3 mAChR	Rabbit	1:500	1:50	Santa Cruz
NOSTRIN	Rabbit	1:10 000	-	Masood Siddique, IBCII, Frankfurt

NOSTRIN	Mouse	1:2000	-	Schilling, Opitz et al. 2006 IBCII, Frankfurt
PECAM-1	Goat	1:	1:100	Santa Cruz
Vinculin	Mouse	1:10 000	-	Sigma
Tag-specific antibodies				
GFP	Rabbit	1:1000	-	Clontech
His	Mouse	1:10 000	-	Novagen
MBP	Mouse	1:10 000	-	New England Biolabs

IB = immunoblotting, IF = immunofluorescence staining

Secondary antibodies

Horseradish peroxidase conjugated goat anti-mouse, goat anti-rabbit and donkey anti-goat secondary antibodies were obtained from Dianova, Hamburg, Germany. All secondary antibodies were used in 1:10 000 dilution for the immunoblot analysis.

FITC-, Cy3- and Cy5-labelled secondary antibodies were obtained from Jackson Immunoresearch, West Grove, USA and used for immunofluorescence analysis in dilutions of 1:300.

6.1.4 Enzymes and recombinant proteins

- Long template polymerase
  Roche, Mannheim, Germany
- Phire Hot Start II DNA Polymerase
  ThermoScientific, Schwerte, Germany
- Pfu DNA Polymerase
  Stratagene, La Jolla, USA
- Quick T4 DNA Ligase
  New England Biolabs, Beverly, USA

- Recombinant Taq DNA polymerase
  GE Healthcare, Freiburg, Germany
- Restriction enzymes
  Fermentas, St. Leon-Rot, Germany
- Taq DNA Polymerase
  New England Biolabs, Beverly, USA

6.1.5 Standards and Kits

- BCA™ Protein Assay Kit
  ThermoScientific, Schwerte, Germany
- Expand Long Template PCR System
  Roche, Mannheim, Germany
- GeneJET Gel Extraction Kit
  ThermoScientific, Schwerte, Germany
- GeneRuler DNA Ladder Mix
  Fermentas, St. Leon-Rot, Germany
- ImmobilonTM WB detection kit
  Millipore, Billerica, USA
- NucleoBond PC 100 MidiPrep Kit
  Macherey-Nagel, Düren, Germany
- NucleoSpin Plasmid MiniPrep Kit
  Macherey-Nagel, Düren, Germany
- QIAquick Gel Extraction Kit
  Qiagen, Hilden, Germany
- Unstained Protein MW Marker
  Fermentas, St. Leon-Rot, Germany

6.1.6 Chemicals and special reagents

- Acetylcholine

- Albumine bovine fraction V
  Sigma, Taufkirchen, Germany
- Amylose resin
  New England Biolabs, Beverly, USA
- Benzonase® Nuclease
  Novagen®, Merck Millipore, Darmstadt, Germany
- Carbachol
- Collagenase A
  Roche
- D(+)-Maltose monohydrate
  Sigma, Taufkirchen, Germany
- Digitonin
  Sigma, Taufkirchen, Germany
- Dynabeads Sheep anti-Rat IgG
  Invitrogen, Karlsruhe, Germany
- GeneJuice ® Transfection Reagent
  Merck Millipore, Darmstadt, Germany
- GSH-Sepharose 4B
  GE Healthcare, Freiburg, Germany
- Ionomycin
- Midori Green DNA Stain
  NIPPON Genetics EUROPE GmbH Dueren, Germany
- Phast GelTM Blue R (Coomassie R 350 stain)
  GE Healthcare, Freiburg, Germany
- Protease inhibitor cocktail tablets
  Roche, Mannheim, Germany
- Protein A/G Plus Agarose
  Santa Cruz Biotechnology, Santa Cruz, USA
- Proteinase K
  Roth, Karlsruhe, Germany
- Ringer Solution
  B.Braun, Melsungen, Germany

Standard chemicals were obtained from Sigma (Taufkirchen, Germany), Fluka (Buchs, Schweiz) or Roth (Karlsruhe, Germany).

6.1.7 Buffers, solutions and gels

- Direct pulldown interaction buffer
  20 mM Tris-HCl pH 8.4
  150 mM NaCl
  2.5 mM $CaCl_2$
  1 mM DTT
  10 % (v/v) Glycerol
  1 % (v/v) Triton X-100

- 6X DNA loading buffer
  0.25 % (w/v) Bromophenol Blue
  0.25 % (w/v) Xylencyanol
  30 % (v/v) Glycerol

- Genotyping lysis buffer
  50 mM Tris-HCl pH 8.0
  50 mM EDTA
  100 µg/ml Proteinase K
  0.5 % (w/v) SDS

- Hot Coomassie Staining Solution
  Phast GelTM Blue R (Coomassie R 350 stain)
  GE Healthcare, Freiburg, Germany

- LB medium (Luria-Bertani medium)
  1 % (w/v) Tryptone
  0.5 % (w/v) Yeast extract
  1 % (w/v) NaCl

- Lung lysis buffer

  50 mM Tris-HCl pH 7.4

  150 mM NaCl

  2 mM EDTA

- MBP (Maltose binding protein) buffer

  20 mM Tris-HCl pH 7.4

  200 mM NaCl

  1 mM EDTA

  1 mM DTT

- Polyacrylamide gels
  - 4X stacking gel buffer

    0.5 M Tris-HCl pH 6.8

    4 % (w/v) SDS

  - 4X resolving gel buffer

    3 M Tris-HCl pH 8.9

    4 % (w/v) SDS
  - Polyacrylamide gel mixture

	Resolving gel	Stacking gel
Acrylamide 40% (w/v)	7.5%, 10% or 12,5%	4%
4x stacking gel buffer	-	1x
4x resolving gel buffer	1x	-
APS	4 mM	4 mM
TEMED	4 mM	4 mM
H_2O	Added to final volume	

- Ponceau S staining solution

  0.2 % (w/v) Ponceau S

  3 % (w/v) Trichloroacteic acid

- Protease and phosphatase inhibitors

  1 mM PMSF

  1 mM Na_3VO_4

  Protease Inhibitor Cocktail (Roche) according to the manufacturer's instructions

  25 mM NaF

  1mM β-Glycerophosphate

- 1X Protein sample buffer

  63 mM Tris-HCl pH 6.8 5

  % (w/v) glycerol

  5 % (w/v) β-mercaptoethanol

  0.005 % (w/v) bromophenol blue

  2.5 % (w/v) SDS

- 1X SDS electrophoresis buffer

  25 mM Tris

  95 mM Glycine

  0.5 % (w/v) SDS

- 1X TAE buffer

  40 mM Tris

  20 mM Acetic acid

  1 mM EDTA pH 8.0

- Wet-Western Blot transfer buffer

  25 mM Tris

  192 mM Glycine

  0.037 % (w/v) SDS

  20 % (v/v) Methanol

6.1.8 Cell culture media and supplements

- Coelenterazine h
  Invitrogen, Karlsruhe, Germany
- DMEM GlutaMAX-I with 4.5 mg/L D-Glucose
  Invitrogen, Karlsruhe, Germany
- Dulbecco´s modified Eagle´s medium (DMEM) with 4500 mg/L glucose, L-glutamine
  PAA Laboratories, Pasching, Austria
- Endothelial cell growth supplement/Heparin
  Promocell, Heidelberg, Germany
- F12 Medium
  Gibco®, Life Technologies GmbH, Darmstadt, Germany
- Fetal Bovine Serum (FBS) Gold
  PAA Laboratories, Pasching, Austria
- Glucose 40%
  B. Braun, Melsungen, Germany
- Hank´s balanced solt solution (HBSS)
  Invitrogen, Karlsruhe, Germany
- Leibovitz's L-15 Medium
  Gibco®, Life Technologies GmbH, Darmstadt, Germany
- Penicilin/Streptomycin
  PAA Laboratories, Pasching, Austria
- Puromycin
  Invitrogen, Karlsruhe, Germany
- Sodium pyruvate 100mM
  Sigma, Taufkirchen, Germany
- Trypsin/EDTA
  PAA Laboratories, Pasching, Austria

6.1.9 Consumables

- Cell Strainer 40 µm
  BD Falcon, Franklin Lakes, USA
- Filter paper
  Whatman, Dassel, Germany
- Fuji Medical x-ray film Super RX
  Fujifilm, Tokyo, Japan
- Histoacryl® Gewebekleber (n-Butyl-2-Cyanoacrylat)
  B. Braun, Melsungen, Germany
- Microscope cover glasses (15 mm diameter)
  Marienfeld Laboratory Glassware, Lauda-Königshofen, Germany
- Microscope slides
  Knittel Gläser, Braunschweig, Germany
- Microscope slides Superfrost® Plus
  ThermoScientific, Schwerte, Germany
- Protran nitrocellulose transfer membrane (pore size 0.2 µm)
  Whatman, Dassel, Germany

Cell culture dishes and flasks were obtained from Greiner, Frickenhausen, Germany and other plastic consumables either from the same company or from Sarstedt, Nümbrecht, Germany.

6.1.10 Equipment

Agarose gel analysis

Gel Doc 2000 (Quantity One software)	BioRad Laboratories Inc., Hercules, CA, USA

Centrifuges

Avanti™ J-E High-Performance Centrifuge	Beckmann Coulter, Krefeld, Germany

Eppendorf centrifuge 5417R	Eppendorf, Hamburg, Germany
Eppendorf centrifuge 5810R	Eppendorf, Hamburg, Germany
Heraeus Biofuge fresco	Heraeus, Hanau, Germany
Optima™ MAX Ultracentrifuge	Beckmann Coulter, Krefeld, Germany

Flow circuit

Pulse Dampener	Cole-Parmer-Instrument Co., Vernon Hills, IL, USA
Peristaltic pump P-1	Pharmacia LKB, Uppsala, Sweden

Parallel plate flow chamber

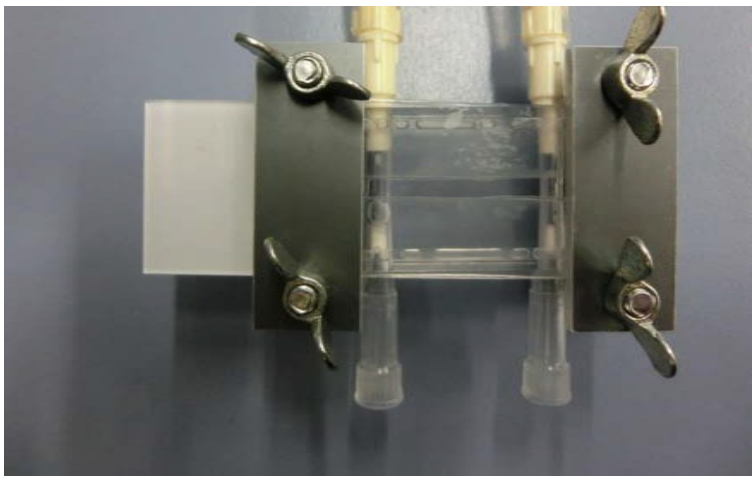

Figure 9 Parallel plate flow chamber , length x width x height = 5cm x 2.4cm x 1.2cm

Microscopes

Leica MZ165 dissecting microscope	Leica, Wetzlar, Germany
Leica Live Cell Imaging microscope	Leica, Wetzlar, Germany
Leica TCS SP5 confocal laser scanning microscope	Leica, Wetzlar, Germany

Immunoblot/SDS-PAGE

MiniProtean II electrophoresis system	BioRad Laboratories Inc., Hercules, CA, USA

PCR	
T Professional Thermocycler	Biometra, Göttingen, Germany
Photometric analysis	
Eppendorf BioPhotometer	Eppendorf, Hamburg, Germany
Wallac Victor3 1420 Multilabel Counter	Perkin Elmer, Fremont, USA
Nanodrop Spectrophotometer ND-100	PeqLab Biotechnologie GmbH, Erlangen, Germany
Others	
Dynal MPC-1 Magnetic particle concentrator	Invitrogen, Karlsruhe, Germany
Thermomixer Comfort	Eppendorf, Hamburg, Germany

6.1.11 NOSTRIN knockout mice

6.1.11.1 Global knockout (KO)

The NOSTRIN targeting vector construction and knockout mouse generation were carried out by genOway (www.genoway.com; Lyon, France). The targeting vector contained two loxP sites, one in the long homology region (6.0 kb, homologous to a sequence containing exons 3, 4 and 5) and a second one in the short homology region (2.0 kb, homologous to exon 6), and a neomycin resistance gene cassette for positive selection flanked by Frt sites. Homologous recombination after introduction of the linearized vector in 129sv/Pas embryonic

stem (ES) cells and neomycin selection resulted in generation of ES cell clones with a recombined NOSTRIN locus containing one loxP site between exon 3 and 4 and the Frt flanked neomycin resistance gene cassette followed by the second loxP-site between exons 5 and 6. ES cell clones containing the recombined NOSTRIN allele were used for injection into C57BL/6J blastocysts and generation of chimera. Male offspring of chimera with the recombined NOSTRIN allele were further mated with C57BL/6J Cre delete females to induce excision of the floxed sequence (exons 4 and 5) to generate the NOSTRIN knockout allele. The presence of the NOSTRIN knockout allele in the offspring was confirmed by Southern blotting and PCR. Heterozygeous NOSTRIN knockout mice were backcrossed into C57BL/6J mice for 6 generations.

6.1.11.2 Endothelial cell specific knockout (ECKO)

NOSTRIN endothelial specific knockout in mice is achieved by Cre-mediated excision of exons 4 and 5 of the NOSTRIN gene in endothelial cells. Two loxP sites and a neomycin resistance gene cassette were introduced by homologous recombination to generate the recombined NOSTRIN locus. Neomycin cassette was excised by crossing with Flp-recombinase-expressing deleter mice to generate NOSTRIN flox/flox control mice (CTL). CTL mice were further bred with Tie2-Cre mice in order to achieve the excision of the loxP-flanked sequence leading to deletion of the exons 4 and 5 in the NOSTRIN KO locus in endothelium.

6.2 Methods

6.2.1 Molecular biological methods

6.2.1.1 Agarose gel electrophoresis

DNA fragments were separated by electrophoresis on 1 or 2 % agarose gels according to their size. Gels were prepared using standard agarose and 1x TAE buffer. For DNA visualization, 1 µl Midori Green DNA Stain was added to the gels. Before loading, samples were mixed with 6x DNA loading buffer. Gels were run at 100 V for 20 – 30 minutes in 1x TAE buffer and finally examined under UV light (Gel Doc 2000, Quantity One).

6.2.1.2 Generation of PCR products

DNA fragments were amplified by polymerase chain reaction (PCR) using thermostable proofreading DNA polymerase Pfu (Stratagene, Fermentas). Primers for cloning were designed with overhangs in their 5' regions containing the appropriate sites for restriction enzymes. All primers that were used are listed under 6.1.1.

PCR mixture:

	Final concentration (reaction volume 50 µl)
10x Pfu reaction buffer	1x
dNTP mix	0,2 mM
Forward Primer	1 pM
Reverse Primer	1 pM
Template DNA	25 ng
Pfu Polymerase	2,5 U
ddH_2O	Added to final volume

PCR reaction settings:

	Temperature	Time
1. Initial denaturation	95°C	3 min
2. Denaturation	95°C	45 sec
3. Annealing	variable*	45 sec
4. Extension	72°C	variable*
5. Final extension	72°C	15 min
6. Cool down	10°C	unlimited

2-4: 35 cycles

* Annealing temperature was determined according to the melting temperature of primers (Tm-5°C) and extension time was calculated depending on the length of the DNA fragment to be amplified (2 minutes per kb of DNA).

The amplified DNA was separated by agarose gel electrophoresis and analysed under UV light. For further processing, fragments of the expected size were excised and extracted from the gel using the GeneJET Gel Extraction Kit according to the manufacturer's instructions. For cloning into the vector, the purified DNA fragment (insert) and the vector were digested with the appropriate restriction enzymes and subsequently ligated with Quick Ligase according to the manufacturer's instructions. Ligation products were then transformed into competent E.coli Mach1 cells using heat shock transformation for 1 min at 42°C and grown on LB-Agar plates containing the appropriate antibiotic overnight at 37°C for selection. On the next day, transformed colonies were picked and grown overnight in LB-Medium supplemented with the appropriate antibiotic at 37°C under vigorous shaking. Plasmid DNA was purified using the NucleoSpin Plasmid MiniPrep Kit according to the manufacturer's instructions. The presence of the amplified cloned fragment was confirmed by digestion with restriction enzymes and analysis of the restricted DNA by agarose gel electrophoresis and by DNA sequencing (Eurofins MWG Operon, Ebersberg, Germany).

6.2.2 Cell biological methods

6.2.2.1 Cell culture and transfection

U2OS cells were cultured in DMEM supplemented with 10% fetal bovine serum, 1 mM sodium pyruvate, 100 U/ml penicillin and 100 µl/ml streptomycin. The cells were grown at 37°C at 5% CO_2 containing air. After reaching confluency, the cells were passaged by trypsin digestion at regular intervals.
Transient transfection was performed with GeneJuice® according to the manufacturer's instructions.

6.2.2.2 Generation of stable cell lines

The genes of interest, mCherry-NOSTRIN, mCherry-NOSTRIN-Δ-SH3, GFP-M2 and GFP-M3, were cloned into the expression vector pIRESpuro2.
U2OS cells were seeded in 6-well-plates at a density of 300 000 cells per well. On the next day, they were transfected with the expression construct using GeneJuice® according to the manufacturer's instructions. After reaching confluency, cells were split into 10cm-dishes. 24 hours past transfection, selection with 0,5 ng/ml puromycin was started. Medium was changed daily in order to remove dead cells and cell debris. After completion of the selection process, expression was confirmed by immunofluorescence and western blot analysis.

6.2.2.3 Immunofluorescence staining and microscopy

U2OS cells were grown on glass coverslips and transfected with expression vectors for the M3R, NOSTRIN, NOSTRIN-Δ-SH3. 24 hours post-transfection, cells were washed with PBS, fixed with 4% paraformaldehyde in PBS solution for 30 minutes, washed with PBS and permeabilized with 50 µg/ml Digitonin in PBS for 15 minutes. After another washing step with PBS, the cells were blocked with 1% BSA in PBS for 30 minutes and then incubated with the

primary antibodies in 1% BSA in PBS for 30 minutes in a humidity chamber. After washing with 0,1 % BSA in PBS, cells were incubated with Cy3-, Cy5- and FITC-conjugated secondary antibodies and DAPI in 1% BSA in PBS for 30 minutes in a humidity chamber. After further washing with 0,1% BSA in PBS, the coverslips were mounted in Moviol supplemented with DABCO. All steps were carried out at room temperature.
Fluorescent images were acquired using a Leica TCS SP5 confocal microscope and edited using ImageJ software.

6.2.2.4 Aequorin-based calcium assay

The Aequorin-based calcium assay was performed according to Preuß B. et al., Clin Exp Immunol, 2014[97]. In detail, CHO cells stably transfected with Aequorin-GFP (CHO/G5A) were grown in Ham's F12 Medium supplemented with 10% FBS, 1% penicillin/streptomycin and 300 µg/ml G418 sulphate. Confluent cells were split and dispensed at a density of 10 000 cells per well of a 96-well-plate in a volume of 100 µl. For luminometry measurements, 96-well-plates with white walls and clear bottom were used.
24 hours after seeding, cells were co-transfected with plasmid containing M3 receptor DNA and either NOSTRIN or NOSTRIN- Δ-F-BAR or mCherry using GeneJuice® according to the manufacturer's instructions. The functional assay was performed 48 hours post-transfection. In order to load the cells with coelenterazine h, growth medium was replaced by Hank's Balanced Salt Solution, containing 10 mM glucose, 1,8 mM $CaCl_2$ and 5 µM coelenterazine h and incubated for 2 hours at 37 °C in a room air incubator. Subsequently, cells were transferred to the measuring device (Wallac Victor3 1420 Multilabel Counter), stimulated with 100 µM carbachol, and fluorescence intensity at a wavelength of λmax = 470 nm was recorded over a time period of 2 min.

6.2.3 Protein biochemical methods

6.2.3.1 Purification of GST fusion proteins

In order to produce glutathione-S-transferase (GST) fusion proteins, Escherichia coli BL21 (DE3) cells were transformed with one of the following constructs: pGEX-2T1-NOSTRIN, pGEX-2T1-NOSTRINΔSH3 (aa1-440) and pGEX-2T1-NOSTRIN-SH3 (aa 433-506).

Bacterial cells were transformed with 20 ng of the appropriate plasmid by chemical transformation and a starter culture of 5 ml LB medium with 100 µg/ml ampicillin (LB/ampicillin) was grown overnight at 37°C. On the following day, the overnight culture was diluted 100 fold with LB/ampicillin and grown at 37°C to an OD600 of 0.4-0.6. Induction of GST-fusion proteins followed after addition of 0.25 mM isopropyl-β-D-1-thiogalactopyranoside (IPTG) and bacteria were grown either overnight at 16°C or for 3 hours at 30°C. After adequate expression time, bacterial cells were harvested by centrifugation at 3500 g at 4°C for 20 minutes. The bacterial pellet was resuspended in 5 ml ice cold PBS (supplemented with protease and phosphatase inhibitors listed under 6.1.7). Bacterial cell walls were disrupted by sonication for 5 times 10 seconds each with breaks of 1 minute in between. After that, Triton-X100 was added to a final concentration of 1 % and the bacterial cell suspension was incubated under gentle rotation at 4°C for 30 min. To obtain the clear bacterial lysate, the bacterial cell suspension was centrifuged at 14 000 g at 4°C for 15 minutes. At the same time, Glutathione (GSH) sepharose beads were prepared by washing of the appropriate volume of GSH-sepharose slurry three times with ice cold PBS. Cleared bacterial lysate was incubated with prewashed beads for 1 hour at 4°C under gentle rotation, centrifuged and washed extensively three times with ice cold lysis buffer and three times with PBS. Washed beads were resuspended in PBS supplemented with 0.1 % (w/v) sodium azide and stored at 4°C.

6.2.3.2 Purification of MBP fusion proteins

In order to prepare the Maltose-Binding Protein (MBP) fusion protein, Escherichia coli BL21 (DE3) cells were transformed with MBP-Loop.
Bacterial cells were transformed with 20 ng of the appropriate plasmid by chemical transformation and a starter culture of 5 ml LB medium with 100 µg/ml ampicillin (LB/ampicillin) was grown overnight at 37°C. On the next day, 400 ml of LB/ampicillin was added to the overnight culture and grown to an OD600 of 0.4 at 37°C with vigorous shaking. Induction of MBP-fusion proteins followed after addition of 0.5 mM isopropyl-β-D-1-thiogalactopyranoside (IPTG). At the same time, 2% (w/v) glucose was added to repress the maltose genes on the E.coli chromosome, which include an amylase that can degrade the amylose on the affinity resin. Bacteria were grown either overnight at 16°C or for 4-6 hours at 37°C. After adequate expression time, bacterial cells were harvested by centrifugation at 3500 g at 4°C for 20 minutes. The bacterial pellet was resuspended in 8 ml MBP buffer supplemented with 1 mM PMSF and 0.1 % (w/v) β−mercaptoethanol. Bacterial cell walls were disrupted by sonication for 5 times 10 seconds each with breaks of 1 minute in between. After that, Triton-X100 was added to a final concentration of 0.5 % (w/v). To obtain the clear bacterial lysate, the bacterial cell suspension was centrifuged at 10 000 g at 4°C for 20 minutes. At the same time, amylose resin was prepared by washing it three times with ice cold PBS. Cleared bacterial lysate was incubated with prewashed amylose resin for 1 – 2 hours at 4°C under gentle rotation, centrifuged and washed three times with MBP buffer supplemented with 1 mM PMSF and 0.1 % β−mercaptoethanol. Washed beads were resuspended in MBP buffer supplemented with 0.1 % (w/v) β−mercaptoethanol and 0.1 % (w/v) sodium azide. To elute the proteins from the amylose resin, they were incubated with 10 mM maltose for 30 minutes. After centrifugation, the supernatant as well as the beads in MBP buffer were stored at 4 °C.

6.2.3.3 Purification of His-tagged proteins

(His)6-tagged Sos was purified from E. coli BL21 using a Ni-NTA matrix (Qiagen) according to the manufacturer's instructions.

6.2.3.4 GST pulldown

For the pulldown experiments, lysates from of GFP-M3 U2OS cells or mouse lung lysates were used. Lysates were prepared using lysis buffer and incubated overnight at 4°C with GSH-Sepharose beads coupled with equal amounts of GST-tagged NOSTRIN or GST–NOSTRIN-Δ-SH3 or GST-NOSTRIN-SH3. Subsequently, beads were centrifuged 3 min, 800 g and washed three times with lysis buffer. Afterwards, beads were boiled in protein sample buffer and bound proteins were resolved by SDS-PAGE followed by immunoblotting (see 6.2.3.5).

For the direct protein interaction studies of NOSTRIN with the 3rd intracellular loop of M3 or with Sos respectively, purified proteins added to the GST-fusion proteins coupled to Sepharose beads. Proteins were incubated for 1 hour at 4°C in direct pulldown incubation buffer (supplemented with protease and phosphatase inhibitors listed under 6.1.7). Subsequently, Sepharose beads were washed three times with direct pulldown incubation buffer and two times with PBS. Bound proteins were further analysed by SDS-PAGE and immunoblotting (see 6.2.3.5).

6.2.3.5 SDS-PAGE and immunoblotting

SDS polyacrylamide gel electrophoresis (SDS-PAGE) was used to electrophoretically separate proteins according to their molecular weight and was carried out in vertical gels using the BioRad Miniprotean II electrophoresis system and the buffers listed under 6.1.7. Separated proteins were either stained with Hot Coomassie Staining solution or electrophoretically transferred

from the gel to a nitrocellulose membrane using the Bio-Rad Wet/Tank blotting unit. Prior to immunoblotting, protein transfer was confirmed by staining the nitrocellulose membrane with Ponceau S staining solution. After short destaining with PBS, the membrane was blocked in 5 % (w/v) BSA/PBS for 1 hour at room temperature, followed by further incubation with the primary antibody, diluted in 5 % (w/v) BSA/PBS at 4°C overnight. After subsequent three rinses with PBS, the membrane was incubated with HRP-coupled secondary antibody for 45 minutes at room temperature and again washed three times with PBS. To detect the HRP signal, ImmobilionTM WB detection reagent from Millipore was used.

6.2.4 Experimental work with animal models

6.2.4.1 Genotyping of transgenic NOSTRIN mice

Genotyping was carried out on 0.5 cm tail biopsies from three weeks old mice. Tail biopsies were lysed in the genotyping lysis buffer at 55°C overnight with constant shaking. Tissue and cell debris were removed by 30 min centrifugation at 14000 g 4°C and genomic DNA was precipitated from supernatant using 50 % (v/v) isopropanol. The pellet was washed with 70 % (v/v) ethanol and isolated DNA was diluted in 300 µl of water. 0,5 µl of DNA solution was used for the genotyping procedure. Genotyping was performed using the indicated primers (sequences are listed under 6.1.1) and the indicated DNA polymerases, according to the manufacturer´s instructions. The reaction was set according to the following schemes:

<u>Global NOSTRIN KO:</u>

1.) Primers: Hom28 (forward primer), Flp11 (reversed primer)
DNA-Polymerase: Long template DNA polymerase

	Temperature	Time
1. Initial denaturation	94°C	5 min
2. Denaturation	94°C	1 min

3. Annealing	64°C	1 min
4. Extension	68°C	4 min
5. Final extension	68°C	7 min
6. Cool down	10°C	unlimited

2 – 4: 40x

2.) Primers: FW2 (forward primer), REV2 (reversed primer)
DNA-Polymerase: Phire DNA Polymerase

	Temperature	Time
1. Initial denaturation	95°C	4 min
2. Denaturation	95°C	30 sec
3. Annealing	64°C	30 sec
4. Extension	72°C	2 min
5. Final extension	72°C	7 min
6. Cool down	4°C	unlimited

2 – 4: 40x

NOSTRIN EC KO

1.) Primers: Flp10 (forward primer), Flp11 (reversed primer)
DNA-Polymerase: Phire DNA Polymerase

	Temperature	Time
1. Initial denaturation	95°C	5 min
2. Denaturation	95°C	1 min
3. Annealing	58°C	1 min
4. Extension	72°C	4 min
5. Final extension	72°C	7 min
6. Cool down	10°C	unlimited

2 – 4: 40x

2.) Primers: FW2 (forward primer), REV2 (reversed primer)
DNA-Polymerase: GoTaq DNA Polymerase

	Temperature	Time
1. Initial denaturation	95°C	3 min
2. Denaturation	94°C	30 sec
3. Annealing	51,7°C	25 sec
4. Extension	72°C	1 min
5. Final extension	72°C	2 min
6. Cool down	10°C	unlimited

2 – 4: 35x

6.2.4.2 Aorta whole-mount staining and microscopy

Male mice at the age of 8 – 10 weeks were anesthesized with isoflurane and sacrificed by decapitation. The thoracic aorta was removed and trimmed of fat and excess tissue in cold PBS. The isolated aorta was cut into 4 stripes and transferred into a 12-well-plate (2 stripes per well) for the staining procedure. The pieces of aorta were fixed with 4% paraformaldehyde in PBS for 10 minutes at 4°C, permeabilized in 0,3 % Triton-X in PBS for 30 minutes at room temperature and blocked in 5% BSA in PBS for 1 hour at room temperature. The pieces of aorta were then incubated with primary antibodies overnight at 4°C with gentle shaking.

After washing with PBS, they were incubated with Cy3-, Cy5- and FITC-conjugated secondary antibodies and DAPI. For actin-staining AlexaFluor-conjugated phalloidin was used. After further washing steps, the aorta segments were mounted in 50% Glycerol in PBS.

Fluorescent images were acquired using a Leica TCS SP5 confocal microscope and edited using ImageJ software.

6.2.4.3 Generation of mouse lung lysates

Male mice at the age of 8 – 10 weeks were sacrificed by decapitation and perfused with Ringer solution in order to remove the blood from the tissue. Lungs were isolated and directly frozen in liquid nitrogen. In order to prepare lysates, frozen lungs were pulverised using mortar and pestle. The powder was then transferred into a reaction tube containing 2 ml of lung lysis buffer and sonicated for 10 seconds. After sonication, Digitonin was added to a final concentration of 0,5% and the lysate was incubated with 0,5% Digitonin and Benzonase according to the manufacturer's instructions for 30 minutes at 4°C under rotation. Subsequently, the lysate was centrifuged in the ultra centrifuge at 25 000 g and 4°C for 30 minutes. Finally, the total protein concentration of the sample was quantified by using the BCA™ Protein Assay. Equal amounts of lysates were boiled with protein sample buffer and used for immunoblot analysis.

6.2.4.4 Isolation of primary mouse lung endothelial cells (MLEC)

In order to obtain mouse lung endothelial cells (MLEC), young mice (P4-P8) were anesthetized with isoflurane and sacrificed by decapitation. Lungs were isolated and placed into dissection buffer (10 % fetal calf serum, 100 U/ml penicillin and 100 µg/ml streptomycin in Hank´s balanced salt solution). After removing excessive connective tissue, the lungs were finely chopped using scissors. Pieces of lung tissue were further digested with Collagenase A for 30-45 minutes at 37°C. After collagenase digestion, the resulting cell suspension was passaged through a disposable 40 µm cell
strainer and centrifuged at 200 g for 5 min. The cell pellet was washed twice with dissection buffer and subsequently incubated with 500 ng/ml of PECAM-1-specific antibody coupled to anti-rat-IgG-coated magnetic beads for 1 hour at 4°C. After incubation, the cells coupled to the magnetic beads were separated from the rest of the suspension using a Dynal MPC-1 Magnetic particle concentrator. The cells coupled to the magnetic beads were washed six times,

resuspended in endothelial cell medium (DMEM GlutaMAX-I, 20 % FBS, 100 U/ml penicillin, 100 µg/l streptomycin and endothelial cell growth supplement) and seeded on gelatine coated cell culture dishes. Cell culture dishes were coated with solution of 1 % (w/v) gelatine in PBS. Primary MLECs were kept until passage two and used for immunofluorescence staining.

6.2.4.5 Aorta stimulation and lysis

Male mice at the age of 8 – 10 weeks were anesthetized with isoflurane and sacrificed by decapitation. The thoracic aorta was removed and trimmed of fat and excess tissue in Leibovitz's media prewarmed to 37°C. The isolated aorta was cut into 4 stripes and transferred into a 12-well-plate (2 stripes per well) for the stimulation.

The aortae were stimulated for 5 min with 10 µM Acetylcholine, 100 µM Carbachol or 1 µM Ionomycin at 37 °C in Leibovitz's media. Immediately after the stimulation, the pieces of aortae were frozen in liquid nitrogen, pulverized with a small mortar and boiled in 80 µl 2x protein sample buffer. After cooling, 20 µl 2x protein sample buffer supplemented with Benzonase® Nuclease was added according to the manufacturer's instructions and incubated for 5 min.

Subsequently, the activating phosphorylation of eNOS at Ser1179 in response to the different stimuli was analyzed by imunoblot.

6.2.4.6 Flow chamber

A Flow circuit consisting of a reservoir for media, a pump and a pulse dampener, all interconnected with tubes, was assembled according to[98] Instead of the described parallel-plate flow chamber, an chamber has been modified according to our needs: The chamber was covered with a Superfrost® Plus microscope slide on which the aorta can be fixed. A 3 mm wide channel was cut in silicone sheets and placed between the chamber and the microscope slide. Small screw clamps were used to fix the slide on the chamber.

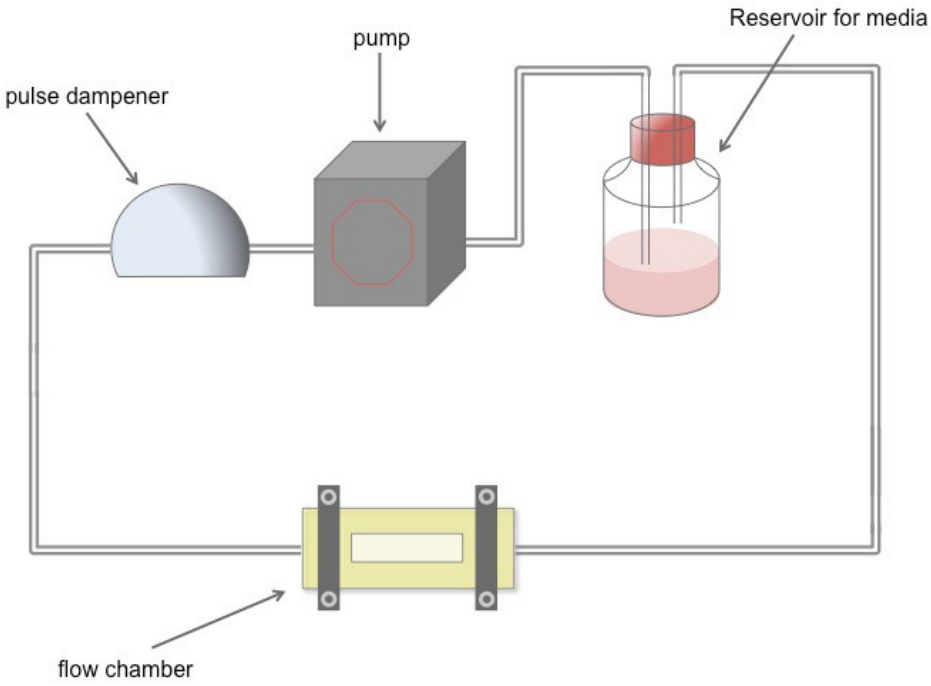

Figure 10 Assembly of the flow circuit modified after[98] For detailed description please refer to text.

Before starting the experiment, the flow circuit was assembled and flushed first with ethanol, then with sterile water.

The aorta was isolated and prepared in Leibovitz's medium supplemented with 10 % FBS and 2% penicillin/streptomycin prewarmed to 37°C. It was cut longitudinally and in 2 pieces. Both pieces of the aorta were fixed on a Superfrost® Plus microscope slide using Histoacryl®, one of the pieces in the physiological direction of the blood flow and one piece perpendicular to it. The slide was then fixed on the chamber and the aortae were exposed to laminar flow of about 5 dynes/cm² for 24 hours. During the experiment, the flow circuit was kept at 37°C.
After the experiment, the aorta was stained as described under 6.2.4.2.

7 Results

7.1 Detailed analysis of the ACh/eNOS signaling axis in the aorta

7.1.1 Loss of NOSTRIN has no influence on protein levels of the M3R

Given that the impaired relaxation of aortic rings from NOSTRIN KO and ECKO mice was restricted to those stimulated with ACh, the hypothesis was derived that the loss of NOSTRIN might directly affect the function of the endothelial acetylcholine receptor M3R. To exclude that the presence or absence of NOSTRIN affects the expression of the M3R, lung lysates from NOSTRIN KO, WT and ECKO and CTL mice were prepared using lysis buffer containing Digitonin and Benzonase. Lung lysates were then used to compare the expression levels of the M3R and eNOS by Immunoblot analysis. PECAM-1 was used as loading control. As shown in Fig. 11, there were no differences in protein expression levels of the M3R. This indicated that the loss of NOSTRIN did not influence the M3R protein levels, as it is the case for eNOS, shown in previous experiments[94]..

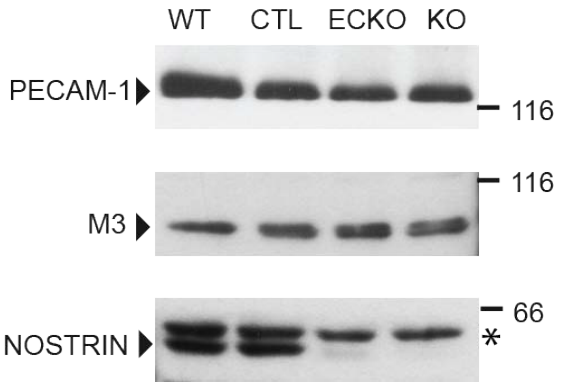

Figure 11 M3R expression levels are not affected by the loss of NOSTRIN. Immunoblot of lung lysates with M3R or NOSTRIN-specific antibodies. NOSTRIN (58 kDa) is present in equal amounts in WT and CTL mice, whereas its expression is abolished in the complete KO and significantly reduced in ECKO mice. Protein levels of M3R are comparable in NOSTRIN KO compared to WT and NOSTRIN ECKO compared to control mice. Immunoblot with PECAM-1-specific antibody was used as loading control. The asterisk in the lower panel indicates an unspecific band detected with the NOSTRIN antibody.

7.1.2 NOSTRIN is needed for the correct spatial localization of the M3R at the plasma membrane of murine aortic ECs

Spatial localization of effector proteins is crucial for signaling events. To determine if NOSTRIN influences the spatial localization of the M3R in aortic endothelial cells, aortae from NOSTRIN KO and WT mice as well as from NOSTRIN ECKO and CTL mice were isolated, stained in *en face* immunofluorescence with a M3R-specific antibody and visualized using confocal microscopy.

In WT and CTL aortae, the M3R is mainly found at the plasma membrane at endothelial cell-cell-contacts. In NOSTRIN KO and ECKO aortae however, this subcellular localization was lost and the M3R staining was restricted to intracellular punctae (Fig. 12).

This finding implies that NOSTRIN is required for the proper subcellular localization of the M3R and targets the receptor to the plasma membrane.

7.1.3 NOSTRIN facilitates the carbachol-induced calcium response in mammalian cells expressing the M3R

Calcium is an important link between the M3R and eNOS activation: The M3R is coupled to G-proteins of the $G\alpha_{q/11}$ family, and in response to ligand binding, it activates phospholipase Cβ leading to the mobilization of intracellular Ca^{2+}. At the same time, an increase in intracellular calcium levels is a major stimulus leading to activation of eNOS[75,83]

In order to test if NOSTRIN affects M3R receptor activation and the ACh-induced Ca^{2+} signal, CHO cells stably expressing GFP-Aequorin were used as a test system[96]. Aequorin is a calcium sensor protein. Upon binding of calcium ions, it converts its prosthetic group, coelenterazine, into excited coelenteramide and CO_2. When the excited group relaxes to the ground state, blue light is emitted, which can then excite GFP. The GFP signal is proportional to the increase in intracellular Ca^{2+} and can be measured luminometrically as

read-out for the increase in intracellular calcium levels and consequently for receptor activation[99].

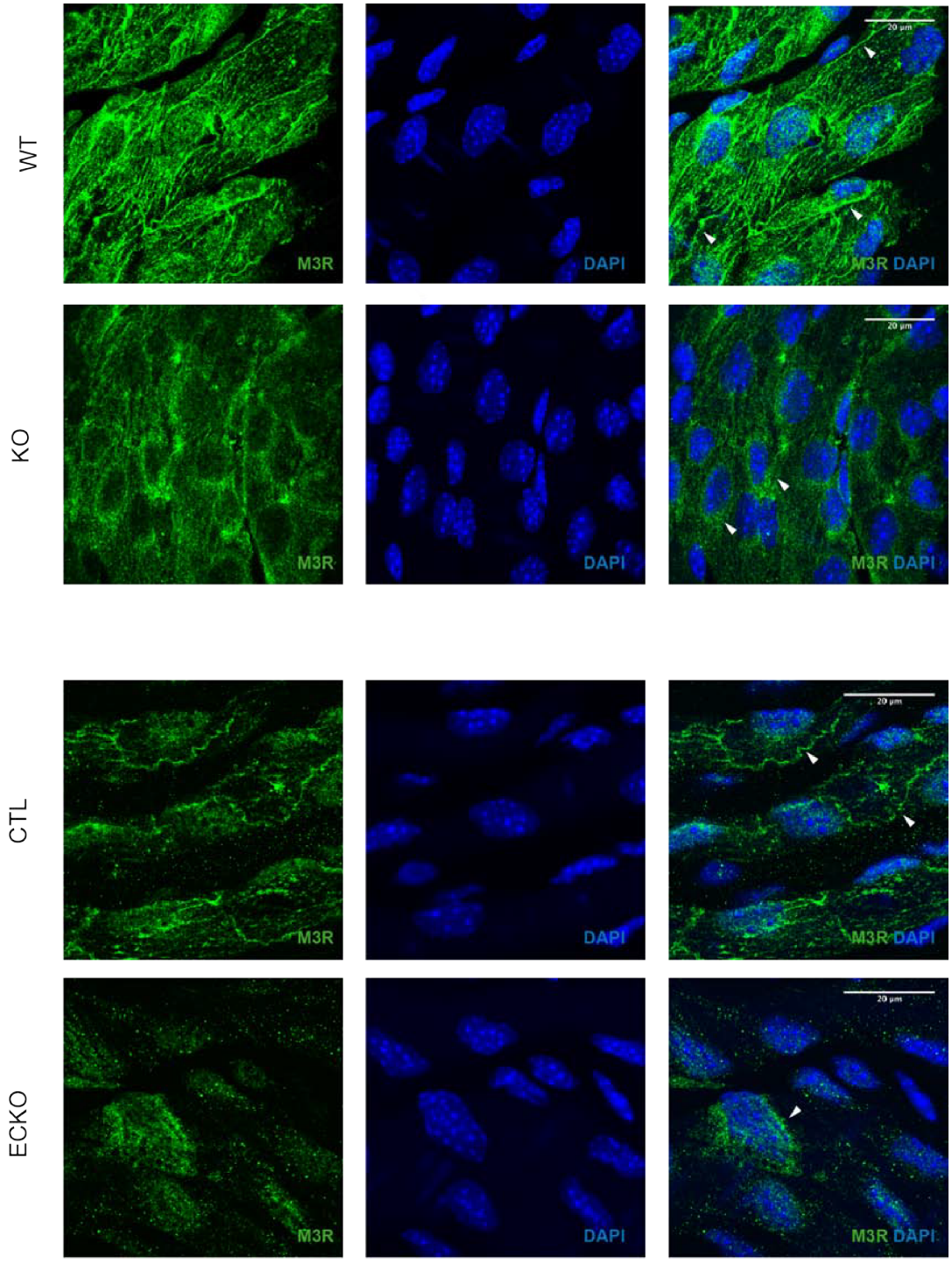

Figure 12 NOSTRIN is necessary for the correct subcellular localization of the M3R in aortic EC. Confocal immunofluorescence microscopy images of *en face* stained aorta explants from mice of the indicated genotype using an M3R-specific antibody in combination with DAPI. Arrowheads point to M3R-specific staining at the plasma membrane in WT and CTL aortae or to intracellular punctae in KO and ECKO aortae. Scale bar 20 µm.

For this assay, CHO/G5A cells were transfected with the M3R and either full size NOSTRIN or a NOSTRIN mutant lacking the F-BAR domain (NOSTRIN-Δ-F-BAR) or mCherry as a control and the intensity of the GFP signal was recorded over time after stimulation with the M3R agonist carbachol. Measurements were performed in quintuplets, the area under the curve (AUC) was calculated and normalized to the mCherry-expressing control condition.

After the application of carbachol, cells expressing the M3R and full length NOSTRIN responded with a strong increase in the GFP signal whereas the carbachol-induced GFP signal was repressed in cells that expressed the M3R in combination with the NOSTRIN-Δ-F-BAR mutant or mCherry (Fig. 13A), suggesting that NOSTRIN facilitates the increase in intracellular calcium after stimulation with the M3R agonist carbachol and that this depends on the NOSTRIN F-BAR domain. However in this experimental set-up the measurements lacked the desired reproducibility, with the consequence that differences measured over three independent experiments were not significantly different (Fig. 13B). Therefore this experiment provided a first indication for a role of NOSTRIN in facilitating the carbachol-induced calcium response in M3R-expressing cells. This was confirmed independently of this study as is discussed in section 8.5.

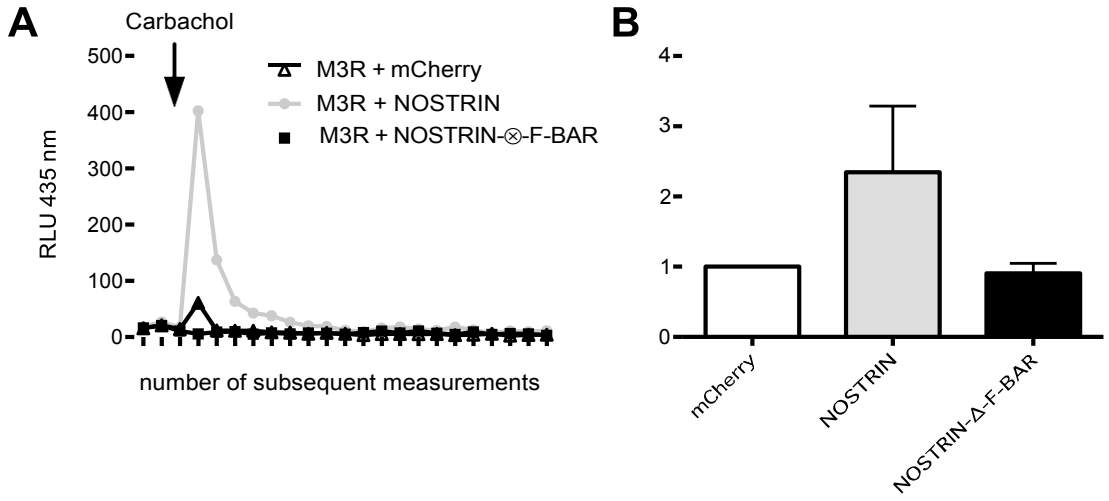

Figure 13 Carbachol-induced calcium-response of CHO/G5A cells transfected with M3R in combination with either mCherry, full size NOSTRIN or NOSTRIN-Δ-F-BAR.**. A Time course of GFP intensity after addition of carbachol** (100µM) in cells transfected as indicated. Single experiment measured in quintuplets. **B** Comparison of the AUC of GFP intensity over time as determined in A and normalized to the mCherry-expressing control condition in three independent experiments (n=3); $p > 0.05$, determined with **two tailed wilcoxon matched pair test** using Graph Pad Prism software. These experiments provide an indication for a role of NOSTRIN in facilitating M3R-dependent signal transduction.

7.1.4 Translocation of eNOS to the Golgi apparatus is decreased in NOSTRIN KO and ECKO aortic endothelial cells

eNOS activation goes along with its translocation to the Golgi complex. NOSTRIN was originally described as a regulator of eNOS subcellular localization in CHO-eNOS cells, facilitating its internalization by interacting with caveolin-1, the large GTPase dynamin and N-WASP[27].

To investigate if endogenous NOSTRIN influences the subcellular localization of eNOS in aortic ECs, aortae from NOSTRIN KO and ECKO mice and their respective controls were isolated and stained for eNOS and the Golgi marker Giantin and fluorescence was visualized by confocal microscopy. Subsequently, the eNOS fraction associated with the Golgi apparatus was quantified and compared between NOSTRIN KO and WT, as well as ECKO and CTL aortae.

A significant reduction of the eNOS positive Golgi area was detected in aortae of NOSTRIN KO and ECKO mice compared to their respective controls (Fig. 14).

In accordance with previous data, this finding implicates that NOSTRIN determines eNOS subcellular localization in aortic ECs. The reduced fraction of eNOS associated with the Golgi complex in KO and ECKO is consistent with an impaired activation of eNOS in the absence of NOSTRIN.

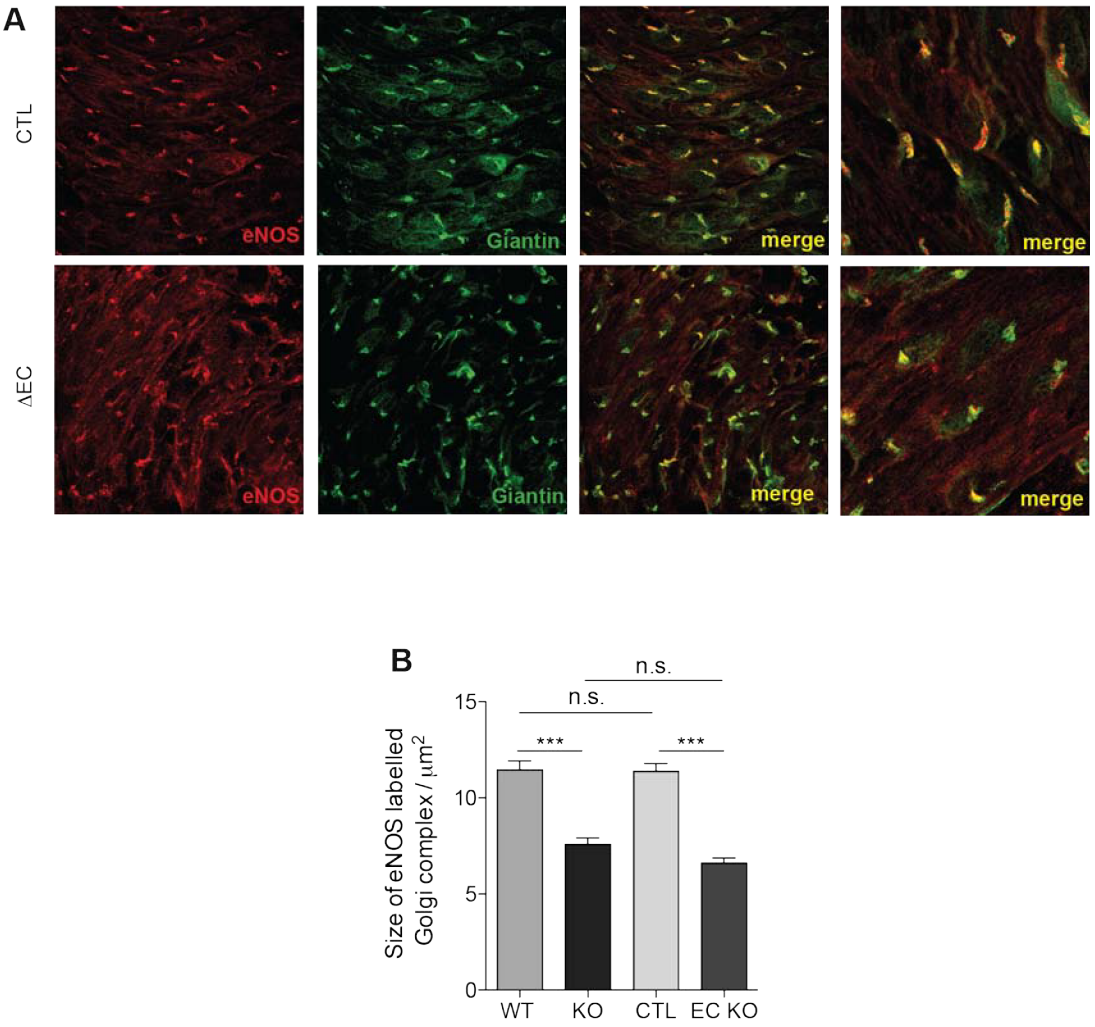

Figure 14 Reduction of the eNOS-positive Golgi area in the aortic endothelium in the absence of NOSTRIN. A Aorta whole-mount staining for eNOS, Giantin and DAPI. **B** Quantification of eNOS-labeled Golgi complexes in NOSTRIN KO and ECKO aortae and their respective controls. Comparison of the size of eNOS labelled Golgi complexes in ≥ 60 ECs (n ≥ 60); p<0,05, determined with 1way ANOVA test in combination with Bonferroni's Multiple Comparison post test using Graph Pad Prism software. The fraction of eNOS associated with the Golgi apparatus is significantly decreased in the aortic endothelium of NOSTRIN KO and ECKO mice. (*** indicates p<0.05; n.s. not significant)

7.1.5 Activation of eNOS in MLECs is impaired in the absence of NOSTRIN

Activation of eNOS is accompanied not only by its internalization and translocation to the Golgi complex, but also by its phosphorylation at activating residues. Phosphorylation at Ser1177 in humans or Ser1179 in mice is the most thoroughly studied activating phosphorylation of eNOS[75]. As the translocation of eNOS to the Golgi complex was reduced in the absence of NOSTRIN, it was

subsequently studied if NOSTRIN influences also the activating phosphorylation of eNOS.

To study the activation of eNOS in response to stimulation with the M3R-agonist carbachol, primary mouse lung endothelial cells (MLEC) were isolated. NOSTRIN KO and WT MLEC of passage 2 were kept under serum-starvation for 6 hours and were afterwards stimulated with 10 µM carbachol for 5 minutes. Cells were fixed, permeabilized and subsequently stained for phospho-Ser1179 eNOS and DAPI and visualized by confocal microscopy.

Starved, non-stimulated MLEC showed a very weak phospho-eNOS signal both in KO and WT MLEC (Fig. 15). After stimulation with carbachol, WT MLEC showed a strong pSer1179-eNOS signal with the strongest intensity at the Golgi apparatus. In contrast in NOSTRIN KO MLEC, the pSer1179-eNOS signal was not enhanced after stimulation with carbachol and there was no staining at the Golgi apparatus (Fig. 15), indicating that NOSTRIN is needed to mediate the activation of eNOS in response to stimulation with the M3R agonist carbachol.

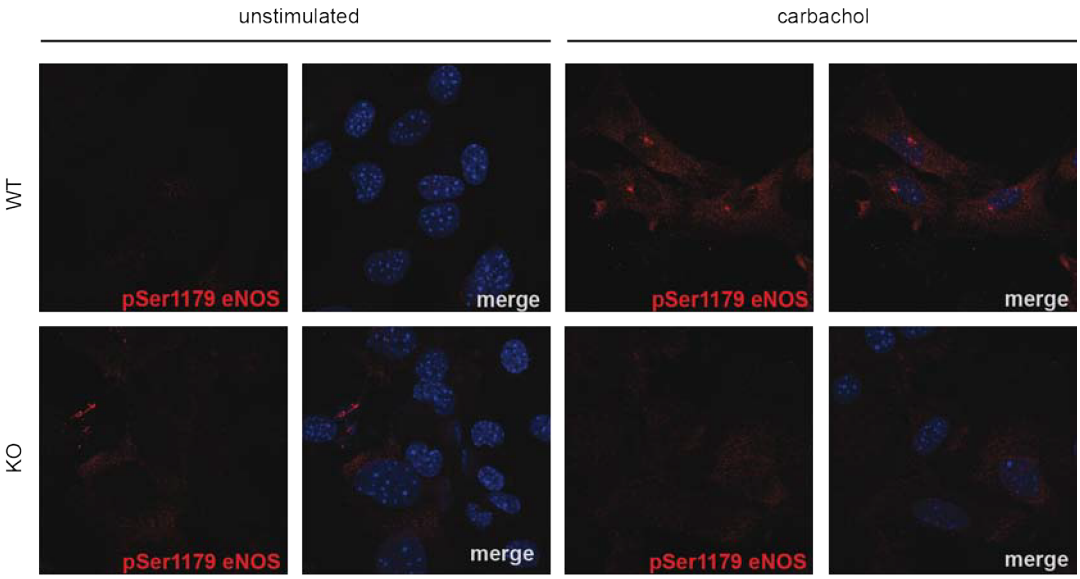

Figure 15 Carbachol fails to activate eNOS in the absence of NOSTRIN. Immunofluorescence staining for pSer1179 eNOS and DAPI in WT and NOSTRIN KO MLEC, after serum starvation (unstimulated) and stimulation with the M3R-agonist carbachol (100µM). Unstimulated WT and KO MLEC show a very weak pSer1179-eNOS staining. Upon stimulation with carbachol, the signal enhances in WT MLEC with the strongest signal at the Golgi apparatus. This activation cannot be detected in NOSTRIN KO MLEC.

7.1.6 NOSTRIN knockout inhibits the Carbachol-induced eNOS phosphorylation in murine aortae

Upon activation, eNOS gets rapidly phosphorylated. To further support the observation that NOSTRIN is needed to mediate the activation of eNOS after stimulation with carbachol, phosphorylation of eNOS at Ser1179 in response to different stimuli was studied in mouse aorta *ex vivo*. For this purpose, aortae from NOSTRIN ECKO and control mice were isolated and stimulated for 5 minutes with ACh, the M3R-agonist carbachol or the calcium ionophore ionomycin. Immediately after the stimulation, the aortae were frozen in liquid nitrogen and further processed for immunoblotting with an eNOS-pSer1179-specific antibody.

In the non-stimulated condition phosphorylation of eNOS at Ser1179 was more pronounced in CTL than in ECKO aortae (Fig. 16). Stimulation with ACh induced a strong phosphorylation in CTL aortae and to a lesser extent in ECKO. The M3R-agonist carbachol induced a phosphorylation of eNOS in CTL but failed to induce phosphorylation of eNOS in NOSTRIN ECKO aortae. Ionomycin induced phosphorylation in both CTL and in ECKO aortae (Fig. 16).

These data indicate that NOSTRIN is involved in the M3R/eNOS signaling axis, as the ACh- as well as the carbachol-induced eNOS phosphorylation were reduced in the absence of NOSTRIN.

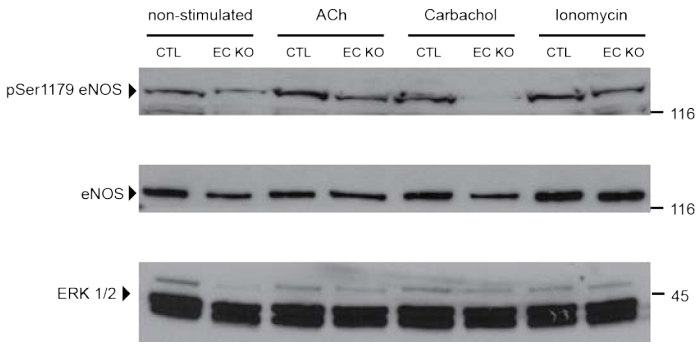

Figure 16 Phosphorylation of eNOS after stimulation of isolated aortae with ACh, carbachol and ionomycin. Aortae of NOSTRIN ECKO and CTL mice were stimulated with ACh (10µM), carbachol (100µM), or ionomycin (1µM) for 5 min. After stimulation, the phosphorylation of eNOS at Ser1179 was analyzed by immunoblot with a pSer1179eNOS-specific antibody. Immunoblotting with eNOS and ERK1/2-specific antibodies, respectively, served as loading controls. In the absence of NOSTRIN the basal as well as ACh- and carbachol-induced eNOS phosphorylation was reduced

7.2 Interaction analysis of the M3R and NOSTRIN

7.2.1 NOSTRIN interacts with M3R-GFP in mammalian cells

Given the influence of NOSTRIN on the ACh/eNOS signaling axis and the altered spatial localization of the M3R in the absence of NOSTRIN, the hypothesis was derived that NOSTRIN might interact with the M3R.

To study if NOSTRIN interacts with the M3R, GST pulldown experiments were performed. For this purpose, different GST-NOSTRIN constructs were used: full length NOSTRIN (GST-NOSTRIN), a mutant where the SH3 domain is deleted (GST-NOSTRIN-ΔSH3; amino acids 1-440) and the isolated SH3 domain (GST-SH3; amino acids 433-506). These GST-NOSTRIN fusion proteins and GST alone were recombinantly expressed in and purified from E-coli BL21.

The M3R was cloned into the pEGFP vector and expressed in U2OS cells as a M3R-GFP fusion protein. Cell lysates were prepared and equal amounts of the lysate were added to the purified GST-tagged proteins coupled to GSH-Sepharose beads. The interaction was analyzed by immunoblot.

GST-NOSTRIN interacted with M3R-GFP expressed in U2OS cells (Fig. 17). The interaction involved the SH3 domain of NOSTRIN, as the GST-NOSTRIN-ΔSH3 mutant failed to interact with the M3R. The SH3 domain alone was not sufficient for binding to the M3R (Fig. 17), indicating that additional motifs in NOSTRIN might be required to mediate the interaction.

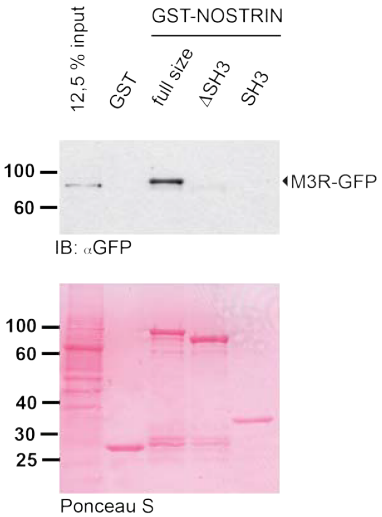

Figure 17 NOSTRIN interacts with M3-GFP in mammalian cells. GST pulldown from U2OS cells expressing M3R-GFP with indicated GST fusion proteins, followed by immunoblotting with a GFP-specific antibody (top). Ponceau S-stained blotting membrane to visualize equal input of GST fusion proteins (bottom). GST-NOSTRIN interacts with the M3R. The interaction requires the SH3 domain of NOSTRIN. However, the SH3 domain alone is not sufficient to mediate the interaction.

7.2.2 NOSTRIN interacts with endogenous M3R in mouse lung lysates

In order to study if NOSTRIN interacts with endogenous M3R, pulldown experiments were performed using the same GST-NOSTRIN fusion proteins as described above and lung lysates from WT mice. NOSTRIN is expressed in vascular ECs and lung tissue being a highly vascularized tissue was found to be one of the tissues with the strongest expression of NOSTRIN[62]. Mouse lung lysate was prepared using lysis buffer containing digitonin and benzonase. Lung lysate was incubated with equal amounts of the different GST-NOSTRIN fusion proteins or GST alone and the GST pulldown performed using GSH-Sepharose beads. The interaction was analyzed by immunoblot.

Full size NOSTRIN interacted with the endogenous M3R. In contrast, neither the ΔSH3 mutant nor the SH3 domain alone interacted with the M3R (Fig. 18), confirming the previous result that the SH3 domain is necessary but not sufficient to mediate the NOSTRIN/M3R interaction.

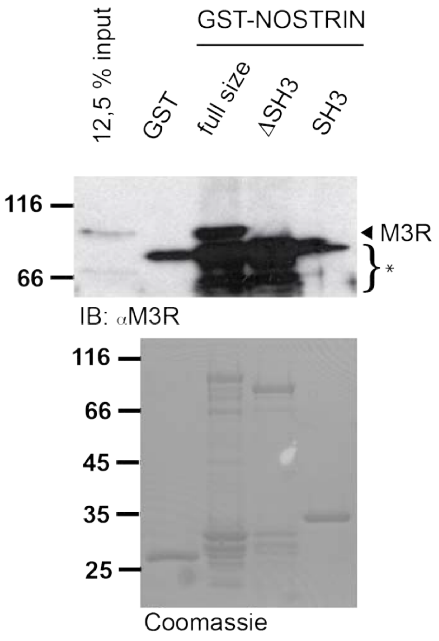

Figure 18 NOSTRIN interacts with the endogenous M3R expressed in lung tissue. GST **p**ulldown from mouse lung lysate with indicated GST fusion proteins followed by immunoblotting with an M3R-specific antibody; * indicates unspecific bands detected with the antibody directed against M3R, most probably originating from cross-reactivity with GST (top). Coomassie-stained gel to visualize equal input of GST fusion proteins (bottom). GST-NOSTRIN interacts with the endogenous M3R. This interaction depends on the SH3 domain of NOSTRIN. However, the SH3 domain alone is not sufficient to mediate the interaction.

7.2.3 NOSTRIN interacts directly with the M3R via the 3rd intracellular loop of the M3R

Several interactions of GPCRs are mediated via their 3rd intracellular loop[84]. To test if this is also the case for the NOSTRIN/M3R interaction, the 3rd intracellular loop of the M3R (i3loop, amino acids 253-492) was cloned into a maltose-binding protein (MBP)-vector. The MBP-tagged i3loop was expressed in bacterial cells and purified. Subsequently, pulldown assays were performed using the purified MBP-tagged i3loop and the previously described GST-tagged NOSTRIN fragments.

The immunoblot analysis confirmed that NOSTRIN interacted with the M3R (Fig. 19) and that this interaction was indeed mediated via the ,3rd intracellular loop of the M3 receptor, since it was sufficient for binding to NOSTRIN. Furthermore this experiment with purified proteins indicated that the interaction of NOSTRIN and the M3R was direct and did not require additional bridging binding partners. Once more, it confirmed that the SH3 domain of NOSTRIN is necessary but not sufficient for binding. As a control, a pulldown assay was performed using the same purified GST-NOSTRIN fragments and his-tagged proline rich domain of Sos, which is known to bind the NOSTRIN SH3 domain[63]. Full size NOSTRIN as well as the SH3 domain alone bound Sos, confirming that the SH3 domain was functional (Fig. 19).

7.2.4 NOSTRIN and M3R-GFP co-localize upon overexpression in mammalian cells

To confirm the NOSTRIN/M3R interaction, the co-localization of M3R and NOSTRIN in mammalian cells was analyzed. First, NOSTRIN was cloned into the mCherry-N1 vector. Subsequently, M3R-GFP and NOSTRIN-mCherry fusion proteins were expressed in U2OS cells. Where indicated, cells were stimulated with the M3R-agonist carbachol for 60 min. Subsequently, cells were visualized using confocal fluorescence microscopy.

Both proteins co-localized at the cell border in non-stimulated cells and preferentially to intracellular punctae after stimulation with carbachol (Fig. 20).

This finding confirms the interaction of NOSTRIN and the M3R as well as their co-localization upon overexpression in mammalian cells

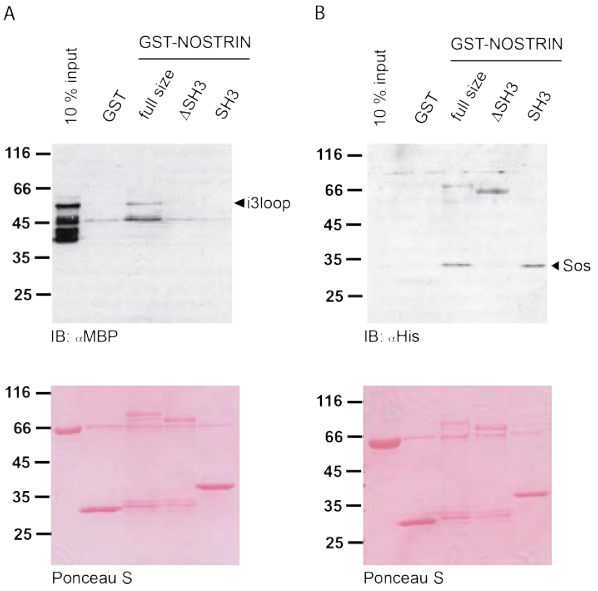

Figure 19 NOSTRIN interacts directly with the i3loop of the M3R. A GST-Pulldown of purified maltose-binding-protein (MBP)-tagged i3loop with indicated GST fusion proteins, followed by immunoblotting with an MBP-specific antibody (top); Ponceau S-stained blotting membrane to visualize equal input of GST fusion proteins (bottom). **B** GST-Pulldown of purified His-tagged Sos proline rich domain with indicated GST fusion proteins, followed by immunoblotting with an His-specific antibody (top); Ponceau S-stained blotting membrane to visualize equal input of GST fusion proteins (bottom). GST-NOSTRIN interacts directly with the i3loop of the M3R. The SH3 domain of NOSTRIN is necessary but not sufficient to mediate the interaction, although the SH3 domain was functional as it binds to Sos.

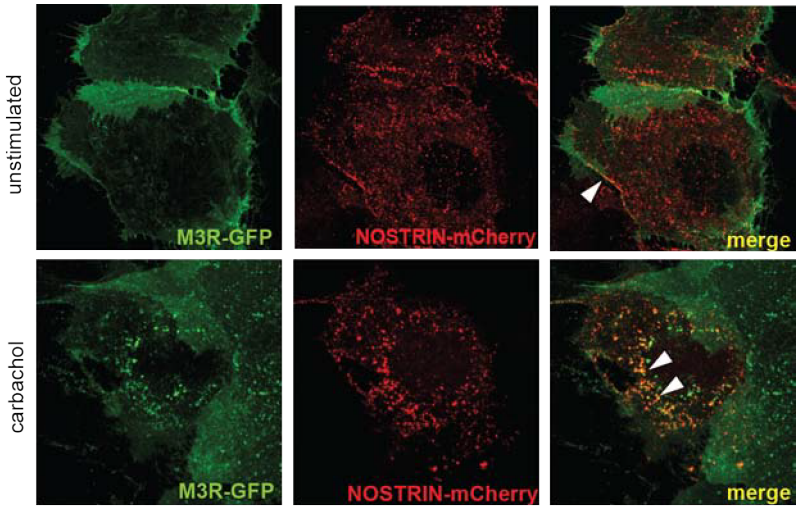

Figure 20 Colocalization of NOSTRIN-mCherry and M3R-GFP upon overexpression in mammalian cells. Confocal fluorescence microscopy image of U2OS cells expressing M3R-GFP and NOSTRIN-mCherry fusion proteins, arrowheads indicating colocalization at the cell-cell-border and in intracellular punctae. Carbachol (100µM) was applied for 60 min, where indicated.

7.3 Summary I

In this study the M3R has been demonstrated to be a novel interaction partner of NOSTRIN. The interaction is direct and is mediated by the 3rd intracellular loop of the M3R. The SH3 domain of NOSTRIN is necessary but not sufficient for the interaction.

The loss of NOSTRIN leads to an altered localization of the M3R in aortic ECs and inhibits the activating phosphorylation of eNOS at Ser1179 as well as the translocation of eNOS to the Golgi complex upon stimulation with the M3R-agonist carbachol. In addition it provides indication, that NOSTRIN facilitates the calcium response upon M3R activation with ACh and carbachol.

.

7.4 Analysis of the role of NOSTRIN in shear stress sensing

The vasculature is continuously exposed to blood flow-associated mechanical forces, which are major determinants of vascular morphogenesis and physiology. However, little is known about the mechanisms by which individual cells sense these mechanical signals and transduce them into changes in intracellular signal transduction and gene expression[100]. Different molecules have been independently proposed as endothelial mechanosensors, including the glycocalyx, cell adhesion molecules, G-proteins, ion channels and GPCRs. Since NOSTRIN interacts with the M3R in endothelial cells, a first explorative study of a possible involvement of NOSTRIN in shear stress sensing was undertaken.

7.4.1 Actin cytoskeleton and stress fibers are misarranged in NOSTRIN KO endothelial cells

Hemodynamic forces in form of fluid shear stress impose profound morphological changes on ECs. ECs elongate and align in the direction of flow through reorganization at the intracellular level, for example reorientation and elongation of actin stress fibers[101,102]. How this external stimulus is transmitted to the endothelial cytoskeleton is not completely understood.

Since the function of many F-BAR proteins is associated with actin dynamics, aortae from NOSTRIN WT and KO mice were isolated and stained *en face* for actin using AlexaFluor® Phalloidin and visualized using confocal microscopy.

In aortic ECs from WT mice, homogenous cortical actin and prominent actin stress fibers could be detected, which were aligned in the direction of the blood flow (Fig. 21). In contrast, in NOSTRIN KO aortic ECs, there were no properly aligned actin stress fibers. Cortical actin was detected but it appeared randomly oriented and showed many irregularities. Importantly, actin stress fibers of the underlying vascular smooth muscle cells were not affected by the loss of NOSTRIN (Fig. 21).

These findings implicate that NOSTRIN is necessary for the orientation and alignment of the actin cytoskeleton in the murine endothelium.

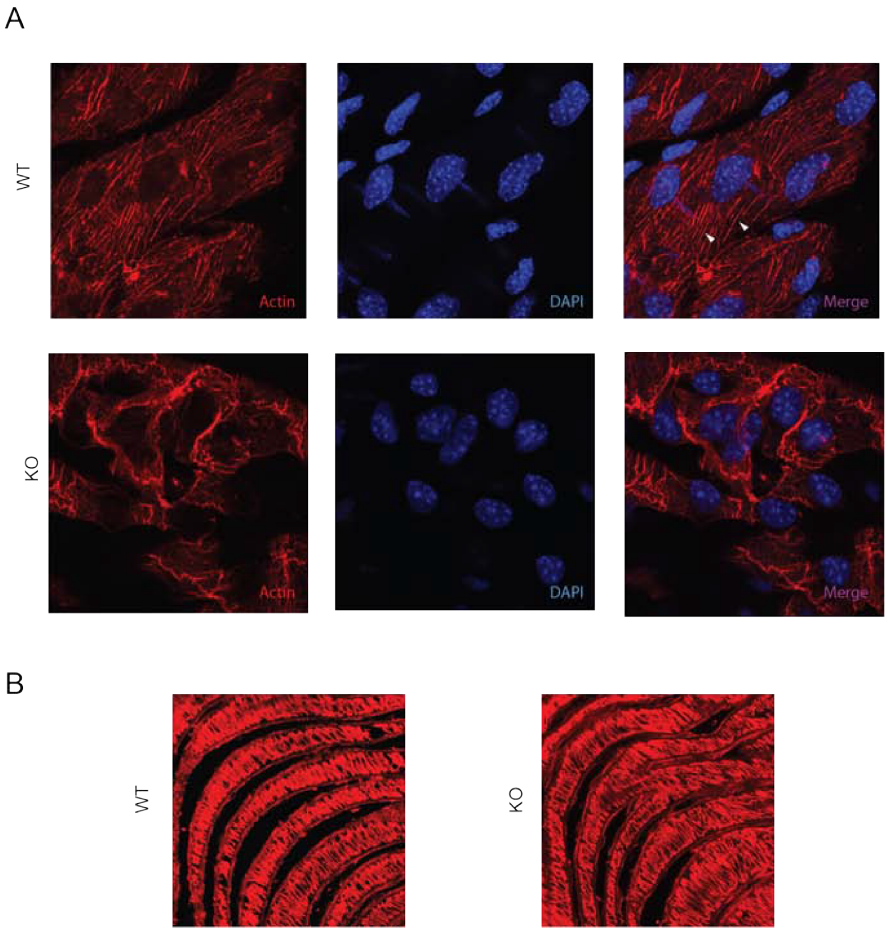

Figure 21 Loss of NOSTRIN leads to a misarrangement of the actin cytoskeleton and stress fibers in the aortic ECs *ex vivo*. *En face* staining for actin and DAPI in WT and NOSTRIN KO mouse aorta explants **A** Aortic endothelial cells **B** Vascular smooth muscle cells (VSMC). In WT aortic EC, the actin cytoskeleton is properly organized in cortical actin and stress fibers, which are aligned in the direction of the blood flow. In NOSTRIN KO aortic EC, the actin cytoskeleton is disorganized and stress fibers are not detectable. The actin cytoskeleton of the underlying VSMC is not affected by the loss of NOSTRIN.

7.4.2 Loss of NOSTRIN inhibits the re-alignment of actin stress fibers with the changing flow direction

Under physiological conditions, actin stress fibers are aligned in the direction of the blood flow. Parallel plate flow chambers are commercially available and used as a standard method to investigate effects of fluid shear stress. Lane et al. refined this method by establishing a novel *in vitro* flow system that allows to change the flow direction on cultured ECs[98]. Given the misarrangement of actin stress fibers in NOSTRIN KO aortae, the question arose if ECs need NOSTRIN for the (re-)alignment of actin stress fibers in response to flow. In order to test the effect of the changing flow direction on the aorta itself, a new flow chamber was build. The flow chamber design and flow circuit was assembled as proposed by Lane et al. However, in contrast to their work, instead of seeding cultured EC, murine aorta explants were fixed in the flow chamber either in the same orientation in respect to the flow as in the intact animal circulation or perpendicular to it. After 24 hours exposure to laminar flow in the physiological direction of flow or perpendicular to it, aortae were stained *en face* for actin and DAPI. ECs of NOSTRIN WT aortae showed prominent stress fibers that were aligned in the direction of flow. After 24 hours exposure to laminar flow, which was perpendicular to the physiological direction of flow, ECs had realigned their stress fibers and their shape in the new flow direction (Fig. 22). In NOSTRIN KO aortae, however, ECs did not show as many prominent stress fibers in the original direction of flow or any rearrangement in the new flow direction (Fig. 22).

These data suggest, that NOSTRIN might play a role in the dynamic remodeling of the cytoskeleton in the response to shear stress in endothelial cells.

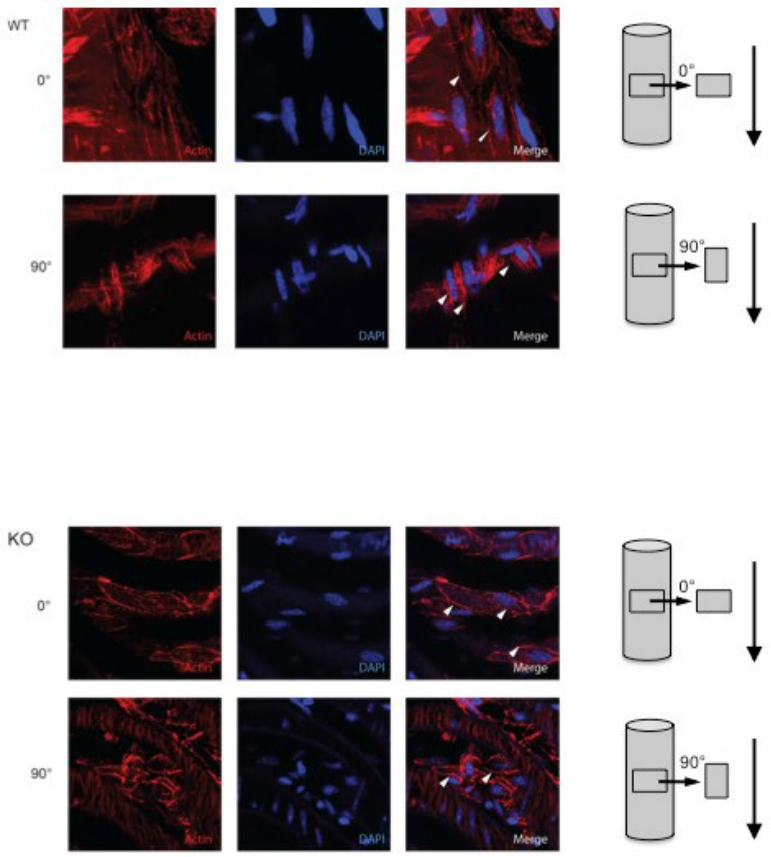

Figure 22 NOSTRIN influences the realignment of actin stress fibers in response to the changing flow direction. NOSTRIN WT (top) and KO (bottom) aorta explants were exposed to laminar flow in the physiological flow direction (rotated by 0°) and perpendicular to it (rotated by 90°) for 24 hrs. *En face* immunofluorescence staining for actin and DAPI. The downward pointing arrow on the right-hand side indicates the direction of flow. Only in WT but not in NOSTRIN KO aortae, ECs realign in the new direction of flow.

7.4.3 Loss of PECAM-1 membrane staining in aortae of NOSTRIN KO mice

Platelet endothelial cell adhesion molecule-1 (PECAM-1) makes up a large portion of endothelial cell intracellular junctions and forms a mechanosensory complex with vascular endothelial cell cadherin and vascular endothelial growth factor receptor 2 which is sufficient to make heterologous cells responsive to flow[103].

To investigate if the expression of NOSTRIN influences the spatial localization of PECAM-1, aortae of NOSTRIN KO and WT mice were isolated and stained for PECAM-1 and DAPI. Whereas PECAM-1 staining at the endothelial cell-cell-

borders is seen in WT aortae, PECAM-1 membrane staining was lost in NOSTRIN KO aortic ECs.

Subsequently, mouse lung lysates were prepared from WT and NOSTRIN KO mice were prepared using lysis buffer, containing digitonin and benzonase and further processed for immunoblot analysis. Interestingly, expression levels of PECAM-1 were equal in mouse lung lysates from NOSTRIN KO and WT mice. This finding sugests a possible role of NOSTRIN in the localization of PECAM-1 with consequences for shear stress sensing.

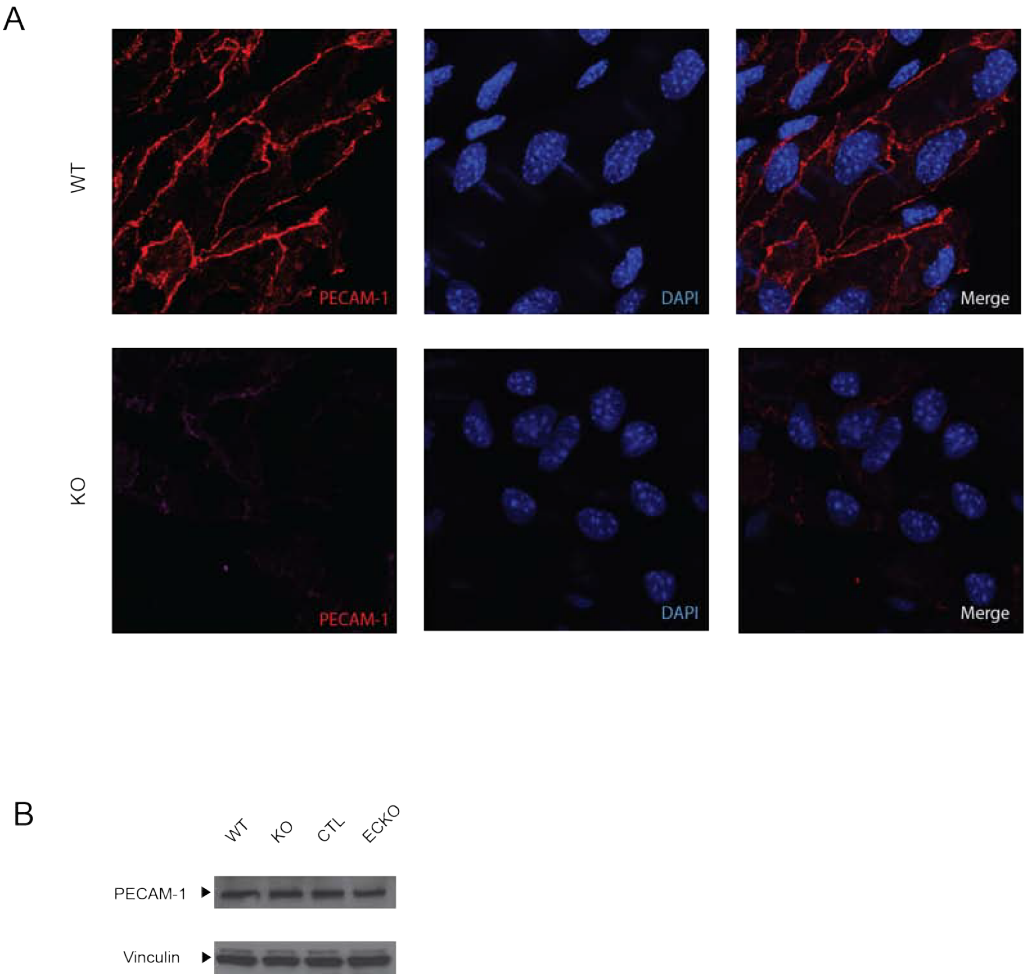

Figure 23 A: Localization of PECAM-1 at the cell-cell-contacts is lost in the absence of NOSTRIN. *En face* staining for PECAM-1 and DAPI in WT and NOSTRIN KO aortae. WT aortic ECs show a regular PECAM-1 staining at cell-cell-contacts whereas he membrane staining is lost in NOSTRIN KO aortic ECs**. B: PECAM-1 expression levels in mouse lung lysates of NOSTRIN KO, EC KO and their respective controls are equal.** Immunoblot of mouse lung lysates with PECAM-1 specific antibody. Vinculin serves as loading control.

7.5 Summary II

This first explorative study shows misarrangement of the actin cytoskeleton and PECAM-1 in aortae of NOSTRIN KO mice *ex vivo*. Furthermore, the ability of the ECs to realign their actin stress fibers with the changing direction of flow is lost in the absence of NOSTRIN.

These data suggest that NOSTRIN might play a role in shear sensing or in mediating the response to shear stress in endothelial cells.

8 Discussion

NOSTRIN was originally identified as eNOS interaction partner, regulating eNOS subcellular localization by interacting with dynamin, N-WASP and caveolin[62,27,64]. *In vivo*, the loss of NOSTRIN leads to hypertension and an inhibition of the vasorelaxation upon stimulation with ACh (Tanja Hindemith, unpublished data;[94]). However, the mechanism behind this phenotype - in particular the restriction of the effect to the stimulation with ACh - was not clear. The results of the present work reveal that NOSTRIN interacts directly with the M3R and is required for its correct spatial localization at the plasma membrane of aortic endothelial cells. In the absence of NOSTRIN, the function of the M3R was markedly impaired, resulting a reduced activation of eNOS.

8.1 The F-BAR protein NOSTRIN as novel interaction partner of the M3R

The results of the present work identify NOSTRIN as novel interaction partner of the M3R. Several F-BAR proteins have been reported to interact with transmembrane receptors. Among others, PACSIN1 interacts with NMDA receptors during glutamatergic synapse maturation[39], PSTPIP2 mediates CD2 receptor signaling in T-lymphocytes[104] and CIP4 regulates internalization of EGFR and PDGFRβ[105,41]. Furthermore, NOSTRIN is known to interact with FGFR1[63]. However, the interaction of NOSTRIN with the M3R is to my knowledge the first example of an F-BAR protein interacting with a GPCR.

8.2 NOSTRIN interacts with the functionally important i3loop of the M3R

The interaction is direct and involves the SH3 domain of NOSTRIN, since deletion of the SH3 domain abolishes the interaction. SH3 domains are important protein interaction modules, which specifically recognize proline-rich

ligands and regulate the assembly of multi-protein complexes and thus the local concentration and subcellular distribution of binding partners [18].

The SH3 domain of NOSTRIN alone is not sufficient to bind to the M3R, indicating that additional motifs in NOSTRIN might be required. On the side of the M3R the interaction with NOSTRIN involves the i3loop. The i3loop is located between transmembrane domain V and VI, comprises 240 amino acids (amino acid 253-492 of full length human M3R) and is the largest of the intracellular loops. It has a recognized role in receptor regulation and is involved e.g. in G-protein coupling[106,107], and the interaction with G-protein coupled receptor kinase-2 (GRK2) and β-arrestin[108,109], both critically involved in GPCR desensitization[110,111]. Furthermore the i3loop has been implicated in M3R dimerization[112]. The i3loop contains 7 (mouse) or 8 proline residues (human sequence), respectively, but no canonical PXXP motif. Interestingly, the i3loop possesses sequences with similarity to recently identified non-consensus and atypical SH3 domain ligands[113,114,115], possibly responsible for the binding to the NOSTRIN SH3 domain.

8.3 NOSTRIN dictates the correct spatial localization of the M3R

In the present work it is shown that the correct spatial localization of the M3R at the endothelial cell membrane of the mouse aorta is lost in the absence of NOSTRIN. The subcellular distribution of the GPCRs is in part determined by their recycling properties. The molecular details of GPCR recycling vary considerably between different family members and cell types and there is no single consensus mechanism. The current knowledge about the factors that govern M3R trafficking in the cardiovascular system is very limited. Overexpression studies in HeLa and COS-7 cells indicate that the M3R undergoes constitutive recycling from the plasma membrane through the endosomal pathway in a clathrin-independent manner. Upon agonist-stimulation the M3R has been reported to switch to clathrin-dependent endocytosis and the i3loop has been suggested to be involved in the agonist-dependent switch between these two alternative endocytic pathways[116]. Moreover, the related

mAChR subtype 2 (M2R), which is the predominant mAChR form in cardiomyocytes, has been reported to be internalized by caveolar sequestration in a dynamin-dependent mechanism[117]. Therefore the precise mechanism of M3R endocytosis and recycling and the molecular components involved are currently unknown.

In general, F-BAR proteins as other members of the BAR protein superfamily have been shown to be involved in several forms of endocytosis, both clathrin-dependent and –independent[118,119]. In addition to endocytosis, BAR proteins of the SNX-BAR family have been shown to form part of the retromer complex, which is critically involved in the endosomal sorting and recycling of membrane-associated cargo proteins[120,121,122]. Therefore, it is conceivable that NOSTRIN could be involved in the trafficking of the M3R at several of the discrete steps of receptor recycling. In line with this notion, it has been proposed that NOSTRIN localizes to rab11-positive (and to a lesser extend rab5-positve) endosomes and might function at endosomal tubule intermediates to mediate microtubule-dependent trafficking of recycling endosomes[123].

In general, proper subcellular localization of proteins within the eukaryotic cell provides the physiological context for their function. Given that proteins cannot diffuse as quickly as small-molecule second messengers, the subcellular localization of signaling proteins in proximity to their downstream targets is crucial for many signal transduction circuits. Examples suggest that aberrant targeting of proteins contributes to the pathogenesis of many human diseases, including metabolic, cardiovascular, and neurodegenerative diseases, as well as cancer. Known diseases caused by mistargeting of GPCRs are e.g. retinitis pigmentosa and blindness through aberrant trafficking of Rhodopsin[124], nephrogenic diabetes insipidus through mislocalized vasopressin receptor in kidney epithelia[125] and hypogonadotropic hypogonadism through misrouted gonadotropin-releasing hormone receptor[126].

8.4 Acetylcholine-induced activation of eNOS depends on NOSTRIN

In tis current study it is shown, that in the absence of NOSTRIN, eNOS activity was compromised, evident as impaired Golgi translocation and phosphorylation at the activating Ser1179 site. This is highly consistent with the impaired acetylcholine-induced vasodilatation of isolated aortic rings and the reduced NO and cGMP levels observed in NOSTRIN KO and ECKO mice and confirms the role of NOSTRIN as an important regulator of eNOS function.
However, the inhibition of vasorelaxation in the absence of NOSTRIN occurred not generally in response to eNOS-activating stimuli, but specifically upon ACh stimulation. This suggests that NOSTRIN is not generally necessary for the activity of eNOS, but rather is involved in the activation in response to specific signals such as ACh. This would be in line with the notion that specific portions of the cellular eNOS pool are preassembled into larger signaling complexes, allowing for controlled spatial activation and/or local NO production[65,77]

8.5 NOSTRIN facilitates increase in intracellular calcium after stimulation with the M3R agonist carbachol

Calcium is an important link between M3R and eNOS activation: The M3R is a GPCR that couples to $G\alpha_{q/11}$ leading upon activation to an increase in intracellular calcium levels[127,128]. At the same time, increase in intracellular calcium is an important activator for eNOS. The data from the aequorin-assay in this present study suggested that NOSTRIN might be necessary for the increase in intracellular calcium upon stimulation with the M3R agonist carbachol in CHO/G5A cells transfected with the M3R. However, the results in this experimental setup were statistically not significant. For this reason, the experimental setup was changed and Ca^{2+} was assessed using the Ca^{2+} indicator Fura-2 in MLEC (not part of this study). The loss of NOSTRIN in MLECs isolated from NOSTRIN KO mice dramatically reduced the number of MLEC that respond to acetylcholine with mobilization of intracellular calcium

from around 48% in WT to almost null in NOSTRIN KO cells[94]. This confirmed the findings from the initial experiments presented in this present study, that NOSTRIN is crucial for M3R-dependent rise in intracellular Ca^{2+} levels.
In respect to the heterogeneous ACh response observed in WT cells it should be noted that this is considered a typical behavior of endothelial cells and aortic endothelium and has been attributed to the heterogeneous expression pattern of the M3R[119,129]. Importantly, it was found that NOSTRIN KO endothelial cells respond readily with mobilization of intracellular calcium to the addition of calcium ionophor A23187. Since A23187 facilitates Ca^{2+} influx through plasma membrane Ca^{2+} channels, which subsequently triggers the phospholipase C-dependent mobilization of Ca^{2+} from intracellular stores[130], this indicates that in the absence of NOSTRIN mechanisms downstream of phospholipase C activation are intact and the failure to mobilize Ca^{2+} from intracellular stores lies upstream and is most likely associated with the malfunctioning of the M3R itself.

8.6 NOSTRIN as regulator of the M3R/eNOS signaling axis

In this study it is shown that NOSTRIN in addition to its role in regulating eNOS is necessary for the functionality of the M3R acetylcholine receptor. Although endothelial cells express the M3R, and ACh is routinely used in *in vitro* studies to assess endothelial cell function and NO production[86,87,88,89,90,91,92], there is considerable debate about the *in vivo* relevance of ACh for the regulation of vascular tone and resistance. Indeed, ACh is produced by perivascular nerve fibers, but they are restricted to some arterial vascular beds. Rather, endothelial cells have been shown to serve as the endogenous source for ACh[131,132] and e.g. in the coronary vasculature generate the transmitter in sufficient amounts to induce NO release[133]. Such observations argue in favor of an important physiological role of ACh in the regulation of vascular tone. The question, which aspects of the phenotype in NOSTRIN KO and ECKO mice are dependent on the impaired function of ACh and which might be independent, and should be addressed in future experiments with M3R KO and ECKO mice for comparison.

8.7 Interaction of NOSTRIN with the M3R provides a possible mechanistic explanation for diastolic dysfunction in NOSTRIN ECKO mice

The findings of this present work describe NOSTRIN as a novel regulator of M3R/eNOS signaling axis and provide a possible mechanistic explanation for the vascular phenotype of NOSTRIN KO and ECKO mice.

NOSTRIN KO and ECKO mice exhibit elevated blood pressure ([94], Tanja Hindemith, unpublished work) and this is in line with the important function of NO as mediator of vessel relaxation. In accordance with these findings, hypertension is a hallmark characteristic in eNOS knockout mice[134,135].

Furthermore, NOSTRIN ECKO mice develop diastolic dysfunction, characterized by an impaired active cardiac relaxation and increased stiffness[94]. The occurrence of diastolic dysfunction in NOSTRIN ECKO mice is in line with the recognized role of endothelial-derived NO to promote cardiomyocyte relaxation[74,77]. However, the phenotype is more severe than in eNOS KO mice, where additional stresses are needed to evoke diastolic dysfunction; e.g. chronic pressure overload[134], or the simultaneous deletion of the two other NOS isoforms nNOs and iNOS[136]. This indicates that NOSTRIN possibly has additional roles or binding partners, which might contribute to the cardiovascular phenotype in NOSTRIN KO mice. In NOSTRIN ECKO mice the systolic heart function is not compromised and there was no cardiac hypertrophy in mice at the age of 8 to 10 weeks, however at this stage we cannot exclude the development of hypertrophy at later time points.

In humans, diastolic dysfunction often precedes diastolic heart failure or heart failure with preserved ejection fraction (HFpEF), which is a major cause of mortality in the elderly population[137]. In contrast to heart failure with reduced ejection fraction, which includes systolic dysfunction and where the identification of key pathological mechanisms led to the development of targeted pharmacological interventions and improvement in disease prognosis,

the pathophysiological mechanisms underlying HFpEF are far from being understood.

To my knowledge there are no studies addressing cardiovascular function in M3R KO mice and endothelial cell-specific M3R knockout mice do not even exist, which makes it difficult to relate these findings to the *in vivo* functionality of the M3R. Interestingly, a region encompassing the NOSTRIN gene (2q24.3–2q31.1) has been identified as a novel locus for hypertension in a Kyrgyz family[68], pointing toward a possible role of NOSTRIN as an important pathophysiological factor.

8.8 NOSTRIN in flow-induced signaling in endothelial cells

In this first explorative study, it was found that in the absence of NOSTRIN aortic ECs show misarranged cortical actin and stress fibers and loss of PECAM-1 membrane staining. Furthermore, the ECs fail to realign their shape and stress fibers with the changing flow direction in NOSTRIN KO aortae. Elucidating how ECs sense and respond to flow is important for understanding both normal vascular function and the development of vascular diseases and a major challenge in the field. Although the data presented here are just first observations that require further investigation and validation, they implicate a role of NOSTRIN in shear sensing and/or mechanotransduction.

8.9 Stress fibers and realignment of EC in the changing direction of flow is lost in aortic EC of NOSTRIN KO mice

Among the most dramatic and obvious changes in response to fluid shear stress are the morphological changes of endothelial cells under flow conditions. Confluent ECs undergo a transition from a polygonal cobblestone-like pattern to a uniformly spindle-shaped monolayer where the main cell axis is aligned in the direction of flow[138]. The transition is reversible upon cessation of flow[139], is dependent on active protein synthesis[140] and specific to ECs as it is observed in

neither vascular smooth muscle cells nor fibroblasts[141,142]. This adaptation to flow is believed to contribute to reducing shear gradients along the EC surface and failure of ECs to align in the direction of flow correlates very well with sustained activation of inflammatory signaling and is a hallmark of atheroprone regions and atherogenesis[143,144].

A further response to shear stress is a distinct transformation of the actin cytoskeleton, resulting in rearrangement of actin filaments into bundles of stress fibers aligned in the direction of flow[145].

The temporal response of ECs to shear stress and the self-alignment of the stress fibers are not completely understood. Previous studies have established that ECs initially enhance their attachments to the extracellular matrix and neighboring cells, followed by a loss of the dense peripheral bands and an increase in motile behavior. Cells subsequently increase their stress fibers as cell alignment and elongation begin[146].

The Rho family of small GTPases are major regulators of the actin cytoskeleton and they are critical for the shear stress response[147]. A mathematical model has been proposed to explain the coupled dynamics of actin stress fibers, adhesion sites, and Rho GTPases when the cell is exposed to flow[148]. According to this model, the presence of aligned actin stress fibers prevents the cell to change its morphology. A diffuse chemical signal triggered by sheared adhesions activates integrins, which then bind ligands and trigger signals that inhibit Rho and possibly activate Rac. A transient decrease in activated Rho causes a drop in myosin-dependent contractility that is necessary for the maintenance of the adhesions at the ends of the stress fibers, and therefore leads to the stress fibers' disassembly. This frees the cell to change its shape. The transient rise in activated Rac enhances lamellipodial actin network growth at the cell boundary, accelerating the cell shape change. Activation of Rac is polarized to the downstream edge of the cell, which enhances the ultimate elongation of the cell in the direction of flow. Finally, recovery of Rho activity in the newly aligned cell mediates the reassembly of the stress fibers and their alignment with the new long axis of the cell. The stress fibers then fix the cell alignment in the direction of flow.

One possible way how NOSTRIN could influences the process of morphological change and actin stress fiber induction in ECs under flow conditions is via its interaction with small GTPases. Previous work of our group showed that NOSTRIN interacts with small GTPases of the Rho family, preferably with Rac1, to a lesser extent with cdc4, but not with RhoA[63]. Furthermore it was shown that that NOSTRIN interacts with Rac1 in its active form but not in its inactive form and that overexpression of NOSTRIN induces activation of Rac1[63]. The lack of the NOSTRIN-dependent Rac activation could underlie the inability of NOSTRIN KO ECs to rearrange the actin cytoskeleton in the direction of flow. In line with this hypothesis, several members of the F-BAR protein family are known to regulate actin dynamics by interacting with Rho GTPases. For example, CIP4 binds activated cdc42 and its overexpression leads to a decrease in stress fibers in Swiss 3T3 fibroblasts[149], Toca-1 interacts with active cdc42 and promotes actin polymerization through activation of N-WASP [24] and PACSIN1 is proposed to mediate Rac1 activation in neuronal filopodia protrusions via recruitement of its GEF Sos1[150].

Furthermore, direct interaction of NOSTRIN with actin cannot be excluded as actin gamma1 was identified as a putative interaction partner in a yeast-two-hybrid screen with NOSTRIN aa362-506 as bait[151].

Clearly, the function of NOSTRIN in the regulation of actin dynamics needs to be addressed experimentally in further studies.

8.10 Loss of PECAM-1 membrane staining in NOSTRIN KO aortae

En face staining of NOSTRIN KO aortae revealed a loss of PECAM-1 membrane staining whereas PECAM-1 expression levels were not affected by the absence of NOSTRIN, indicating that NOSTRIN influences the subcellular localization of PECAM-1. This is of particular interest, since PECAM has been proposed to function as a mechanosensor in ECs, although the precise molecular machinery and mechanism of action are unknown to date.

PECAM-1 is a transmembrane glycoprotein which is expressed in blood and vascular cells and has important roles in regulating endothelial junctional integrity, transendothelial migration, and angiogenesis[152].

In confluent ECs, PECAM-1 is primarily localized at cell-cell junctions where it mediates homophilic binding between adjacent EC[153].

PECAM-1 is of particular interest in mechanotransduction as it gets rapidly phosphorylated following the application of fluid shear stress[154]. Moreover, the cell-cell junction, where PECAM-1 is situated, has shown to be the region of greatest shear-induced tension[155], and a subcellular compartment that is rich in many of the signaling molecules known to be activated following the application of shear stress[156].

There is increasing evidence that PECAM-1 serves as a scaffold for mechanochemical signaling: The association of PECAM-1 with VE-Cadherin and VEGFR2 is possibly the most frequently studied mechanosensory complex in ECs. It has been shown that it confers the ability to sense and respond to the hemodynamic force of flowing blood[103], as well as well as tensional force using a magnetic tweezers system[157].

In addition, PECAM-1 was also found in a complex with $G\alpha_{q/11}$[158]. Rapid activation of heterotrimeric G-proteins is known as one of the earliest flow-mediated responses in endothelial cells[159] and may play a role in the EC's ability to discriminate between flow profiles[158]. $G\alpha_{q/11}$ acts upstream of PECAM-1 as G protein activation is required for the dissociation of the complex in response to dynamic flow. Knockout of the scaffold PECAM-1 lead to a disruption of $G\alpha_{q/11}$ trafficking and pro-inflammatory signaling. The $G\alpha_{q/11}$ PECAM-1 complex might be part of a larger macromolecular structure assembled at the endothelial cell junction.

As mentioned above, in this current study it is shown, that in the absence of NOSTRIN the localization of PECAM-1 is altered, suggesting that NOSTRIN acts upstream of PECAM-1. A different functional interaction between PECAM-1 and NOSTRIN has been reported previously and the following model of PECAM-1 mediated induction of NOSTRIN expression and eNOS trafficking was proposed, that places NOSTRIN downstream of PECAM-1 action: the cytoplasmic tail of PECAM-1 serves as scaffold for STAT3 (signal transducer

and activator of transcription 3) binding. Upon activation, STAT3 translocates into the nucleus and activates the transcription of the NOSTRIN gene. Increased NOSTRIN expression mediates eNOS trafficking and intracellular localization[160].

At the current stage the functional interplay between NOSTRIN and PECAM-1 is incompletely understood and further studies are needed to decipher the relationship and crosstalk between PECAM-1, NOSTRIN, eNOS, and $G\alpha_{q/11}$ as well as their role in signaling complexes at the endothelial cell junction and in mechanostransduction.

8.11 Conclusion

This work was conducted in order to address the mechanism causing the inhibited vasodilation specifically upon stimulation with acetylcholine in NOSTRIN KO and ECKO mice and to explore additional roles of NOSTRIN in endothelial signal transduction.

Experimental data presented in this work identifies NOSTRIN as a novel interaction partner of the M3R being the first example of an F-BAR protein regulating a GPCR. NOSTRIN interacts directly with the M3R and is required for its correct spatial localization at the plasma membrane of aortic endothelial cells. In the absence of NOSTRIN, the function of the M3R was markedly impaired, resulting in abolition of the calcium response to the M3R agonist carbachol and an impaired activation of eNOS.

Therefore, this work confirms that NOSTRIN is an important regulator of eNOS function and identified a potential role of NOSTRIN in the development of endothelial dysfunction and cardiovascular disease.

Furthermore, it was found that in the absence of NOSTRIN aortic ECs show misarranged cortical actin and stress fibers and loss of PECAM-1 membrane staining. In addition, the EC's ability to realign their shape and their stress fibers with the changing flow direction is lost in NOSTRIN KO aortae.

Taken together, these data clearly point to the possibility that NOSTRIN plays a role in shear sensing or in mediating the response to shear stress in aortic

endothelial cells. Undoubtedly, there is much that remains to be elucidated in order to fully explore the underlying molecular mechanisms. I anticipate my experiments as a starting point for further studies of the role of NOSTRIN as well as the M3R in shear sensing and cellular signaling in response to shear stress.

8.12 Outlook

In the present work, the role and function of the F-BAR protein NOSTRIN in the acetylcholine/eNOS signaling axis and a possible role of NOSTRIN in shear stress sensing and mechanostransduction in EC was discussed. However, several issues remain to be investigated in more detail in future.

There is much that remains to be elucidated in order to understand the molecular and cellular processes that regulate M3R trafficking and localization in the endothelium. Given that NOSTRIN localizes to rab11- and to a lesser extent rab5-positive endosomes[161], this might be a starting-point to identify the M3R's trafficking route in ECs and see if NOSTRIN is involved.

Furthermore, NOSTRIN KO and ECKO mice should be subjected to more detailed analysis in order to investigate the role of NOSTRIN in cardiovascular biology *in vivo*. Against the background of the controversial discussion of the physiological significance of the M3R in ECs and to clarify which of the described findings are M3R-specific, it would be important to investigate the vascular and cardiac phenotype of endothelial specific M3R KO mice.

Given that NOSTRIN is critical for the proper localization of a number of membrane-associated proteins, e.g. eNOS, M3R, PECAM-1, this function should be studied in a broader context, taking structural aspects of membrane dynamics, specific phospholipid interactions and vesicular trafficking into account.

I have begun to look at a possible role of NOSTRIN in shear stress sensing and mechanotransduction, but many issues remain to be resolved. Based on the previously described observations it is tempting to decipher the molecular mechanisms that underlie the regulation of the actin cytoskeleton, stress fiber induction and cell alignment by NOSTRIN and its interaction with PECAM-1.

Furthermore, investigating atherosclerosis in NOSTRIN KO and ECKO mice may be worthwhile as vascular mechanotransduction has long been recognized as important factor for the localization of atherosclerotic lesions and PECAM-1 is a critical mediator of atherosclerosis[162,163,164].

To understand how the several documented mechanosensors are integrated at the cellular and molecular level and how they affect specific processes in EC are major future challenges in the field. These efforts should ultimately lead to a better understanding of the function of endothelial mechano-activated pathways in physiology, their dysregulation in atherogenesis and other disorder conditions, and their potential as therapeutic targets for the prevention and treatment of cardiovascular disease.

9 References

1. Frost A, Unger VM, De Camilli P. The BAR Domain Superfamily: Membrane-Molding Macromolecules. *Cell*. 2009;137(2):191-196. doi:10.1016/j.cell.2009.04.010.

2. Rao Y, Haucke V. Membrane shaping by the Bin/amphiphysin/Rvs (BAR) domain protein superfamily. *Cell Mol Life Sci*. 2011;68(24):3983-3993. doi:10.1007/s00018-011-0768-5.

3. Lippincott J, Li R. Involvement of PCH family proteins in cytokinesis and actin distribution. *Microsc Res Tech*. 2000;49(2):168-172. doi:10.1002/(SICI)1097-0029(20000415)49:2<168::AID-JEMT9>3.0.CO;2-T.

4. Aspenström P. Roles of F-BAR/PCH proteins in the regulation of membrane dynamics and actin reorganization. *Int Rev Cell Mol Biol*. 2009;272:1-31. doi:10.1016/S1937-6448(08)01601-8.

5. Peter BJ, Kent HM, Mills IG, et al. BAR domains as sensors of membrane curvature: the amphiphysin BAR structure. *Science*. 2004;303(5657):495-499. doi:10.1126/science.1092586.

6. Shimada A, Niwa H, Tsujita K, et al. Curved EFC/F-BAR-Domain Dimers Are Joined End to End into a Filament for Membrane Invagination in Endocytosis. *Cell*. 2007;129(4):761-772. doi:10.1016/j.cell.2007.03.040.

7. Masuda M, Takeda S, Sone M, et al. Endophilin BAR domain drives membrane curvature by two newly identified structure-based mechanisms. *The EMBO Journal*. 2006;25(12):2889-2897. doi:10.1038/sj.emboj.7601176.

8. Ren G, Vajjhala P, Lee JS, Winsor B, Munn AL. The BAR domain proteins: molding membranes in fission, fusion, and phagy. *Microbiol Mol Biol Rev*. 2006;70(1):37-120. doi:10.1128/MMBR.70.1.37-120.2006.

9. Millard TH, Bompard G, Heung MY, et al. Structural basis of filopodia formation induced by the IRSp53/MIM homology domain of human IRSp53. *The EMBO Journal*. 2005;24(2):240-250. doi:10.1038/sj.emboj.7600535.

10. Lee SH, Kerff F, Chereau D, Ferron F, Klug A, Dominguez R. Structural basis for the actin-binding function of missing-in-metastasis. *Structure*. 2007;15(2):145-155. doi:10.1016/j.str.2006.12.005.

11. Mattila PK, Pykäläinen A, Saarikangas J, et al. Missing-in-metastasis and IRSp53 deform PI(4,5)P2-rich membranes by an inverse BAR domain-like mechanism. *The Journal of Cell Biology*. 2007;176(7):953-964. doi:10.1083/jcb.200609176.

12. Itoh T, Erdmann KS, Roux A, Habermann B, Werner H, De Camilli P. Dynamin and the Actin Cytoskeleton Cooperatively Regulate Plasma Membrane Invagination by BAR and F-BAR Proteins. *Developmental Cell*. 2005;9(6):791-804. doi:10.1016/j.devcel.2005.11.005.

13. Frost A, De Camilli P, Unger VM. F-BAR Proteins Join the BAR Family Fold. *Structure*. 2007;15(7):751-753. doi:10.1016/j.str.2007.06.006.

14. Henne WM, Kent HM, Ford MGJ, et al. Structure and Analysis of FCHo2 F-BAR Domain: A Dimerizing and Membrane Recruitment Module that Effects Membrane Curvature. *Structure*. 2007;15(7):839-852. doi:10.1016/j.str.2007.05.002.

15. Ahmed S, Bu W, Lee RTC, Maurer-Stroh S, Goh WI. F-BAR domain proteins: Families and function. *Commun Integr Biol*. 2010;3(2):116-121.

16. Heath RJW, Insall RH. F-BAR domains: multifunctional regulators of membrane curvature. *Journal of Cell Science*. 2008;121(12):1951-1954. doi:10.1242/jcs.023895.

17. Aspenström P, Fransson Å, Richnau N. Pombe Cdc15 homology proteins: regulators of membrane dynamics and the actin cytoskeleton. *Trends in Biochemical Sciences*. 2006;31(12):670-679. doi:10.1016/j.tibs.2006.10.001.

18. Mayer BJ. SH3 domains: complexity in moderation. *Journal of Cell Science*. 2001;114(Pt 7):1253-1263.

19. Liu BA, Jablonowski K, Raina M, Arcé M, Pawson T, Nash PD. The human and mouse complement of SH2 domain proteins-establishing the boundaries of phosphotyrosine signaling. *Mol Cell*. 2006;22(6):851-868. doi:10.1016/j.molcel.2006.06.001.

20. Peck J, Douglas G, Wu CH, Burbelo PD. Human RhoGAP domain-containing proteins: structure, function and evolutionary relationships. *FEBS Lett*. 2002;528(1-3):27-34.

21. Henne WM, Boucrot E, Meinecke M, et al. FCHo Proteins Are Nucleators of Clathrin-Mediated Endocytosis. *Science*. 2010;328(5983):1281-1284. doi:10.1126/science.1188462.

22. Roberts-Galbraith RH, Gould KL. Setting the F-BAR: functions and regulation of the F-BAR protein family. *Cell Cycle*. 2010;9(20):4091-4097.

23. Liu S, Xiong X, Zhao X, Yang X, Wang H. F-BAR family proteins, emerging regulators for cell membrane dynamic changes-from structure to human diseases. *J Hematol Oncol*. 2015;8(1):47. doi:10.1186/s13045-015-0144-2.

24. Ho H-YH, Rohatgi R, Lebensohn AM, et al. Toca-1 mediates Cdc42-dependent actin nucleation by activating the N-WASP-WIP complex.

Cell. 2004;118(2):203-216. doi:10.1016/j.cell.2004.06.027.

25. Tian L, Nelson DL, Stewart DM. Cdc42-interacting protein 4 mediates binding of the Wiskott-Aldrich syndrome protein to microtubules. *J Biol Chem*. 2000;275(11):7854-7861.

26. Modregger J, Ritter B, Witter B, Paulsson M, Plomann M. All three PACSIN isoforms bind to endocytic proteins and inhibit endocytosis. *Journal of Cell Science*. 2000;113 Pt 24:4511-4521.

27. Icking A, Matt S, Opitz N, Wiesenthal A, Müller-Esterl W, Schilling K. NOSTRIN functions as a homotrimeric adaptor protein facilitating internalization of eNOS. *Journal of Cell Science*. 2005;118(Pt 21):5059-5069. doi:10.1242/jcs.02620.

28. Insall RH, Machesky LM. Actin dynamics at the leading edge: from simple machinery to complex networks. *Developmental Cell*. 2009;17(3):310-322. doi:10.1016/j.devcel.2009.08.012.

29. Aspenström P, Richnau N, Johansson A-S. The diaphanous-related formin DAAM1 collaborates with the Rho GTPases RhoA and Cdc42, CIP4 and Src in regulating cell morphogenesis and actin dynamics. *Experimental Cell Research*. 2006;312(12):2180-2194. doi:10.1016/j.yexcr.2006.03.013.

30. Chitu V, Pixley FJ, Macaluso F, et al. The PCH family member MAYP/PSTPIP2 directly regulates F-actin bundling and enhances filopodia formation and motility in macrophages. *Mol Biol Cell*. 2005;16(6):2947-2959. doi:10.1091/mbc.E04-10-0914.

31. Nikki M, Meriläinen J, Lehto V-P. FAP52 regulates actin organization via binding to filamin. *J Biol Chem*. 2002;277(13):11432-11440. doi:10.1074/jbc.M111753200.

32. Kostan J, Salzer U, Orlova A, et al. Direct interaction of actin filaments with F-BAR protein pacsin2. *EMBO Rep*. 2014;15(11):1154-1162. doi:10.15252/embr.201439267.

33. Kaksonen M, Toret CP, Drubin DG. Harnessing actin dynamics for clathrin-mediated endocytosis. *Nat Rev Mol Cell Biol*. 2006;7(6):404-414. doi:10.1038/nrm1940.

34. Ferguson SM, Ferguson S, Raimondi A, et al. Coordinated actions of actin and BAR proteins upstream of dynamin at endocytic clathrin-coated pits. *Developmental Cell*. 2009;17(6):811-822. doi:10.1016/j.devcel.2009.11.005.

35. Mayor S, Pagano RE. Pathways of clathrin-independent endocytosis. *Nat Rev Mol Cell Biol*. 2007;8(8):603-612. doi:10.1038/nrm2216.

36. McMahon HT, Boucrot E. Molecular mechanism and physiological functions of clathrin-mediated endocytosis. *Nat Rev Mol Cell Biol*.

2011;12(8):517-533. doi:10.1038/nrm3151.

37. Frost A, Perera R, Roux A, et al. Structural Basis of Membrane Invagination by F-BAR Domains. *Cell*. 2008;132(5):807-817. doi:10.1016/j.cell.2007.12.041.

38. Daumke O, Roux A, Haucke V. BAR Domain Scaffoldsin Dynamin-Mediated Membrane Fission. *Cell*. 2014;156(5):882-892. doi:10.1016/j.cell.2014.02.017.

39. Pérez-Otaño I, Luján R, Tavalin SJ, et al. Endocytosis and synaptic removal of NR3A-containing NMDA receptors by PACSIN1/syndapin1. *Nat Neurosci*. 2006;9(5):611-621. doi:10.1038/nn1680.

40. de Kreuk BJ, Anthony EC, Geerts D, Hordijk PL. The F-BAR Protein PACSIN2 Regulates Epidermal Growth Factor Receptor Internalization. *Journal of Biological Chemistry*. 2012;287(52):43438-43453. doi:10.1074/jbc.M112.391078.

41. Hu J, Troglio F, Mukhopadhyay A, et al. F-BAR-containing adaptor CIP4 localizes to early endosomes and regulates Epidermal Growth Factor Receptor trafficking and downregulation. *Cellular Signalling*. 2009;21(11):1686-1697. doi:10.1016/j.cellsig.2009.07.007.

42. Endris V, Wogatzky B, Leimer U, et al. The novel Rho-GTPase activating gene MEGAP/ srGAP3 has a putative role in severe mental retardation. *Proc Natl Acad Sci USA*. 2002;99(18):11754-11759. doi:10.1073/pnas.162241099.

43. Gunnarsson C, Foyn Bruun C. Molecular characterization and clinical features of a patient with an interstitial deletion of 3p25.3-p26.1. *Am J Med Genet A*. 2010;152A(12):3110-3114. doi:10.1002/ajmg.a.33353.

44. Shuib S, McMullan D, Rattenberry E, et al. Microarray based analysis of 3p25-p26 deletions (3p- syndrome). *Am J Med Genet A*. 2009;149A(10):2099-2105. doi:10.1002/ajmg.a.32824.

45. Elstner M, Morris CM, Heim K, et al. Single-cell expression profiling of dopaminergic neurons combined with association analysis identifies pyridoxal kinase as Parkinson's disease gene. *Ann Neurol*. 2009;66(6):792-798. doi:10.1002/ana.21780.

46. Need AC, Ge D, Weale ME, et al. A genome-wide investigation of SNPs and CNVs in schizophrenia. McCarthy MI, ed. *PLoS Genet*. 2009;5(2):e1000373. doi:10.1371/journal.pgen.1000373.

47. Wilson NKA, Lee Y, Long R, et al. A Novel Microduplication in the Neurodevelopmental Gene SRGAP3 That Segregates with Psychotic Illness in the Family of a COS Proband. *Case Rep Genet*. 2011;2011(2):585893-585895. doi:10.1155/2011/585893.

48. Wong K, Ren XR, Huang YZ, et al. Signal transduction in neuronal

migration: roles of GTPase activating proteins and the small GTPase Cdc42 in the Slit-Robo pathway. *Cell*. 2001;107(2):209-221.

49. Marco S, Giralt A, Petrovic MM, et al. Suppressing aberrant GluN3A expression rescues synaptic and behavioral impairments in Huntington's disease models. *Nat Med*. 2013;19(8):1030-1038. doi:10.1038/nm.3246.

50. Holbert S, Dedeoglu A, Humbert S, Saudou F, Ferrante RJ, Néri C. Cdc42-interacting protein 4 binds to huntingtin: neuropathologic and biological evidence for a role in Huntington's disease. *Proc Natl Acad Sci USA*. 2003;100(5):2712-2717. doi:10.1073/pnas.0437967100.

51. Yamamoto H, Sutoh M, Hatakeyama S, et al. Requirement for FBP17 in invadopodia formation by invasive bladder tumor cells. *J Urol*. 2011;185(5):1930-1938. doi:10.1016/j.juro.2010.12.027.

52. Pichot CS, Arvanitis C, Hartig SM, et al. Cdc42-interacting protein 4 promotes breast cancer cell invasion and formation of invadopodia through activation of N-WASp. *Cancer Res*. 2010;70(21):8347-8356. doi:10.1158/0008-5472.CAN-09-4149.

53. Hu J, Mukhopadhyay A, Truesdell P, et al. Cdc42-interacting protein 4 is a Src substrate that regulates invadopodia and invasiveness of breast tumors by promoting MT1-MMP endocytosis. *Journal of Cell Science*. 2011;124(Pt 10):1739-1751. doi:10.1242/jcs.078014.

54. Hartig SM, Ishikura S, Hicklen RS, et al. The F-BAR protein CIP4 promotes GLUT4 endocytosis through bidirectional interactions with N-WASp and Dynamin-2. *Journal of Cell Science*. 2009;122(Pt 13):2283-2291. doi:10.1242/jcs.041343.

55. Roach W, Plomann M. PACSIN3 overexpression increases adipocyte glucose transport through GLUT1. *BIOCHEMICAL AND BIOPHYSICAL RESEARCH COMMUNICATIONS*. 2007;355(3):745-750. doi:10.1016/j.bbrc.2007.02.025.

56. Bai S, Zeng R, Zhou Q, et al. Cdc42-interacting protein-4 promotes TGF-B1-induced epithelial-mesenchymal transition and extracellular matrix deposition in renal proximal tubular epithelial cells. *Int J Biol Sci*. 2012;8(6):859-869. doi:10.7150/ijbs.3490.

57. Wise CA, Gillum JD, Seidman CE, et al. Mutations in CD2BP1 disrupt binding to PTP PEST and are responsible for PAPA syndrome, an autoinflammatory disorder. *Hum Mol Genet*. 2002;11(8):961-969.

58. Baum W, Kirkin V, Fernández SBM, et al. Binding of the intracellular Fas ligand (FasL) domain to the adaptor protein PSTPIP results in a cytoplasmic localization of FasL. *J Biol Chem*. 2005;280(48):40012-40024. doi:10.1074/jbc.M502222200.

59. Shoham NG, Centola M, Mansfield E, et al. Pyrin binds the PSTPIP1/CD2BP1 protein, defining familial Mediterranean fever and

PAPA syndrome as disorders in the same pathway. *Proc Natl Acad Sci USA*. 2003;100(23):13501-13506.doi:10.1073/pnas.2135380100.

60. Tsuboi S, Takada H, Hara T, et al. FBP17 Mediates a Common Molecular Step in the Formation of Podosomes and Phagocytic Cups in Macrophages. *J Biol Chem*. 2009;284(13):8548-8556. doi:10.1074/jbc.M805638200.

61. Ferguson PJ, Bing X, Vasef MA, et al. A missense mutation in pstpip2 is associated with the murine autoinflammatory disorder chronic multifocal osteomyelitis. *Bone*. 2006;38(1):41-47. doi:10.1016/j.bone.2005.07.009.

62. Zimmermann K, Opitz N, Dedio J, Renne C, Müller-Esterl W, Oess S. NOSTRIN: a protein modulating nitric oxide release and subcellular distribution of endothelial nitric oxide synthase. *Proc Natl Acad Sci USA*. 2002;99(26):17167-17172. doi:10.1073/pnas.252345399.

63. Kovacevic I, Hu J, Siehoff-Icking A, et al. The F-BAR protein NOSTRIN participates in FGF signal transduction and vascular development. *The EMBO Journal*. 2012;31(15):3309-3322. doi:10.1038/emboj.2012.176.

64. Schilling K, Opitz N, Wiesenthal A, et al. Translocation of endothelial nitric-oxide synthase involves a ternary complex with caveolin-1 and NOSTRIN. *Mol Biol Cell*. 2006;17(9):3870-3880. doi:10.1091/mbc.E05-08-0709.

65. Oess S, Icking A, Fulton D, Govers R, Müller-Esterl W. Subcellular targeting and trafficking of nitric oxide synthases. *Biochem J*. 2006;396(3):401. doi:10.1042/BJ20060321.

66. Mookerjee RP, Wiesenthal A, Icking A, et al. Increased Gene and Protein Expression of the Novel eNOS Regulatory Protein NOSTRIN and a Variant in Alcoholic Hepatitis. *Gastroenterology*. 2007;132(7):2533-2541. doi:10.1053/j.gastro.2006.12.035.

67. Wiesenthal A, Hoffmeister M, Siddique M, et al. NOSTRINbeta--a shortened NOSTRIN variant with a role in transcriptional regulation. *Traffic*. 2009;10(1):26-34. doi:10.1111/j.1600-0854.2008.00850.x.

68. Kalmyrzaev B, Aldashev A, Khalmatov M, et al. Genome-wide scan for premature hypertension supports linkage to chromosome 2 in a large Kyrgyz family. *Hypertension*. 2006;48(5):908-913. doi:10.1161/01.HYP.0000244107.13957.2b.

69. Bilusic M, Bataillard A, Tschannen MR, et al. Mapping the genetic determinants of hypertension, metabolic diseases, and related phenotypes in the lyon hypertensive rat. *Hypertension*. 2004;44(5):695-701. doi:10.1161/01.HYP.0000144542.57306.5e.

70. Kirsch T, Kaufeld J, Korstanje R, et al. Knockdown of the hypertension-associated gene NOSTRIN alters glomerular barrier function in zebrafish (Danio rerio). *Hypertension*. 2013;62(4):726-730.

doi:10.1161/HYPERTENSIONAHA.113.01882.

71. Xiang W, Chen H, Xu X, Zhang M, Jiang R. Expression of endothelial nitric oxide synthase traffic inducer in the placentas of women with pre-eclampsia. *Int J Gynaecol Obstet*. 2005;89(2):103-107. doi:10.1016/j.ijgo.2004.12.041.

72. Xiang W, Chen H, Guo Y, Shen H. Expression of endothelial nitric oxide synthase traffic inducer in the placenta of pregnancy induced hypertension. *J Huazhong Univ Sci Technol Med Sci*. 2006;26(3):356-358.

73. Davignon J, Ganz P. Role of endothelial dysfunction in atherosclerosis. *Circulation*. 2004;109(23 Suppl 1):III27-III32. doi:10.1161/01.CIR.0000131515.03336.f8.

74. Balligand JL, Feron O, Dessy C. eNOS Activation by Physical Forces: From Short-Term Regulation of Contraction to Chronic Remodeling of Cardiovascular Tissues. *Physiological Reviews*. 2009;89(2):481-534. doi:10.1152/physrev.00042.2007.

75. Fleming I. Molecular mechanisms underlying the activation of eNOS. *Pflugers Arch*. 2010;459(6):793-806. doi:10.1007/s00424-009-0767-7.

76. Massion PB, Balligand JL. Modulation of cardiac contraction, relaxation and rate by the endothelial nitric oxide synthase (eNOS): lessons from genetically modified mice. *The Journal of Physiology*. 2003;546(Pt 1):63-75. doi:10.1113/jphysiol.2002.025973.

77. Massion PB, Feron O, Dessy C, Balligand JL. Nitric oxide and cardiac function: ten years after, and continuing. *Circulation Research*. 2003;93(5):388-398. doi:10.1161/01.RES.0000088351.58510.21.

78. Behrendt D, Ganz P. Endothelial function. From vascular biology to clinical applications. *Am J Cardiol*. 2002;90(10C):40L–48L.

79. Förstermann U, Sessa WC. Nitric oxide synthases: regulation and function. *Eur Heart J*. 2012;33(7):829–37–837a–837d. doi:10.1093/eurheartj/ehr304.

80. Morris SM. Recent advances in arginine metabolism: roles and regulation of the arginases. *British Journal of Pharmacology*. 2009;157(6):922-930. doi:10.1111/j.1476-5381.2009.00278.x.

81. Rubin RP. A brief history of great discoveries in pharmacology: in celebration of the centennial anniversary of the founding of the American Society of Pharmacology and Experimental Therapeutics. *Pharmacol Rev*. 2007;59(4):289-359. doi:10.1124/pr.107.70102.

82. Wess J. M USCARINICA CETYLCHOLINER ECEPTORK NOCKOUTM ICE: Novel Phenotypes and Clinical Implications*. *Annu Rev Pharmacol Toxicol*. 2004;44(1):423-450.

doi:10.1146/annurev.pharmtox.44.101802.121622.

83. Felder CC. Muscarinic acetylcholine receptors: signal transduction through multiple effectors. *FASEB J*. 1995;9(8):619-625.

84. Wess J, Blin N, Mutschler E, Blüml K. Muscarinic acetylcholine receptors: structural basis of ligand binding and G protein coupling. *Life Sciences*. 1995;56(11-12):915-922.

85. Furchgott RF, Zawadzki JV. The obligatory role of endothelial cells in the relaxation of arterial smooth muscle by acetylcholine. *Nature*. 1980;288(5789):373-376.

86. Bény J-L, Nguyen MN, Marino M, Matsui M. Muscarinic receptor knockout mice confirm involvement of M3 receptor in endothelium-dependent vasodilatation in mouse arteries. *J Cardiovasc Pharmacol*. 2008;51(5):505-512. doi:10.1097/FJC.0b013e31816d5f2f.

87. Khurana S, Chacon I, Xie G, et al. Vasodilatory effects of cholinergic agonists are greatly diminished in aorta from M3R-/- mice. *Eur J Pharmacol*. 2004;493(1-3):127-132.doi:10.1016/j.ejphar.2004.04.012.

88. Orii R, Sugawara Y, Sawamura S, Yamada Y. M_3muscarinic receptors mediate acetylcholine-induced pulmonary vasodilation in pulmonary
hypertension. *Biosci Trends*. 2010;4(5):260-266.

89. Gericke A, Steege A, Manicam C, Böhmer T, Wess J, Pfeiffer N. Role of the M3 muscarinic acetylcholine receptor subtype in murine ophthalmic arteries after endothelial removal. *Investigative Ophthalmology & Visual Science*. 2014;55(1):625-631. doi:10.1167/iovs.13-13549.

90. Gericke A, Sniatecki JJ, Mayer VGA, et al. Role of M1, M3, and M5 muscarinic acetylcholine receptors in cholinergic dilation of small arteries studied with gene-targeted mice. *AJP: Heart and Circulatory Physiology*. 2011;300(5):H1602-H1608. doi:10.1152/ajpheart.00982.2010.

91. Gericke A, Sniatecki JJ, Goloborodko E, et al. Identification of the Muscarinic Acetylcholine Receptor Subtype Mediating Cholinergic Vasodilation in Murine Retinal Arterioles. *Investigative Ophthalmology & Visual Science*. 2011;52(10):7479-7484. doi:10.1167/iovs.11-7370.

92. Lamping KG, Wess J, Cui Y, Nuno DW, Faraci FM. Muscarinic (M) receptors in coronary circulation: gene-targeted mice define the role of M2 and M3 receptors in response to acetylcholine. *Arteriosclerosis, Thrombosis, and Vascular Biology*. 2004;24(7):1253-1258. doi:10.1161/01.ATV.0000130661.82773.ca.

93. Eglen RM, Hegde SS, Watson N. Muscarinic receptor subtypes and smooth muscle function. *Pharmacol Rev*. 1996;48(4):531-565.

94. Kovacevic I, Müller M, Kojonazarov B, et al. The F-BAR Protein

NOSTRIN Dictates the Localization of the Muscarinic M3 Receptor and Regulates Cardiovascular Function. *Circulation Research*. 2015;117(5):460-469. doi:10.1161/CIRCRESAHA.115.306187.

95. Icking A, Schilling K, Wiesenthal A, Opitz N, Müller-Esterl W. FCH/Cdc15 domain determines distinct subcellular localization of NOSTRIN. *FEBS Lett*. 2006;580(1):223-228. doi:10.1016/j.febslet.2005.11.078.

96. Tunaru S, Lättig J, Kero J, Krause G, Offermanns S. Characterization of determinants of ligand binding to the nicotinic acid receptor GPR109A (HM74A/PUMA-G). *Molecular Pharmacology*. 2005;68(5):1271-1280. doi:10.1124/mol.105.015750.

97. Preuß B, Tunaru S, Henes J, Offermanns S, Klein R. A novel luminescence-based method for the detection of functionally active antibodies to muscarinic acetylcholine receptors of the M3 type (mAchR3) in patients' sera. *Clin Exp Immunol*. March 2014:n/a–n/a. doi:10.1111/cei.12324.

98. Lane WO, Jantzen AE, Carlon TA, et al. Parallel-plate flow chamber and continuous flow circuit to evaluate endothelial progenitor cells under laminar flow shear stress. *J Vis Exp*. 2012;(59):e3349-e3349. doi:10.3791/3349.

99. Baubet V, Le Mouellic H, Campbell AK, Lucas-Meunier E, Fossier P, Brúlet P. Chimeric green fluorescent protein-aequorin as bioluminescent Ca2+ reporters at the single-cell level. *Proc Natl Acad Sci USA*. 2000;97(13):7260-7265.

100. Wang N, Tytell JD, Ingber DE. Mechanotransduction at a distance: mechanically coupling the extracellular matrix with the nucleus. *Nat Rev Mol Cell Biol*. 2009;10(1):75-82. doi:10.1038/nrm2594.

101. Levesque MJ, Nerem RM. The elongation and orientation of cultured endothelial cells in response to shear stress. *J Biomech Eng*. 1985;107(4):341-347.

102. McCue S, Noria S, Langille BL. Shear-induced reorganization of endothelial cell cytoskeleton and adhesion complexes. *Trends Cardiovasc Med*. 2004;14(4):143-151. doi:10.1016/j.tcm.2004.02.003.

103. Tzima E, Irani-Tehrani M, Kiosses WB, et al. A mechanosensory complex that mediates the endothelial cell response to fluid shear stress. *Nature*. 2005;437(7057):426-431. doi:10.1038/nature03952.

104. Bai Y, Ding Y, Spencer S, Lasky LA, Bromberg JS. Regulation of the association between PSTPIP and CD2 in murine T cells. *Exp Mol Pathol*. 2001;71(2):115-124. doi:10.1006/exmp.2001.2388.

105. Toguchi M, Richnau N, Ruusala A, Aspenström P. Members of the CIP4 family of proteins participate in the regulation of platelet-derived growth

factor receptor-beta-dependent actin reorganization and migration. *Biol Cell*. 2010;102(4):215-230. doi:10.1042/BC20090033.

106. Wess J, Brann MR, Bonner TI. Identification of a small intracellular region of the muscarinic m3 receptor as a determinant of selective coupling to PI turnover. *FEBS Lett*. 1989;258(1):133-136.

107. Wu G, Benovic JL, Hildebrandt JD, Lanier SM. Receptor docking sites for G-protein betagamma subunits. Implications for signal regulation. *J Biol Chem*. 1998;273(13):7197-7200.

108. Wu G, Bogatkevich GS, Mukhin YV, Benovic JL, Hildebrandt JD, Lanier SM. Identification of Gbetagamma binding sites in the third intracellular loop of the M(3)-muscarinic receptor and their role in receptor regulation. *J Biol Chem*. 2000;275(12):9026-9034.

109. Wu G, Krupnick JG, Benovic JL, Lanier SM. Interaction of arrestins with intracellular domains of muscarinic and alpha2-adrenergic receptors. *J Biol Chem*. 1997;272(28):17836-17842.

110. Marchese A, Paing MM, Temple BRS, Trejo J. G protein-coupled receptor sorting to endosomes and lysosomes. *Annu Rev Pharmacol Toxicol*. 2008;48(1):601-629. doi:10.1146/annurev.pharmtox.48.113006.094646.

111. Kang DS, Tian X, Benovic JL. Role of β-arrestins and arrestin domain-containing proteins in G protein-coupled receptor trafficking. *Current Opinion in Cell Biology*. 2014;27:63-71. doi:10.1016/j.ceb.2013.11.005.

112. Hu J, Thor D, Zhou Y, et al. Structural aspects of M_3 muscarinic acetylcholine receptor dimer formation and activation. *FASEB J*. 2012;26(2):604-616. doi:10.1096/fj.11-191510.

113. Saksela K, Permi P. SH3 domain ligand binding: What"s the consensus and where"s the specificity? *FEBS Lett*. 2012;586(17):2609-2614. doi:10.1016/j.febslet.2012.04.042.

114. Jia CYH, Nie J, Wu C, Li C, Li SS-C. Novel Src homology 3 domain-binding motifs identified from proteomic screen of a Pro-rich region. *Mol Cell Proteomics*. 2005;4(8):1155-1166. doi:10.1074/mcp.M500108-MCP200.

115. Li SS-C. Specificity and versatility of SH3 and other proline-recognition domains: structural basis and implications for cellular signal transduction. *Biochem J*. 2005;390(Pt 3):641-653. doi:10.1042/BJ20050411.

116. Dessy C, Kelly RA, Balligand JL, Feron O. Dynamin mediates caveolar sequestration of muscarinic cholinergic receptors and alteration in NO signaling. *The EMBO Journal*. 2000;19(16):4272-4280. doi:10.1093/emboj/19.16.4272.

117. Suetsugu S, Kurisu S, Takenawa T. Dynamic shaping of cellular membranes by phospholipids and membrane-deforming proteins. *Physiological Reviews*. 2014;94(4):1219-1248. doi:10.1152/physrev.00040.2013.

118. Rao Y, Rückert C, Saenger W, Haucke V. The early steps of endocytosis: from cargo selection to membrane deformation. *Eur J Cell Biol*. 2012;91(4):226-233. doi:10.1016/j.ejcb.2011.02.004.

119. Marie I, Bény J-L. Calcium imaging of murine thoracic aorta endothelium by confocal microscopy reveals inhomogeneous distribution of endothelial cells responding to vasodilator agents. *J Vasc Res*. 2002;39(3):260-267.

120. van Weering JRT, Cullen PJ. Membrane-associated cargo recycling by tubule-based endosomal sorting. *Seminars in Cell and Developmental Biology*. 2014;31:40-47. doi:10.1016/j.semcdb.2014.03.015.

121. van Weering JRT, Sessions RB, Traer CJ, et al. Molecular basis for SNX-BAR-mediated assembly of distinct endosomal sorting tubules. *The EMBO Journal*. 2012;31(23):4466-4480. doi:10.1038/emboj.2012.283.

122. Bonifacino JS, Hurley JH. Retromer. *Current Opinion in Cell Biology*. 2008;20(4):427-436. doi:10.1016/j.ceb.2008.03.009.

123. Zobel T, Brinkmann K, Koch N, et al. Cooperative functions of the two F-BAR proteins Cip4 and Nostrin in the regulation of E-cadherin in epithelial morphogenesis. *Journal of Cell Science*. 2015;128(3):499-515. doi:10.1242/jcs.155929.

124. Deretic D, Williams AH, Ransom N, Morel V, Hargrave PA, Arendt A. Rhodopsin C terminus, the site of mutations causing retinal disease, regulates trafficking by binding to ADP-ribosylation factor 4 (ARF4). *Proc Natl Acad Sci USA*. 2005;102(9):3301-3306. doi:10.1073/pnas.0500095102.

125. Tan CM, Nickols HH, Limbird LE. Appropriate polarization following pharmacological rescue of V2 vasopressin receptors encoded by X-linked nephrogenic diabetes insipidus alleles involves a conformation of the receptor that also attains mature glycosylation. *J Biol Chem*. 2003;278(37):35678-35686. doi:10.1074/jbc.M301888200.

126. Knollman PE, Janovick JA, Brothers SP, Conn PM. Parallel regulation of membrane trafficking and dominant-negative effects by misrouted gonadotropin-releasing hormone receptor mutants. *J Biol Chem*. 2005;280(26):24506-24514. doi:10.1074/jbc.M501978200.

127. Wess J. Molecular biology of muscarinic acetylcholine receptors. *Crit Rev Neurobiol*. 1996;10(1):69-99.

128. Caulfield MP, Birdsall NJ. International Union of Pharmacology. XVII.

Classification of muscarinic acetylcholine receptors. *Pharmacol Rev*. 1998;50(2):279-290.

129. Boittin F-X, Alonso F, Le Gal L, Allagnat F, Bény J-L, Haefliger J-A. Connexins and M3 muscarinic receptors contribute to heterogeneous Ca(2+) signaling in mouse aortic endothelium. *Cell Physiol Biochem*. 2013;31(1):166-178. doi:10.1159/000343358.

130. Dedkova EN, Sigova AA, Zinchenko VP. Mechanism of action of calcium ionophores on intact cells: ionophore-resistant cells. *Membr Cell Biol*. 2000;13(3):357-368.

131. Haberberger RV, Bodenbenner M, Kummer W. Expression of the cholinergic gene locus in pulmonary arterial endothelial cells. *Histochem Cell Biol*. 2000;113(5):379-387.

132. Kummer W, Haberberger R. Extrinsic and intrinsic cholinergic systems of the vascular wall. *Eur J Morphol*. 1999;37(4-5):223-226.

133. Milner P, Ralevic V, Hopwood AM, et al. Ultrastructural localisation of substance P and choline acetyltransferase in endothelial cells of rat coronary artery and release of substance P and acetylcholine during hypoxia. *Experientia*. 1989;45(2):121-125.

134. Ruetten H, Dimmeler S, Gehring D, Ihling C, Zeiher AM. Concentric left ventricular remodeling in endothelial nitric oxide synthase knockout mice by chronic pressure overload. *Cardiovasc Res*. 2005;66(3):444-453. doi:10.1016/j.cardiores.2005.01.021.

135. Shesely EG, Maeda N, Kim HS, et al. Elevated blood pressures in mice lacking endothelial nitric oxide synthase. *Proc Natl Acad Sci USA*. 1996;93(23):13176-13181.

136. Shibata K, Yatera Y, Furuno Y, et al. Spontaneous development of left ventricular hypertrophy and diastolic dysfunction in mice lacking all nitric oxide synthases. *Circ J*. 2010;74(12):2681-2692.

137. Abbate A, Arena R, Abouzaki N, et al. Heart failure with preserved ejection fraction: refocusing on diastole. *Int J Cardiol*. 2015;179:430-440. doi:10.1016/j.ijcard.2014.11.106.

138. Malek AM, Izumo S. Mechanism of endothelial cell shape change and cytoskeletal remodeling in response to fluid shear stress. *Journal of Cell Science*. 1996;109 (Pt 4):713-726.

139. Remuzzi A, Dewey CF, Davies PF, Gimbrone MA. Orientation of endothelial cells in shear fields in vitro. *Biorheology*. 1984;21(4):617-630.

140. Malek AM, Greene AL, Izumo S. Regulation of endothelin 1 gene by fluid shear stress is transcriptionally mediated and independent of protein kinase C and cAMP. *Proc Natl Acad Sci USA*.

1993;90(13):5999-6003.

141. Eskin SG, McIntire LV. Hemodynamic effects on atherosclerosis and thrombosis. *Semin Thromb Hemost*. 1988;14(2):170-174. doi:10.1055/s-2007-1002771.

142. Malek AM, Jackman R, Rosenberg RD, Izumo S. Endothelial expression of thrombomodulin is reversibly regulated by fluid shear stress. *Circulation Research*. 1994;74(5):852-860.

143. Hahn C, Schwartz MA. Mechanotransduction in vascular physiology and atherogenesis. *Nat Rev Mol Cell Biol*. 2009;10(1):53-62. doi:10.1038/nrm2596.

144. Davies PF. Endothelial transcriptome profiles in vivo in complex arterial flow fields. *Ann Biomed Eng*. 2008;36(4):563-570. doi:10.1007/s10439-007-9400-0.

145. Wechezak AR, Wight TN, Viggers RF, Sauvage LR. Endothelial adherence under shear stress is dependent upon microfilament reorganization. *J Cell Physiol*. 1989;139(1):136-146. doi:10.1002/jcp.1041390120.

146. Galbraith CG, Skalak R, Chien S. Shear stress induces spatial reorganization of the endothelial cell cytoskeleton. *Cell Motil Cytoskeleton*. 1998;40(4):317-330. doi:10.1002/(SICI)1097-0169(1998)40:4<317::AID-CM1>3.0.CO;2-8.

147. Tzima E. Role of small GTPases in endothelial cytoskeletal dynamics and the shear stress response. *Circulation Research*. 2006;98(2):176-185. doi:10.1161/01.RES.0000200162.94463.d7.

148. Civelekoglu-Scholey G, Orr AW, Novak I, Meister JJ, Schwartz MA, Mogilner A. Model of coupled transient changes of Rac, Rho, adhesions and stress fibers alignment in endothelial cells responding to shear stress. *Journal of Theoretical Biology*. 2005;232(4):569-585. doi:10.1016/j.jtbi.2004.09.004.

149. Aspenström P. A Cdc42 target protein with homology to the non-kinase domain of FER has a potential role in regulating the actin cytoskeleton. *Current Biology*. 1997;7(7):479-487.

150. Wasiak S, Quinn CC, Ritter B, et al. The Ras/Rac guanine nucleotide exchange factor mammalian Son-of-sevenless interacts with PACSIN 1/syndapin I, a regulator of endocytosis and the actin cytoskeleton. *J Biol Chem*. 2001;276(28):26622-26628. doi:10.1074/jbc.M100591200.

151. Kovacevic I. Functional characterization of NOSTRIN in signal transduction and vascular development. 2012.

152. Privratsky JR, Newman PJ. PECAM-1: regulator of endothelial junctional integrity. *Cell Tissue Res*. 2014;355(3):607-619. doi:10.1007/s00441-

013-1779-3.

153. Newton JP, Buckley CD, Jones EY, Simmons DL. Residues on both faces of the first immunoglobulin fold contribute to homophilic binding sites of PECAM-1/CD31. *J Biol Chem*. 1997;272(33):20555-20563.

154. Osawa M. Evidence for a role of platelet endothelial cell adhesion molecule-1 in endothelial cell mechanosignal transduction: is it a mechanoresponsive molecule? *The Journal of Cell Biology*. 2002;158(4):773-785. doi:10.1083/jcb.200205049.

155. Fung YC, Liu SQ. Elementary mechanics of the endothelium of blood vessels. *J Biomech Eng*. 1993;115(1):1-12.

156. Fleming I, Fisslthaler B, Dixit M, Busse R. Role of PECAM-1 in the shear-stress-induced activation of Akt and the endothelial nitric oxide synthase (eNOS) in endothelial cells. *Journal of Cell Science*. 2005;118(Pt 18):4103-4111. doi:10.1242/jcs.02541.

157. Collins C, Guilluy C, Welch C, et al. Localized tensional forces on PECAM-1 elicit a global mechanotransduction response via the integrin-RhoA pathway. *Curr Biol*. 2012;22(22):2087-2094. doi:10.1016/j.cub.2012.08.051.

158. Otte LA, Bell KS, Loufrani L, et al. Rapid changes in shear stress induce dissociation of a Gq/11-platelet endothelial cell adhesion molecule-1 complex. *The Journal of Physiology*. 2009;587(10):2365-2373. doi:10.1113/jphysiol.2009.172643.

159. Gudi SR, Clark CB, Frangos JA. Fluid flow rapidly activates G proteins in human endothelial cells. Involvement of G proteins in mechanochemical signal transduction. *Circulation Research*. 1996;79(4):834-839.

160. McCormick ME, Goel R, Fulton D, Oess S, Newman D, Tzima E. Platelet-Endothelial Cell Adhesion Molecule-1 Regulates Endothelial NO Synthase Activity and Localization Through Signal Transducers and Activators of Transcription 3-Dependent NOSTRIN Expression. *Arteriosclerosis, Thrombosis, and Vascular Biology*. 2011;31(3):643-649. doi:10.1161/ATVBAHA.110.216200.

161. Zobel T, Brinkmann K, Koch N, et al. Cooperative functions of the two F-BAR proteins Cip4 and Nostrin in the regulation of E-cadherin in epithelial morphogenesis. *Journal of Cell Science*. 2015;128(7):1453-1453. doi:10.1242/jcs.170944.

162. Goel R, Schrank BR, Arora S, et al. Site-specific effects of PECAM-1 on atherosclerosis in LDL receptor-deficient mice. *Arteriosclerosis, Thrombosis, and Vascular Biology*. 2008;28(11):1996-2002. doi:10.1161/ATVBAHA.108.172270.

163. Harry BL, Sanders JM, Feaver RE, et al. Endothelial cell PECAM-1

promotes atherosclerotic lesions in areas of disturbed flow in ApoE-deficient mice. *Arteriosclerosis, Thrombosis, and Vascular Biology*. 2008;28(11):2003-2008. doi:10.1161/ATVBAHA.108.164707.

164. Stevens HY, Melchior B, Bell KS, Yun S, Yeh J-C, Frangos JA. PECAM-1 is a critical mediator of atherosclerosis. *Dis Model Mech*. 2008;1(2-3):175–81–discussion179. doi:10.1242/dmm.000547.

10 Acknowledgements

First of all, I would like to express my very sincere gratitude to my supervisor Prof. Dr. Ivan Dikic for accepting me as an MD student at IBC II as well as for his general support, motivation and encouragement.

I would also like to thank Prof. Dr. Nina Wettschureck from the MPI Bad Nauheim for agreeing to be my second referee.

A very special thanks goes to my group leader Dr. Stefanie Oess for the opportunity to join her group, for offering her continuous advice and encouragement throughout the course of this thesis, and for sharing her enthusiasm for science with me.
Special thanks go as well to Dr. Igor Kovacevic and Dr. Meike Hoffmeister
for the great effort they have put into training me in the scientific field as well as for their care and friendship and the great atmosphere in the lab. Without their guidance and persistant help this thesis would not have been possible.

I thank Dr. Sorin Tunaru from the MPI Bad Nauheim for sharing his experience with me and providing me with the cells for the aequorin assay.

I am thankful to all the colleagues and co-workers at IBC II for the inspiring discussions, openness, and general support that contributed to the special scientific environment at IBC II. Special thanks go to Dr. Doris Popovic for introducing me to the microscope and her technical assistance.

I also want to express my gratitude to Prof. Dr. Hartmut Leppin, my mentor from the *Studienstiftung,* for his confidence, and his personal guidance and support.

Also, I am grateful to the SFB 834 Endothelial Signaling and Vascular Repair for the conceptual support and the MD scholarship. I recognize that I would not have been able to focus as much on my research without their financial assistance.

And I want to thank my mother Anne and my sister Marit for always believing in me. I am proud that we have constantly grown together into such a strong team.

12 Schriftliche Erklärung

Ich erkläre ehrenwörtlich, dass ich die dem Fachbereich Medizin der Johann Wolfgang Goethe-Universität Frankfurt am Main zur Promotionsprüfung eingereichte Dissertation mit dem Titel

The role of the F-BAR protein NOSTRIN in endothelial signal transduction

in dem Institut für Biochemie II (Kardiovaskuläre Biochemie) unter Betreuung und Anleitung von Prof. Dr. Ivan Dikic mit Unterstützung durch Dr. Stefanie Oess ohne sonstige Hilfe selbst durchgeführt und bei der Abfassung der Arbeit keine anderen als die in der Dissertation angeführten Hilfsmittel benutzt habe. Darüber hinaus versichere ich, nicht die Hilfe einer kommerziellen Promotionsvermittlung in Anspruch genommen zu haben.

Ich habe bisher an keiner in- oder ausländischen Universität ein Gesuch um Zulassung zur Promotion eingereicht. Die vorliegende Arbeit wurde bisher nicht als Dissertation eingereicht.

Vorliegende Ergebnisse der Arbeit wurden in folgendem Publikationsorgan veröffentlicht:

Igor Kovacevic, Miriam Müller, Baktybek Kojonazarov, Alexander Ehrke, Voahanginirina Randriamboavonjy, Karin Kohlstedt, Tanja Hindemith, Ralph Theo Schermuly, Ingrid Fleming, Meike Hoffmeister, Stefanie Oess, The F-BAR Protein NOSTRIN Dictates the Localization of the Muscarinic M3 Receptor and Regulates Cardiovascular Function, Circulation Research, 117(5), 460–469, 2015.

_____ _____

(Ort, Datum) (Unterschrift)